Innovative process design : laminar counterflow recuperator rotational phase separator

Innovative Process Design

laminar counterflow recuperator
rotational phase separator

Erik van Kemenade

Innovative Process Design

laminar counterflow recuperator
rotational phase separator

Erik van Kemenade

A catalogue record is available from the Library Eindhoven University of Technology
ISBN-10: 90-386-2928-1
ISBN-13: 978-90-386-2928-5

Contents

Preface

This text is prepared for the graduate course "Innovative Process Technology" at the Eindhoven University of Technology, department mechanical engineering. The course is intended to provide insight in the relation between scientific (university) research and industrial applications based on the activities in the section Process Technology. Chapter 1, about innovations and intellectual property management is mainly based on the lectures given in 2004 and 2005 by ir. Hein v.d. Heuvel (Patentwerk b.v.) with additional information from Wikipedia. Chapter 2 about the Energy market is excerpted from "The Shell Global Scenario's to 2025" (2006) and BP's "Statistical Review of World Energy 2006". Apart from the lectures of ir. Bart Veltkamp, for compiling chapter 3, "the laminar counterflow recuperator", I had access to the LEVEL energy technology b.v. internal reports, while prof. dr. ir. Bert Brouwers and dr. ir. Eva Mondt supplied the material for chapter 3 and 4 about the rotational phase separator. The latest developments in using phase transfer mechanisms with the heat exchanger and the rotational phase separator, are based on the work of ir. Carlo de Best and ir. Ralph van Wissen together with the lecture of dr. Michael Golombok (Royal Dutch Shell PLC)in 2004.

Eindhoven, August 2006,

Erik van Kemenade

Nomenclature

A	surface [m^2]
c_p	heat capacity [$Jkg^{-1}K^{-1}$]
C_c	Cunningham slip factor
C_m	torque coefficient [-]
D	diffusion coefficient [m^2s^{-1}]
D_h	hydraulic diameter [m]
d_c	channel diameter [m]
d_p	particle diameter [m]
d_p	plate thickness [m]
E	efficiency [-]
$\dot{E}$	energy consumption rate [Js^{-1}]
F	force [N]
F_th	thermophoretic force [N]
f	friction factor [-]
G	angular momentum [Nm]
H	heating value [Jkg^{-1}]
H	height [m]
H	correction factor
j	mass flux per unit length [$kg\ m^{-1}s^{-1}$]
k	total heat transfer coefficient [$Wm^{-2}K^{-1}$]
L	length [m]
M	particle concentration [$mg\ Nm^{-3}$]
$\dot{m}$	mass flow [$kg\ s^{-1}$]
N	number concentration [m^{-3}]
N_s	entropy generation number
n	strain hardening exponent
p	pressure [Pa]
Q	volume vlow [m^3s^{-1}]
R	gas constant 8.134 $JMol^{-1}K^{-1}$
R	radius [m]
r	radial position [m]
Re	Reynolds number
S	entropy generation [W]
Sc	Schmidt number
s	distance [m]
T	temperature [K]
Ta	Taylor number [-]
t	time [s]
u_b	bulk velocity [ms^{-1}]
u_d	deposition velocity [ms−1]
u_f	axial fluid velocity [ms^{-1}]
u_p	particle velocity [ms^{-1}]
u_{th}	thermophoretic velocity[ms^{-1}]
v_{ax}	axial velocity [ms^{-1}]
v_{ax0}	axial velocity at $t = 0$ [ms^{-1}]
v_t	tangential velocity at $t = 0$ [ms^{-1}]
v_{t0}	tangential velocity at $t = 0$ [ms^{-1}]
W	width [m]
w	axial velocity [ms^{-1}]
w	tangential velocity [ms^{-1}]
x	mole fraction
x^*	ratio length/diameter [-]
α	heat transfer coefficient[$Wm^{-2}K^{-1}$]
α	blade angle [rad]
β	axial velocity decay parameter [-]
δ	inner to outer diameter ratio [-]
ϵ	effectivity [-]
ϵ	surface reduction ratio [-]

ϵ	specific energy consumption [Jkg^{-1}]
η	efficiency
ϕ	stochiometric air ratio
$\overline{\phi}$	correction factor [-]
λ	free molecular length [-]
λ	heat conduction coefficient [$Wm^{-1}K^{-1}$]
μ	dynamic viscosity
ρ	density [kg $m^{-}3$]
τ	relaxation time [s]
τ	residence time [s]
θ	angular position [rad]
ω	mass fraction [-]
Ω	angular velocity [rad s^{-1}]

1 Innovations and patents

"Innovation" can be defined as the process of making changes to something established by introducing something new and is a continuation of an invention, a creation (a new device or process) resulting from study and experimentation, in the sense that it involves a change that creates a new dimension of performance. Innovations involve a series of scientific, technological, organisational, financial and commercial activities. The major part of what is called innovation is essentially evolutionary in character: a step forward along a technology trajectory, or from the known to the unknown, with a high chance of success and low uncertainty about outcomes. The subject of this course however is radical innovation: it involves larger leaps of understanding, perhaps demanding a new way of seeing the whole problem, probably taking a much larger risk than many people involved are happy about. The chances of success are difficult to estimate. There may be considerable opposition to the proposal and questions about the ethics, practicality or cost of the proposal may be raised. People may question if this is, or is not, an advancement of a technology or process.

1.1 Goals of innovation

Technological companies need to innovate in order to survive as a lack of innovation leads to stagnation. It is not surprising, therefore, that companies have embraced the management of innovation enthusiastically, with the primary goal of driving growth and, consequently, improving shareholder value. In general, business organisations spend a significant amount of their turnover on innovation i.e. making changes to their established products, processes and services. The amount of investment can vary from as low as a half a percent of turnover for organisations with a low rate of change to anything over twenty percent of turnover for organisations with a high rate of change. The average investment across all types of organizations is about four percent. This budget will typically be spread across various functions including marketing, product design, information systems, manufacturing systems and quality assurance. Organisational innovation programs are most frequently driven by (in

decreasing order of popularity):

1. Improved quality
2. Creation of new markets
3. Extension of the product range
4. Reduced labour costs
5. Improved production processes
6. Reduced materials
7. Reduced environmental damage
8. Replacement of products/services
9. Reduced energy consumption
10. Conformance to regulations

While evolutionary innovation may be focussed on only one of the items above, radical innovation typically adresses more items at the same time. In organisations innovations often fail if it is seen as a mechanistic process "pull lever obtain result", furthermore innovation, implies change, and can be counter to an organisation's orthodoxy. It should be realised however that innovation is "enacted" - recognised, developed, applied and adopted - through individuals.

1.2 innovation diffusion

The life cycle of innovations can be described using the 's-curve' or diffusion curve. The s-curve maps growth of revenue or productivity against time. In the early stage of a particular innovation, growth is relatively slow as the new product establishes itself. At some point customers begin to demand and the product growth increases more rapidly. New incremental innovations or changes to the product allow growth to continue. Towards the end of its life cycle growth slows and may even begin to decline. In the later stages, no amount of new investment in that product will yield a nornal rate of return.

The s-curve is derived from half of a normal distribution curve. There is an assumption that new product are likely to have "product Life". i.e. a start-up phase, a rapid increase in revenue and eventual decline. In fact the great majority of innovations never get off the bottom of the curve, and never produce normal returns.

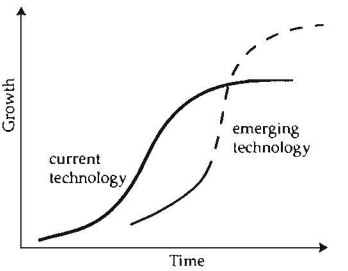

figure 1.1: Innovation S curves

Innovative companies will typically be working on new innovations that will eventually replace older ones. Successive s-curves will come along to replace older ones and continue to drive growth upwards. In the figure above the first curve shows a current technology. The second shows an emerging technology that current yields lower growth but will eventually overtake current technology and lead to even greater levels of growth. The length of life will depend on many factors.

Idea generation leads to opportunity recognition where someone can see an opportunity for developing the idea into a new product, process or service. The opportunity recognition stage involves the idea evaluation stage where ideas are prodded and tested. Often ideas are improved, merged with other ideas and in many cases abandoned. An important test for an idea is that it matches the goals of the organisation and available resources Ű people and money.

If an opportunity is recognised, then the idea moves to a new stage where it can be developed further. The development phase may involve prototype development and marketing testing. Many ideas wait at the end of the development phase for market conditions to be right. There are currently many new products languishing in the laboratories of Philips and Nokia waiting for their moment to begin replacing or even disrupting existing technology. The final stage of the innovation process is realisation and in many cases exploitation where the customer makes the final evaluation.

1.3 Patents

For this section extensive use is made of web resources, mainly Wikipedia and The World Intellectual Property Organization (WIPO).

A patent is a set of exclusive rights granted by a state to a person for a fixed period of time in exchange for the regulated, public disclosure of certain details of a device,

method, process or composition of matter (substance) (known as an invention) which is new, inventive, and useful or industrially applicable.

Although there is evidence suggesting that something like patents was used among some ancient Greek cities, patents in the modern sense originated in Italy. The first patent law was a Venetian Statute of 1474 in which the Republic of Venice issued a decree by which new and inventive devices, once they had been put into practice, had to be communicated to the Republic in order to obtain legal protection against potential infringers. England followed with the Statute of Monopolies in 1623 under King James I. Prior to this time, the crown would issue letters patent (meaning "open letter", as opposed to a letter under seal) providing any person with a "monopoly" to produce particular goods or provide particular services. The first of them was granted by Henry VI in 1449 to a Flemish man a 20 year monopoly on the manufacture of stained glass.

A modern patent provides the right to exclude others from making, using, selling, offering for sale, or importing the patented invention for the term of the patent. A patent is, in effect, a limited property right that the government offers to inventors in exchange for their agreement to share the details of their inventions with the public.

In order to obtain a patent, an applicant must provide a written description of his or her invention in sufficient detail for a person skilled in the art to make and use the invention. This written description is provided in what is known as the patent specification, which often is accompanied by figures that show how the invention is made and how it operates. In addition, at the end of the specification, the applicant must provide the patent office with one or more claims that distinctly point out what the applicant regards as his or her invention. A claim, unlike the body of the specification, is not a detailed description of the invention, but a succinct series of words designed to provide the public with notice of precisely what the patent owner has a right to exclude others from making, using, or selling. Claims are often analogised to a deed or other instrument that, in the context of real property, sets the metes and bounds of an owner's right to exclude. It is the claims that define what a patent covers or does not cover. A single patent may contain numerous claims, each of which is regarded as a distinct invention.

In order for a patent to be granted, that is to take legal effect, the patent application must meet the requirements of the national law, in particular those related to patentability.

A patent is an exclusionary right-it gives the right to exclude others from infringing the patent, but that does not necessarily give the owner of the patent the right to exploit the patent. This is so since many inventions relate to improvements of prior inventions which may still be covered by someone else's patent. For example, if an

inventor takes an existing patented mouse trap design, adds a new feature to make an improved mouse trap, and obtains a patent on the improvement, he or she can only legally build his or her improved mouse trap with permission from the patent holder of the original mouse trap, assuming the original patent is still in force. On the other hand, the owner of the improved mouse trap can exclude the original patent owner from using the improvement.

Patents are typically enforced through civil lawsuits (for example, for a US patent, by an action for patent infringement in a United States federal court). Typically, the patent owner will seek monetary compensation for past infringement, and will seek an injunction prohibiting the defendant from engaging in future acts of infringement. In order to prove infringement, the patent owner must establish that the accused infringer practices all of the requirements of at least one of the claims of the patent.

An important limitation on the ability of a patent owner to successfully assert his or her patent in civil litigation is the accused infringer's right to challenge the validity of that patent. Civil courts hearing patent cases can and often do declare patents invalid. The grounds on which a patent can be found invalid are set out in the relevant patent legislation and vary between countries. Often, the grounds are a sub-set of the requirements for patentability in the relevant country.

The vast majority of patent rights, however, are not determined through litigation, but are resolved privately through patent licensing. Patent licensing agreements are effectively contracts in which the patent owner (the licensor) agrees not to sue the licensee for infringement of the licensor's patent rights. It is not uncommon for companies engaged in complex technical fields to enter into dozens of license agreements associated with the production of a single product. Moreover, it is equally common for competitors in such fields to license patents to each other under cross-licensing agreements in order to gain access to each other's patents. A cross license agreement could be highly desirable to the mouse trap developers discussed above, for example, because it would permit both parties to profit off each other's inventions.

1.4 Patent application

Patent laws usually require that, in order for an invention to be patentable, it must

- be of patentable subject matter, ie a kind of subject-matter that is eligible for patent protection
- be novel

- be non-obvious (in United States patent law) or involve an inventive step (in European patent law)
- be useful (in U.S. patent law) or be susceptible of industrial application (in European patent law)

Usually the term "patentability" only refers to "substantive" conditions, and does not refer to formal conditions such as the "sufficiency of disclosure", the "unity of invention" or the "best mode requirement". Judging patentability is one aspect of the official examination of a patent application performed by a patent examiner. Although the grant of a patent creates a presumption that the claimed invention is patentable, errors in the granting procedure may occur and previously unconsidered prior art may be brought to light only after the patent was granted. Prior to filing a patent application, inventors sometimes obtain a patentability opinion from a patent agent or patent attorney regarding whether an invention satisfies the substantive conditions of patentability.

A patent application is a request pending at a patent office for the grant of a patent for the invention described and claimed by that application. An application consists of a description of the invention (the patent specification), together with official forms and correspondence relating to the application. The term patent application is also used to refer to the process of applying for a patent, or to the patent specification itself.

In order to obtain the grant of a patent, a person, either legal or natural, must file an application at a patent office with jurisdiction to grant a patent in the geographic area over which coverage is required. This will often be a national patent office, such as the United Kingdom Patent Office or the United States Patent and Trademark Office (USPTO), but could be a regional body, such as the European Patent office. Once the patent specification complies with the laws of the office concerned, a patent may be granted for the invention described and claimed by the specification.

The process of "negotiating" or "arguing" with a patent office for the grant of a patent, and interaction with a patent office with regard to a patent after its grant, is known as patent prosecution. Patent prosecution is distinct from patent litigation which relates to legal proceedings for infringement of a patent after it is granted

Depending upon the office at which a patent application is filed, that application could either be an application for a patent in a given country, or may be an application for a patent in a range of countries. The former are known as "national (patent) applications", and the latter as "regional (patent) applications". National applications are generally filed at a national patent office, such as the United Kingdom Patent Office, to obtain a patent in the country of that office. The application may either be

filed directly at that office, or may result from a regional application or from an international application under the Patent Cooperation Treaty (PCT), once it enters the national phase. A regional patent application is one which may have effect in a range of countries. The European Patent Office (EPO) is an example of a Regional patent office. The EPO grants patents which can take effect in some or all countries contracting to the European Patent Convention (EPC), following a single application process. Filing and prosecuting an application at a regional granting office is advantageous as it allows patents in a number of countries to be obtained without having to prosecute applications in all of those countries. The cost and complexity of obtaining protection is therefore reduced.

It is important to file a patent application before publicly disclosing the details of the invention. In general, any invention which is made public before an application is filed would be considered prior art (although the definition of the term "prior art" is not unified at the international level, in many countries, it consists of any information which has been made available to the public anywhere in the world by written or oral disclosure). In countries which apply the above definition of the term 'prior art', the applicant's public disclosure of the invention prior to filing a patent application would prevent him/her from obtaining a valid patent for that invention, since such invention would not comply with the "novelty" requirement. Some countries, however, allow for a grace period, which provides a safeguard for applicants who disclosed their inventions before filing a patent application, and the novelty criteria may be interpreted differently depending on the applicable law. If it is inevitable to disclose your invention to, for example, a potential investor or a business partner, before filing a patent application, such a disclosure should be accompanied by a confidentiality agreement.

At present, no "world patents" or "international patents" exist. In general, an application for a patent must be filed, and a patent shall be granted and enforced, in each country in which you seek patent protection for your invention, in accordance with the law of that country. In some regions, a regional patent office, for example, the European Patent Office (EPO) and the African Regional Intellectual Property Organization (ARIPO), accepts regional patent applications, or grants patents, which have the same effect as applications filed, or patents granted, in the member States of that region. Further, any resident or national of a Contracting State of the Patent Cooperation Treaty (PCT) may file an international application under the PCT. A single international patent application has the same effect as national applications filed in each designated Contracting State of the PCT. However, under the PCT system, in order to obtain patent protection in the designated States, a patent shall be granted by each designated State to the claimed invention contained in the international ap-

plication.

1.5 Filing an application

In obtaining patent rights for an inventor, the practitioner first drafts an application typically by interviewing the inventor to understand the nature of the invention and help clarify novel features (and often to ascertain what is already known to people familiar with the general field of the invention - such already-known material is termed the prior art), and to obtain drawings and written notes regarding the features of the invention and the background. During this initial phase, termed "patent preparation", the practitioner may also seek to determine precisely who contributed to the making of the invention (because an incorrect listing of inventors may incurably invalidate any patent that might result from an application), and to find out whether any publications, offers for sale, or other such public disclosures of the invention were made. These issues are important because under certain circumstances, public disclosures or offers to sell an invention prior to filing an application for a patent may prevent or the issuance of a patent for the invention, under the laws or regulations of some jurisdictions (in the United States, the laws preventing obtaining patents because of previous disclosures or offers to sell are termed "statutory bars").

After drafting an application for patent, complying with any further rules (such as having the inventor or inventors review the application prior to filing), and obtaining the applicant's permission, the practitioner then files the patent application with the patent office. Usually, the practitioner seeks to file the application as soon as possible, because in a majority of jurisdictions (such as Europe and Japan) if two or more applications for the same subject matter are filed, then only the party who filed first will be entitled to seek a patent (this is known as the "first-to-file rule"). Even in other jurisdictions (such as the United States, which does not follow the "first-to-file rule"), early filing may prevent the use of certain materials from being applied against the patent application as prior art while the patent application is pending before the patent office.

The filing date of an application is important as it sets a cutoff date after which any public disclosures will not form prior art (but the priority date must also be considered), and also because, in most jurisdictions (notably, not the USA) the right to a patent for an invention lies with the first person to file an application for protection of that invention. It is therefore generally beneficial to file an application as soon as possible.

In order to obtain a filing date the documents filed must comply with the regula-

tions of the patent office in which it was filed. A full specification complying with all rules may not be required to obtain a filing date, for example in the United Kingdom, claims and an abstract are not required to obtain a filing date, but can be added later. However, no subject matter can be added to an application after the filing date and so it is vital that an application discloses all material relevant to the application at the time of filing. If the requirements for the award of a filing date are not met, the Patent Office will notify the Applicant of the deficiencies. Depending upon the law of the patent office in question, correction may be possible without moving the filing date, or the application may be awarded a filing date adjusted to the date on which the requirements are completed.

A patent application may make a claim to priority from another previously filed application, in order to take advantage of the filing date of information disclosed in that earlier application. Claiming priority is desirable because the earlier effective filing date reduces the number of prior art disclosures, increasing the likelihood of obtaining a patent. The priority system is principally useful in filing patent applications in many countries, as the cost of the filings can be delayed by up to a year, without any of the applications made earlier for the same invention counting against later applications. The rules relating to priority claims are derived from the Paris Convention for the Protection of Industrial Property and countries which provide a priority system in conformity with the Paris convention are said to be convention countries. These should not be confused with the rules under the Patent Cooperation Treaty (PCT), outlined above.

Patent applications are generally published 18 months after the earliest priority date of the application. Prior to that publication the application is confidential to the patent office. After publication, depending upon local rules, certain parts of the application file may remain confidential, but it is common for all communications between an Applicant (or his agent) and the patent office to be publicly available. The publication of a patent application marks the date at which it is publicly available and therefore at which it forms full prior art for other patent applications worldwide.

After filing, and when requested, a patent application is researched to reveal prior art which may be relevant to the patentability of the invention. The search report is published, generally with the application 18 months after the priority date with the application, and as such is a public document. The search report is useful to the applicant to determine whether the application should be pursued or if there is prior art that prevents the grant of a useful patent, in which case the application may be abandoned before incurring further expense. Some jurisdictions, for example the USA, do not conduct a separate search, but rather search and examination are combined. In that case, a separate search report is not issued and it is not until the

application is examined that the applicant is informed of prior art that the patent office examiner considers relevant.

Examination is the process of ensuring an application complies with the requirements of the relevant patent laws. Examination is generally an iterative process, in which the patent office writes to the applicant notifying him/her of its objections to which the applicant responds with arguments and/or amendments to overcome the objections. Amendments and arguments may then be accepted or rejected, triggering further response, and so forth, until a patent is issued or the application is abandoned.

Many jurisdictions require periodic payment of maintenance fees in order to retain the validity of a patent after it is issued and during its term. Failure to timely pay the fees results in loss of the patent's protection. The validity of an issued patent may also be subject to post-issue challenges of various types, some of which may cause the patent office to re-examine the application.

The word "infringement" means an encroachment upon the domain belonging to a patentee that is described by the claims of her/his patent. If a patent is analogised to real property, the claims correspond to the boundary recited in the deed. Invasion of the boundary of a landowner's real estate is called trespass, while invasion of a patentee's claims is called infringement. A determination of patent infringement involves a two-step process. First, the claims are analysed by studying all of the relevant patent documents. Second, the claims must "read on" the accused device or process. This merely means that the device or process is examined to see if it is substantially described by the claims; in other words, the claims are tested to see whether they describe the accused infringement. Infringement can be direct, indirect, or contributory. Anyone who makes, uses, or sells the patented invention is a direct infringer. If a person actively encourages another to make, use, or sell the invention, the person so inducing is liable for indirect infringement. Contributory infringement can be committed by knowingly selling or supplying an item for which the only use is in connection with a patented invention. Good faith or ignorance is no defense for direct infringement, but it can be for indirect or contributory infringement.

1.6 Economic rationale

There are four primary justifications for granting patents: innovation, disclosure, production investment, and designing around.

First, in accordance with the original definition of the term "patent", it is argued that patents facilitate and encourage disclosure of innovations into the public domain for the common good. If inventors did not have the legal protection of patents,

they may prefer or tend to keep their inventions secret. Awarding patents generally makes the details of new technology publicly available, for exploitation by anyone after patent protection ends, or for further improvement by other inventors (who may in turn patent these improvements). Furthermore, when a patent's term has expired, the public record ensures that the patentee's idea is not lost to humanity.

Second, it is broadly believed that patents incentivize economically efficient research and development (R&D). Many large modern corporations have annual R&D budgets of hundreds of millions or even billions of dollars. Without patent protection, R&D spending would be significantly less or eliminated altogether, limiting the possibility of technological advances or breakthroughs. Corporations would be much more conservative about the R&D investments they made, as third parties would be free to exploit any developments. This second justification is closely related to the basic idea underlying traditional property rights: why build a house if another person could freely occupy it?

Third, in many industries (especially those with high fixed costs and low marginal costs and low reverse engineering costs - pharmaceuticals and computer software being the two prototyical examples), once an invention exists and has been tested, the cost of actually turning it into a product is typically six times or more the R&D cost. Unless there is some way to prevent copies from competing at the marginal cost of production, companies will not make that productisation investment.

Fourth, many believe that patent rights create an incentive for companies to develop workarounds to patented inventions, thereby creating improved or alternative technologies that might not otherwise have been developed.

One interesting side effect of modern day patent usage is that the small-time inventor can use the exclusive right status to become a licensor. This allows the inventor to accumulate capital quickly from licensing the invention and may allow rapid innovation to occur because he/she may choose to not manage a manufacturing buildup for the invention. Thus, time and energy can be spent on pure innovation and allow others to concentrate on manufacturability.

There are arguments in opposition to patent rights. Granting a patent confers a "negative right" upon a patent owner, because he or she may legally exclude competitors from using or exploiting the invention, even if the competitor subsequently (either subsequent to the date of invention, or to the priority date, depending upon the relevant patent law - see First to file and first to invent) independently develops the same invention. It is argued that monopolies create inefficiency, and that if the grant of a patent is, assumed to be, the grant of a monopoly, the patent system may stifle competition and result in higher prices, lower quality, and shortages.

All patents are published and so there is a tension to the applicant between includ-

ing sufficient detail to secure patent protection and including excessive information and thereby giving away "trade secrets" to the disadvantage of their company. It has been argued that the sufficiency requirements of patents are not rigorous enough and that patents are sometimes granted without any knowledge being imparted to society. It has also been suggested that market incentives alone would be sufficient incentive to innovate even in the absence of patents.

1.7 Scope

In this text the abstract concepts mentioned above are made concrete using two examples from the research carried out by the section Process Technology of the Eindhoven University of Technology. The two concepts that made it to commercial products are the laminar counterflow heat exchanger and the rotational phase separator. Both examples have in common that they were conceived within projects with a different aim and both could not have been developed within the framework of the initial research alliance. Recognition and subsequent patenting of the concepts has been the key element for further development in both cases utilising changing research and development environments as the products mature.

Both products are also similar in that they have their origins in basic scientific research while the course of development was guided by the interaction of science and engineering. Contrary to the scientific publications, in here detailed attention is given to the influence of the iterative development path concept - model - prototypes - experiments on the final product.

The innovations were conceived and are still mainly applied in the field of energy supply and conservation and consequently are not direct consumer products. The general public is less interested in heaving an energy supply at reasonable cost and less in the technology behind it. Market influences on the innovations under discussion are mainly felt through the interaction between government regulations regarding pollutant emissions or energy conservation and the need of market parties for cost efficient solutions and priorities seem to change from year to year. Technological innovation, with a typical incubation time of 10 to 20 years can not follow these short time fluctuations of interest so the key for successful innovations in this market is to provide a better and cheaper product or process with a multitude of applications inside and outside the energy market. Further development of a concept can be achieved by developing the general idea for applications that are of interest in a specific time frame and/or specific process. Such fruitful areas for development for the heat exchanger and the phase exchanger have been or are (amongst others): nuclear

energy, gas-fired cogeneration, air conditioning, coal/biomass combustion, industrial gas cleaning and oil/gas production. Each individual development has advanced the leve of understanding of the basic process and technological know-how opening up further applications.

2 Energy market

Since the industrial revolution, coal has been gradually superseded by oil and to a lesser degree gas as the main energy source (Shell 2006). Global economic growth has once again become more dependent on energy as a result, notably, of the rapid development of China and India. A "global middle class" is now knocking on the door of prosperity, with energy a fundamental enabler. With China the world's manufacturing hub, global economic growth as a whole has become more energy-intensive again.

A second source of strain is energy security, a concept rooted in geology and technology as well as in politics and international relations. The reserves debate took on a new impetus as markets were confronted: with inconsistencies in reserves categorisations by companies; with unease about longer-term access and supply reliability from some important non-OECD (Organisation for Economic Co-operation and Development) regions; and even with some observers expressing doubts about the state and nature of the vast reserves bases in the Middle East. Production of conventional oil and gas in non-OPEC countries appears about to plateau within a decade or so. A number of producer countries, within and outside of OPEC, may also find it in their interests to keep production at a lower plateau for a longer period, as their concerns for future generations may outweigh pressures for immediate revenue maximisation. The notion that supplies are flexible enough to meet demand in almost any foreseeable circumstance can no longer taken for granted. It is clear that massive investment must be made -and protected- in very challenging regions for the energy consumer to carry on turning the car key or switching on the light without even thinking about where the gasoline, or electricity, comes from.

The third major discontinuity is the one introduced by regulatory and market developments that make carbon a commodity in its own right, even though the price of that commodity is negative (i.e. the price to dispose of it is positive). The energy system will therefore be operating, to an unprecedented extent, as an energy and carbon system. The public, in Europe but also in many parts of the US, and in developing countries most at risk -expect this system to deliver both high growth and a

low-carbon economy. In all scenarios, the "carbon" discontinuity makes its impact felt by influencing legislation and regulation of markets, by fostering the development of alternative fuels, and by affecting the whole structure of relative prices throughout the value chain.

2.1 Energy for the developing world

The correlation between overall primary energy growth and GDP (gross domestic product) growth had decreased from 1.2 in the mid-1960s to a low of 0.3 by 2000, as the oil price shocks of the 1970s fostered higher efficiency, technological change and diversification of supply. Since 2000, however, this long-term trend of reducing energy content per unit GDP growth has reversed, and the correlation more than doubled from around 0.3 to 0.7.

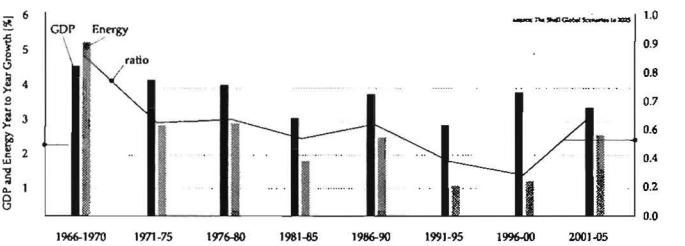

figure 2.1: world total energy growth versus GDP growth

This relationship can be further analysed as a combination of income elasticity and price elasticity. The energy ladder econometric studies indicate that, in general:

- Low-income countries are highly dependent on traditional energy sources (with the risk that deforestation makes their needs increasingly hard to satisfy)
- Once countries reach the threshold of about USD 3000 per capita GDP, energy demand explodes as industrialisation and personal mobility take off
- From around USD 15,000, demand grows more slowly as services begin to dominate
- Beyond USD 25,000, it is possible for economic growth to continue without significant energy increases (although the true picture may differ if one corrects for the relocation of energy-intensive industries to lower-income countries)

With global economic growth fuelled, in large part, by the development of Asia and the "BRICs" (Brazil, Russia, India, and China), the energy ladder becomes an essential consideration for the global energy markets. However, the intensity of energy usage at each stage of development, including on the high-income "plateaux", differs widely across countries. While Japan and some European countries have per capita income levels similar to US ones, their per capita energy consumption is only about half of the US level. This reflects different geographical and climatic conditions, but also the cumulative impact of policies directed at improving energy conservation (whether to reduce trade imbalances or, increasingly, to protect the environment). A critical uncertainty for the world's energy outlook is which of the two paths -the American or the Euro-Japanese one -China, India and other emerging markets will now follow.

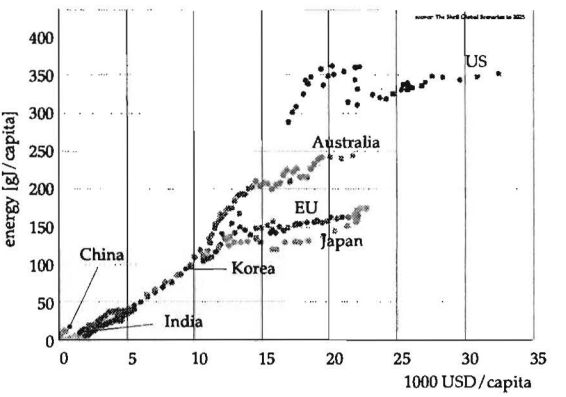

figure 2.2: the energy ladder 1965-2000

China's energy efficiency has remained substantially lower than the world average. Whereas the Chinese economy requires almost 1.5 barrels of oil to produce USD 1000 of output, the global economy needs only half that amount. This is of critical importance because, having doubled its oil demand over the last ten years to 6.4 million bbl/d, of which around 3 million bbl/d is now imported, China is now the world's second largest oil consumer. Even more strikingly, China accounted for no less than 40% of the new demand for oil in the 2001-2004 period. This rapid growth will continue: "depending on how demand for energy services are met, China could quadruple its domestic product between 1998 and 2020 with energy use rising by 70-130%. By contrast, the OECD's share of global oil demand dropped from around 75% in the mid-1960s to slightly more than 60% in the early 2000s. In terms of total

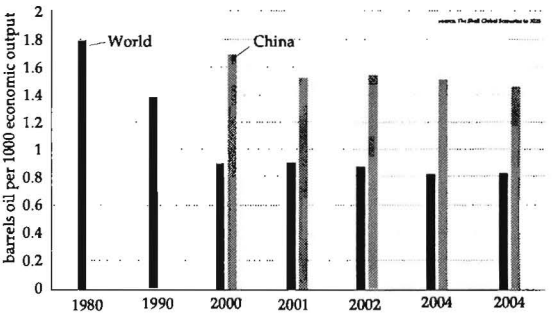

figure 2.3: oil intensity in China and the global economy

primary energy demand, stressing that few governments in the world are as determined as the Chinese one to promote higher energy efficiency, the IEA (International Energy Agency) forecasts that it will be sufficient for China's energy consumption to rise by 2.2% pa in 2002-2030 in order for China's economy to expand by 5% pa during this period. Oil demand growth would be considerably more rapid at 3.7% pa, however. The fastest increase is forecast for gas, whose demand would rise by 4.6% pa. The IEA projections imply therefore that China's demand elasticity with respect to income is falling below the world average. As a result, the energy intensity of the Chinese economy will decline and gradually approach that of the world economy. However, if this occurs at a slow pace, tensions in global energy markets will not be removed, or might even be increased if Chinese growth is stronger than the projected 5%, or if energy-efficiency policies face difficulties when implemented at the local level. Making room for the BRICs in world energy consumption will therefore imply much higher levels of energy investment worldwide. As discussed below, it will also compound the CO2 emission challenge to a degree unforeseen when the Kyoto Protocol was signed in 1992.

2.2 Reserves and energy security

The second discontinuity is concerns -whether for geological and technological reasons or for political ones- over security of energy supplies. The increased risk of

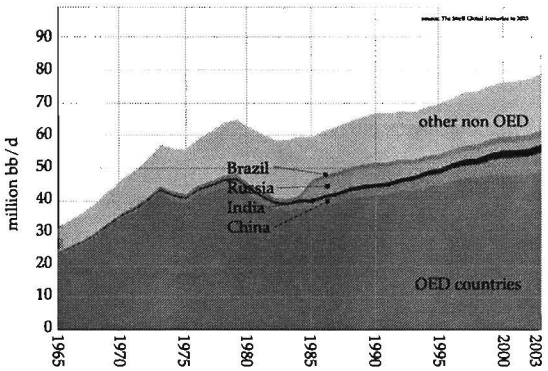

figure 2.4: world oil consumption: making room for the BRICS

reaching a peak in oil supplies in the relatively near future has been debated for decades. However, the failure of previous warnings to materialise is no reason to dismiss the new ones. Whether one is concerned about conventional oil and gas or about energy supply in general, the essential question is the extent to which the price mechanism can be trusted to generate the appropriate signals, investments and technological developments in time for economic growth and development to proceed smoothly.

The static image of reserves has long since given way to a dynamic relationship between needs and capacities in which the key is investment -whether in exploration, in alternative technologies, or in new distribution and organisational infrastructures. Energy investments in producing countries with high export dependency are increasingly accompanied by diplomatic, military and human development assistance from importing countries, concerned about their security of supply.

2.2.1 Peak debate

The most visible component of the debate concerns expected ultimate recoverable reserves. The "Hubbert peak" debate, named after the Shell Oil geophysicist who predicted in 1956 that US oil production would peak in the early 1970s, is again in full swing, albeit now globally. Uncertainties in statistical and geological data have potentially huge implications: a sensitivity study by the US Department of Energy indicated timings for oil production to plateau as divergent as 2040 and 2015, depending on the resource base assumptions at the optimistic and pessimistic ends of the range.

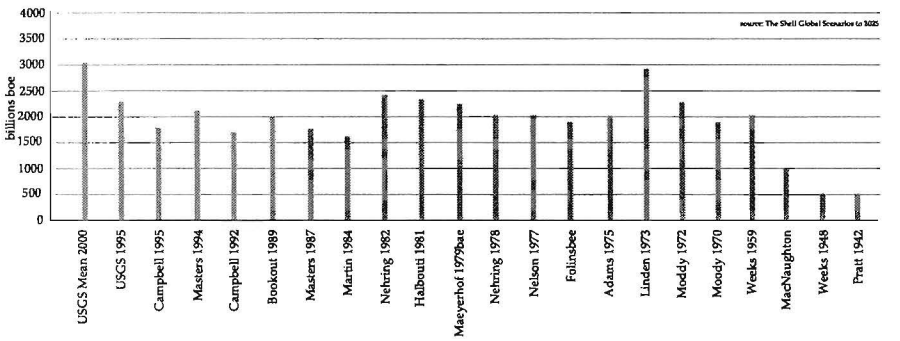

figure 2.5: sixty years of estimates of world crude oil reserves

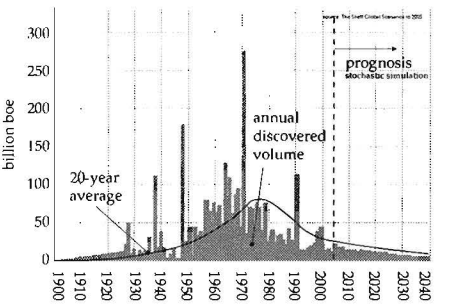

figure 2.6: annual discovered reserves

While major new finds cannot be ruled out, recent statistics do provide worrisome signals. Reserves estimates have increased over time but the annual average increase in proven oil reserves, which stood at 4.5% in the 1980s, has slowed down considerably since the early 1990s to around 1%. Discoveries only replaced some 45% of production since 1999. In addition, the number of discoveries is increasing but discoveries are getting smaller in size. The 25 biggest fields hold some 33% of discovered reserves and the top 100 fields 53%: all but two of the giant fields were discovered before 1970. A simple extrapolation of the volumes discovered annually suggests that volumes to be found between now and 2050 could be as low as 500 billion boe. However, this magnitude of undiscovered potential is considered conservative by some, who believe it is influenced too much by the declining exploration successes of late and by cautious views about the commercial viability of future finds. Limiting the discussion to conventional hydrocarbons would give an increasingly incomplete

picture as unconventionals become more important.

The presently known conventional gas reserves are equivalent to about 85% of known oil reserves, but only a quarter has so far been produced. Gas reserves increased on average at a rate of 3.3% pa over the last two decades, and discoveries more than replaced produced volumes.

Overall, the gas supply outlook is generally reported to be robust. However, significant efforts and investment will be needed in developing infrastructure to move gas to major consuming markets. The environment in each of the scenarios would present different challenges to the timeliness and adequacy of such infrastructure. This would in turn entail challenges before the end of the scenario period on the availability of adequate supplies to gas to some markets. Geographic concentration of gas reserves creates other types of challenges for importing countries. Russia, Iran and Qatar together contain over 55% of the world's proved reserves. Reserves in North America and Europe, 4% and 3% respectively of the world's proved reserves are in decline. It seems unlikely that significant new conventional gas volumes will be discovered so gas supply sources will remain highly concentrated.

Enhanced recovery of resources has been a key feature of the oil and gas industry from its inception, prolonging the life of many fields well beyond initial expectations. The present average oil recovery factor is nearly 30%, but technological progress could still increase the recovery factor by 10-15%. This would lift the available reserves by about 530 billion barrels, or 17 years of consumption at present levels. For gas, there seems to be less scope, with an expected recovery factor of around 70% of the conventional resource base.

In Europe, the key issue is the region's heavy dependence on Russia, which accounts for around 40% of its gas imports. A competitive market develops, with harmonised regulation for crossborder trade. This framework recognises the need to unbundle the ownership of infrastructure, such as pipelines, from the rest of the value chain for competition and investment to develop. While strong regulation is likely to increase the cost of gas market development, regulatory relaxation for specific "strategic" investments is possible. Diversity of supply drives simultaneous development of LNG and pipeline supply. LNG is a price-taker as it competes for market share with long-term contract pipeline gas.

In the US, there is growing realisation that the indigenous resource base is under pressure. Even maintaining production near current levels probably requires sustained high prices; this concern is compounded by the fear that significant increases in gas imports from outside North America may increase global gas prices. NGOs voice strong opposition to the opening of federal lands. Concerns about physical security and regulatory hurdles delay the development of import infrastructure.

In Asia, China and India emerge as the new growth poles for LNG demand, and shop for the best overall value (price, infrastructure, upstream share). Iran and Qatar target Asia as the main market to unlock resources and revenues.

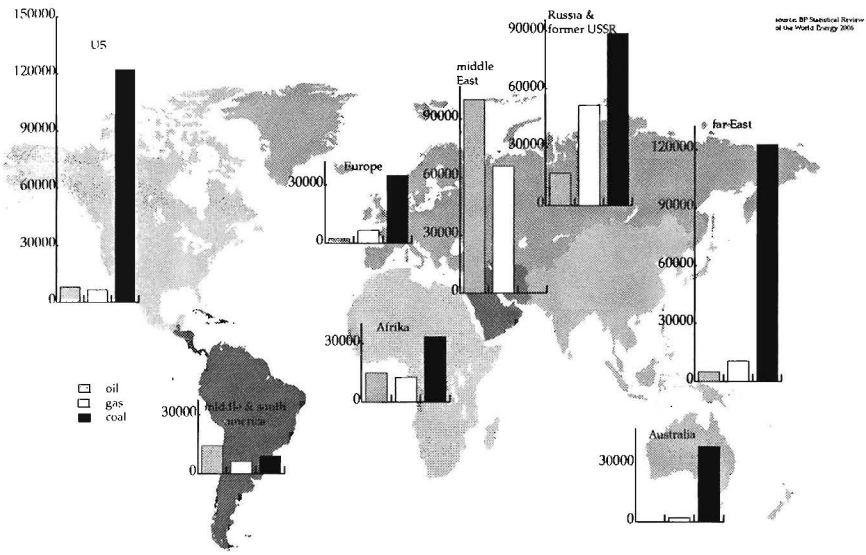

figure 2.7: proven oil gas and coal reserves in millions ton equivalent of oil

2.2.2 Resource holders perspective

Production levels by OPEC member countries will be an increasingly important variable, both for price formation and for security of supply. OPEC's announced growth aspirations to 2010 outstrip expected total market growth; indeed, in all three of our scenarios, OPEC's "market share" is set to increase. The growing domestic consumption of energy by OPEC countries and the paths they follow to development are increasingly important considerations. Most OPEC countries remain dependent on oil revenues and many face rapid demographic growth. Their energy consumption is bound to rise steeply, and they will need increasingly higher oil prices to balance their national budgets and to keep their social expenditure per capita at least constant. Insufficiently diversified economies, such as those of the Middle East and Russia, often have a preference for many years of stable revenues over short-term oil production and revenue maximisation.

Alternatively, countries may produce more and ring-fence a part of their revenues in a fund for future generations, as Kuwait and Norway have done. The trends we have described suggest that, if they remain cohesive in the low-growth scenario, OPEC members can defend a floor-price for their oil. By contrast, maintaining a ceiling-price in periods of high demand will be more elusive, especially if spare capacity will be expanded only in ways that make commercial sense for the individual cartel member. Indeed, 2004-2005 events challenge the traditional assumption that OPEC will be able to balance the world's oil markets over the longer term without major price increases. The steep rise in reserves declared by all OPEC countries in the early 1980s, and the few revisions since then, suggest that oil production has been replaced by new reserves although there is little discussion of these matters. Political considerations, resulting in opposition to investment by foreign companies, may alter the pace of exploration and production from country to country. Altogether, a new balance must be found between the producer ("resource-holder") countries' perspective in which economic diversification and job creation matter immensely, and the need for higher levels of investment -including international investment -at a time when the IEA is beginning to worry that the world is falling behind in this respect.

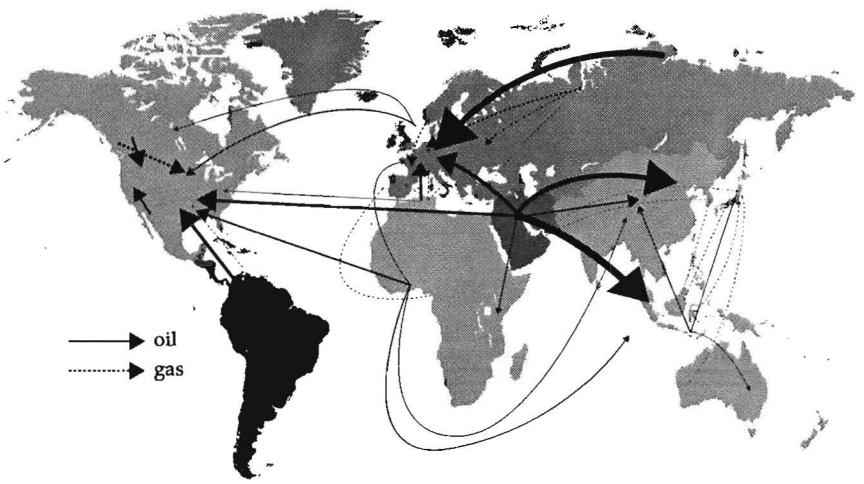

figure 2.8: major export routes for oil and gas

2.2.3 Coal, renewables and nuclear

Coal dominates and maintains its share of the global power market. For China, this alleviates energy security concerns while also raising major logistical problems -coal already represents 60% of Chinese rail freight traffic. New clean technologies (e.g. Integrated Gasification Combined Cycle (IGCC) and CO2 sequestration) enhance its use in the power sector, while Coal-to-Liquids (CTL) technology does so in the transport sector.

Renewables and indigenous energy sources are stimulated by government policy, particularly in Europe. Renewables grow by more than 10% per annum and gradually achieve close to 5% market share by 2025. Wind is the fastest growing non-hydro renewable, followed by solar. Solar photovoltaic (PV) rapidly develops, at a rate of almost four times that of solar thermal, as PV provides extensive distributed and centralised power generation solutions. Ocean energy, predominantly from waves and tidal flows, sees increased installed capacity over this period.

Nuclear energy faces public opposition in Europe and North America, but the example of China and the concerns about the impact of coal lead to a gradual reassessment. The next generations of power plants may therefore achieve the levels of support needed for politicians to take the risk of launching new construction programmes in a number of European countries and in the US.

2.3 Emissions

While political stances remain widely divergent, a quick look at reports by leading insurers and re-insurers1 shows clearly that climate change has become a significant risk on the balance sheet of companies.

Compared with a pre-industrial level of around 280 ppm, CO2 concentration in the atmosphere is now at 380 ppm. After years of intense controversy, it is generally accepted that this reflects largely the impact of human activities and that this "anthropogenic" change has been a key driver in the rise of average temperatures in recent decades. It is also accepted that levels in the range of 700-1000 ppm would lead to very damaging impacts, possibly calling for the relocation of millions of people, as described notably in scenarios developed by the Intergovernmental Panel on Climate Change (IPCC). A level of 500-550 ppm is expected to help avoid the worst calamities.2 Containing the increase in CO2 concentration within 500-550 ppm will require considerable effort: according to the most recent IPCC assessment, such a level could already be reached by 2050 with further increases throughout the 21st century unless precautionary action is taken.

Such action should be considered a matter of some urgency, in light of recent changes in our understanding of climate history. The earth's natural cycles -highly predictable variations in sunlight due to three types of orbital movement -are well researched and are often invoked as alternative explanations for any warming trend beyond short-term oscillation. However, far from providing alternative explanations of the present, they have had the effect of cooling the earth and have offset man-induced global warming. Indeed, ice cores in Antarctica show that CO2 oscillated during a long sequence of ice ages and interglacial periods between 240 and 275 ppm. Anthropogenic warming is more than likely to have begun as early as 6000 years ago, as a result of changes in land use resulting from neolithic agricultural revolution and, later, flooding in large areas for rice cultivation in China and India.

Carbon emissions can be reduced through qualitatively different changes. Key options are to:

1. Impose efficiency gains, to reduce demand growth

2. Consider alternatives that are cleaner

3. Add "tailpipe solutions" such as sequestration, which solve the problem after the event, quite often at high cost.

Examples of all three options are reviewed in the following chapters. Different combinations of such policies can be expected to prevail in different regions, with the US more inclined to support technology based solutions and the EU favouring a precautionary approach, through taxes and standards.

The Kyoto Protocol, ratified by 127 countries representing 55% of total CO2 emissions in 1990, came into force on February 16, 2005. Its essential feature is the combination of a discretionary political and administrative decision -to cap carbon emissions- with a set of market mechanisms (trading schemes) in order to achieve that political objective in a cost-effective manner. In addition, the Kyoto process is open-ended: progress achieved in one period is expected to drive more ambitious objectives in terms of emission capping and in terms of the range of participating countries. How this happens in Kyoto can be compared, if not to the EU integration process, at least to the process of global trade liberalisation. Under the first commitment period from 2008 to 2012, industrialised countries are the only ones to face binding targets regarding the emission of the main greenhouse gases (GHGs), including CO2. These targets reflect underlying national differences in emissions, wealth and capacity. They now apply to all developed countries, except Australia (which vowed to stick to the agreed targets) and the US.

The US exception matters immensely, as the country accounted for 36of GHG emissions in 1990, against 30% for the EU, 17% for Russia and 9% for Japan. Yet, while the US is likely to stay out of the Protocol, states such as New York and California are coming up with schemes of their own. Efforts to reduce other pollutants -notably in power generation -may also provide other channels through which Kyoto-like cap-and-trade schemes could materialise in the US. Kyoto signatories can resort to four policy options that encourage a broader view of ecosystem management and that give an essential role to market pricing mechanisms through "cap-and-trade" instruments:

- First, remembering that about 20% of present carbon emissions are due to deforestation, countries are allowed to subtract from their industrial carbon emissions certain increases in carbon sequestered in "sinks" such as forests.

- Second, the Protocol recognises emissions trading, which allows countries to buy allowances from other countries that reduce their emissions beyond their commitment.

- Third, under the Joint Implementation scheme, an investor from a country with a commitment may obtain carbon credits from the implementation of a project in another country member of the Protocol.

- Fourth, while the Clean Development Mechanism (CDM) is also project related, it involves countries that have not adoptedcommitments, thereby potentially expanding the ways in which credits can be claimed. The "pricing-in" of carbon in the economy 2005 may well be remembered as the year when what is known as "the energy industry" became "the energy-and-carbon industry".

While a genuine "hydrogen economy" may take decades to materialise -if it ever does- economists can make the case that we have already moved from the age of hydrocarbons to that of hydrogen and carbon, as both commodities now carry a price tag. Atoms of carbon are convenient "vehicles" to deliver hydrogen into the world's billions of combustion chambers. Until Kyoto, what happened to the atoms of carbon was of concern to ecologists but not to economists. This is no longer the case. The price discovery mechanism behind the carbon emissions schemes -notably the European Emissions Trading Scheme (EU ETS) - has been patterned after similar markets for nitrogen oxide and sulphur oxide set up in the US to achieve efficient pollution abatement. As a result of the EU ETS, a whole new set of markets can be expected to develop to help companies, investors and speculators to unbundle the rights and

liabilities attached to the carbon part of hydrocarbons from those attached to the hydrogen part. These markets can develop before engineers have put in place the capacities and systems needed to manage carbon separately from hydrogen, e.g. through various forms of sequestration and processing. In this sense, the economy is ahead of the energy infrastructure.

There are many paths to a lower carbon world but they all require step-change evolutions. A further shift to natural gas, nuclear energy, renewables and bio products will all need to be a critical part of a comprehensive approach to keep CO2 concentrations below 550 ppm; so will carbon capture and storage, and advanced vehicle technologies. Taking into account existing commitments for the Kyoto period and assuming a carbon price of euro 13.5/tonne CO2 the European Commission has simulated a carbon-abatement case in which a 21% reduction in world CO2 emissions compared to the reference case comes from both reduction in energy demand and decrease in the carbon intensity of the energy mix. The biggest loser is projected to be coal, followed by oil. Natural gas, by contrast, is not affected as the downward pressure on gas consumption is compensated by coal-to-gas substitutions. The market shares lost by coal and oil are taken up by nuclear and renewable energies. Within the renewables category, the Commission's model foresees a 20-fold increase in wind, solar and small hydro. Clearly, different paths to a lower carbon world are possible; an alternative one has been outlined, for example, by the World Business Council for Sustainable Development (WBCSD). All forecasts have in common, however, a decline in the income elasticity of energy demand and rapid development of nuclear and renewables.

As a worst case let us look at the scenario that the Kyoto Protocol unravels as one country after another follows the US lead and bails out. Without any sense of reciprocity, governments go their own way on the issue of climate change. While the EU tries to put on a brave front and insists that controls on GHG emissions will be implemented across its 30-country zone, "free-riding" by other nations soon makes this policy untenable. A number of countries, for instance, will accept payments for carbon credits while not really pursuing environmentally sound policies. With its competitiveness eroding in the face of products coming into the global marketplace from other jurisdictions where companies bear no climate-change-related regulatory costs, Brussels eventually abandons its GHG control programme. Those parties who have not signed up to the Protocol may nevertheless promote higher efficiency in the use of hydrocarbon fuels as part of their energy security and environmental agendas. Societal pressure will in fact lead states, such as China, to stimulate cleaner technologies to address the impact of burning coal or of vehicle emissions. Reductions in GHG emissions, however, are largely incidental to these local pressures. A lower-

carbon economy develops therefore, reflecting not so much the consumer's choice but rather lower global economic growth, national aspirations to self-sufficiency as well as concerns over local pollution.

2.4 Short term forecast

In the case of a fast increasing shortage of oil, it is most likely that synthetic production of fuels from coal will fill the gap. The mondial coal reserves are enormous and there is ample experience with the technology both for coal and biomass combustion through the Fischer-Trops process, like being used in the Buggenum power plant. This solution is much appreciated in China with their large coal reserves. Gas to liquids solutions (GTL) can provide liquid fuels from natural gas, as Shell is doing in their Bintulu plant (Malaysia), but in general this option is less attractive as a the gas demand is expected to rise even faster than the oil demand in the coming years and also the gas supplies are limited. Gas heaters and power plants are attractive as they are cheap and quick to build. Furthermore the gas reserves are mainly found in combination with oil, about 80 % of the gas is supplied by seven countries so they can form a monopoly like OPEC. Coal is found in a much larger geographical area.

If sufficient oil supply continuous for a little while, the Hydrogen economy can be prepared. Technology (fuel cells) have to improve quite lot however to make a hydrogen economy possible, not to speak of the distribution yet to be developed. Large scale production of bio-fuels is not likely, considering the amount of conventional fuels needed to sustain production and the competition with food production. The EU only stimulates Bio-fuel production as just a little less CO2 is produced, the main reason being that the current agricultural system can be maintained. The main problem is however: who is to be concerned about global warming when confronted with a sudden shortage of oil ?

It depends on technology and price developments if the large tar fields in Venezuela and Canada will be developed or that a straight change to natural gas will occur. Large scale use of coal can be expected in all cases. Public opposition to nuclear energy may lessen as no recent calamities have occurred and in that case nuclear power will increase fast. Uranium however can never provide the definitive solution as it is only suited for the production of electricity. That many countries are concerned to a large extend with global warming while looking for other energy sources is unlikely. Emerging economies will use the argument that the present high CO2 levels are the consequence of unlimited emissions for 150 years by the western industrialised countries.

3 Laminar counterflow recuperator

The laminar counterflow recuperator represents the case where during scientific research a new heat exchanger concept was developed. The opening to succesful application in a different market was present as the operations of the inventor were not restricted to a singular market as might have been the case for a large company. Although the original aim was to license the invention, market circumstances forced the inventor to pursue the development until the manufacturing stage.

3.1 Thermionic energy conversion

The laminar counterflow heat exchanger is an offspin of the research on thermionic energy conversion by the TU/e and LEVEL energy technology b.v.. A Thermionic Energy Converter (TEC) is essentially a diode; the basic components of a TEC are shown in figure 3.1. One of the electrodes, the emitter, is supplied with heat of high temperature (1500 - 2000 K). Electrons are evaporated thermionically into the evacuated, or rarefied-vapour filled interelectrode space. The other electrode, the collector (800 - 1000 K), is kept at a lower temperature and the electrons condense on it. Part of the heat, that is removed from the emitter by evaporating the electrons, is transported to the collector by the electrons. The remaining part is converted into electrical energy.

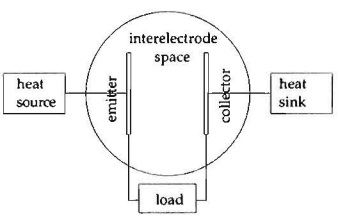

figure 3.1: diagram of a thermionic converter

Thermodynamically the thermionic converter can be treated as any other heat en-

gine. The path from point 1 to 2 in the T-S diagram (figure 3.2) represents the heating of the electrons and ohmic losses. The electrons are emitted at a constant temperature (2-3). In a close spaced diode the electrons travel through the interelectrode space at a constant temperature (3-4). In the case that an ignited plasma is present, the electrons will experience a sharp rise and decrease in temperature. The path from point 4 to 1 represents the condensing of the electrons on the collector, where electrical energy is produced. By adding the TEC to simple combustion systems, the thermodynamic efficiency can be raised to produce both heat and electricity (cogeneration).

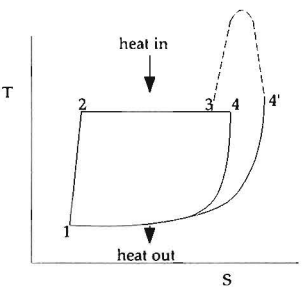

figure 3.2: TS diagram of a thermionic converter

3.1.1 Research history

The start of the study of thermionics coincides with the invention of the electrical lamp. Because Edison had troubles during his experiments with the life time of the filaments in his electrical lamp, he used more filaments in one evacuated glass enclosure. During his experiments it was observed that an electric current could be made to flow between two electrodes in vacuum (the filaments) if one of them was heated. Although the effect was of no interest to Edison and his group, the effect was duly reported (Preece 1885).

Thirty years went by before emission of electrons was analysed and investigated by Richardson (1912). Schlichter (1915) recognised that this process could be used to convert heat to electricity and a patent was issued in 1923. Though Langmuir (1923) and his co-workers formulated the fundamentals for the understanding of the process in 1923, no further interest was shown in this conversion technique for many years. In 1941 Gurtovoy published experimental data demonstrating the conversion of heat into electricity by means of a thermionic converter. In 1957 the threshold of practical thermionic conversion was reached by several groups.

One of the earliest combustion heated thermionic converters is reported by Martini (1963). This work started in 1959, but since it was aimed at military applications, information about this work is scarce. Most of the early work on small scale thermionics was carried out in the USA and France. In 1969 Shefsiek published a realistic design of a TEC, already featuring a heat pipe collector and a SiC-CVD hot shell. A survey of practical TEC's being developed is given by Wolff (1989).

The following research effort was focused on the development of space applications. In that application, the high heat reject temperature is advantageous as in space only radiant heat rejection is possible. Since the power of the radiator depends to the fourth power on the absolute temperature, the heat rejection temperature is of decisive importance.

The designs of the Thermo Electric Corporation (TECO) served as an example for the early Eindhoven University of Technology (EUT) designs. An overview of the work done by TECO is presented in an article of Goodale (1982). The converters feature a tri-layer hot shell, consisting of a graphite shell coated on the outside with SiC and on the inside with tungsten, or molybdenum. Both a bell-shaped and a cylindrical converter were constructed (figure 3.3). With the TECO converters power- and life tests were performed. Unfortunately, the TECO combustion heated converter program was stopped years ago to devote all their effort to space nuclear thermionics under president Reagan's Star Wars project.

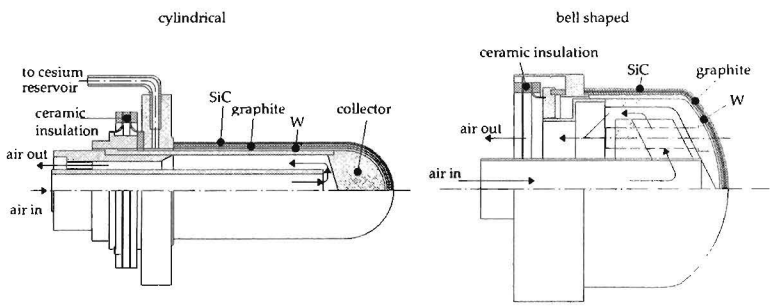

figure 3.3: cylindrical and bell-shaped thermionic converters developed by the Thermal Electric Corporation

3.1.2 research at the TU/e

Research at the Eindhoven University of Technology (EUT) was initiated in the seventies by the search at the Chemistry Department for suitable emitter materials. The

objective was to raise the performance of the TEC by materials development. A new emitter material was developed, based on a directionally solidified metal-ceramic eutectic (Wolff 1982). Beside the emitter material, the confinement which serves to protect the TEC from the combustion environment, the hot shell and the electrical insulation between emitter and collector, the ceramic seal, were studied. This study evolved in the design and construction of a water-cooled TEC (figure 3.4). Several problems occurred during the operation of the water-cooled TEC. After start-up, the collector head became too hot, causing explosive boiling of the cooling water. Furthermore, the sapphire spacers crushed the brittle hot shell.

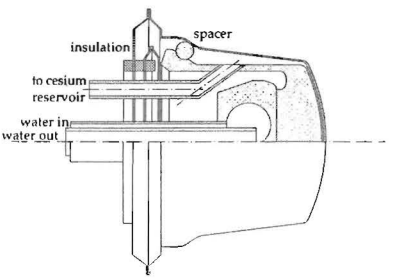

figure 3.4: water cooled TEC designed at the EUT (Gubbels 1986)

Research was taken over by the Department of Mechanical Engineering. The objective was to redesign the water cooled TEC to an air-cooled TEC (figure 3.5) with a heat pipe collector for measurement purposes (Veltkamp 1989). Air cooling has the advantage over water-cooling that the rejected heat is available at a higher temperature level, thus increasing the Carnot efficiency. Due to the lower heat capacity and consequently lower heat exchange capacity as compared to water cooling, air cooling requires a larger heat exchange area and flow rate. A geometry that allows for the necessary heat exchange area in the bell shaped collector is rather complex. A heat pipe collector eliminates this disadvantage as this passive isothermal element can amplify the heat exchange area at a more convenient location outside the TEC.

3.1.3 Thermionic cogeneration system

In thermionic cogeneration systems, the heat demand has the priority, while the electricity produced is a bonus. The heat produced by cooling the converter is not dumped as in space applications, but used to heat the house. In its simplest form the thermionic cogeneration system consists of a burner, heating the TEC which in turn heats the boiler. Such a system operates at very low efficiencies as the exhaust gases

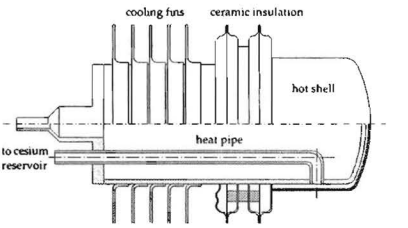

figure 3.5: air cooled TEC designed at the EUT (Veltkamp 1989)

cannot be lower in temperature than the emitter, leading to a low burner efficiency. Furthermore, it takes time to heat the TEC and therefore electricity is not immediately produced when starting the burner. Heating systems without thermal storage switch on and off frequently and consequently electricity is produced during a fraction of the operating period of the burner only. Therefore two subsystems have to be considered: a recuperator to regenerate heat from the flue gases and a thermal storage to increase the operating time of the thermionic converter.

Only a small part of the energy present in the fuel is converted to work because the temperature of the flue gases cannot be lower than the emitter temperature. By using the heat in the flue gases to preheat the air or air-fuel mixture, the efficiency can be increased. The heat can be transferred by recuperation or regeneration. A counterflow recuperator is the best solution thermodynamically, but even in that case not all the heat can be recuperated due to the difference in heat capacity between the flue gases and air. Furthermore, the fuel (natural gas) can only be preheated to about 900 K to prevent carbonisation. An example of a recuperative burner system is given by Veltkamp (1993) (figure 3.6). Air streams through a recuperator where it is heated by the flue gases. Natural gas is injected in the air stream and the mixture is burned in a vortex burner. The flue gases heat one of the headers of the recuperator which radiates to the hot shell.

One little question remained however: how do you make a recuperator able to withstand the high temperatures ? Metals are not able to withstand the extreme temperatures, so ceramic materials have to be used. The brittle ceramics are susceptible to thermoschock, so the local temperature differences in the construction have to be small. For a heat exchanger this implies that it has to have a high effectivity and that the heat capacity flows (mass flow times heat capacity) are almost equal to each other, see figure 3.7. To keep the temperature difference over the dividing walls small, they should be thin. To maintain structural integrity in a thin walled structure, the channels should be small, leading to a laminar velocity profile. Realising that this concept

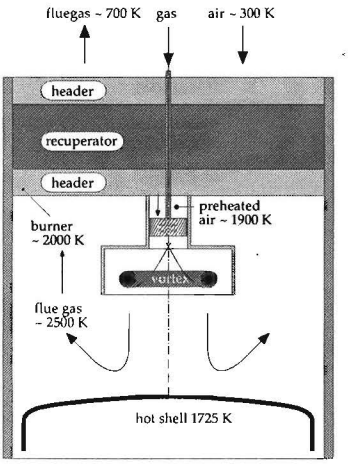

figure 3.6: burner structure with recuperator (Veltkamp 1993)

of a heat exchanger has far more potential than high temperature applications alone, Level applied for a patent in 1993. Thermionic energy conversion reserarch continued at the university for two more years, but was stopped in 1995 as the economical prospects were not favourable (van Kemenade 1995).

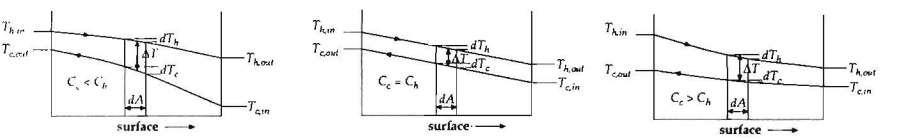

figure 3.7: temperature profiles in a counterflow heat exhanger

3.1.4 Test rig

Before continuing with the development of the heat exchanger, we have a look at the test rig for the thermionic energy converter as the technology gained during the construction has been put to good use in the further developments of both the heat exchanger and the rotational phase separator.

The hot shell of the prototype TEC (fig 3.8) was made by first deepdrawing the molybdenum shell and subsequently coating it with a layer of TiN to act as a diffusion barrier and a SiC layer. The two major points are the isostatic tension during the

drawing process and the critical bending radius. The isostatic component of the stress in the hot shell can be calculated when the initial blank radius is known. The reduc-

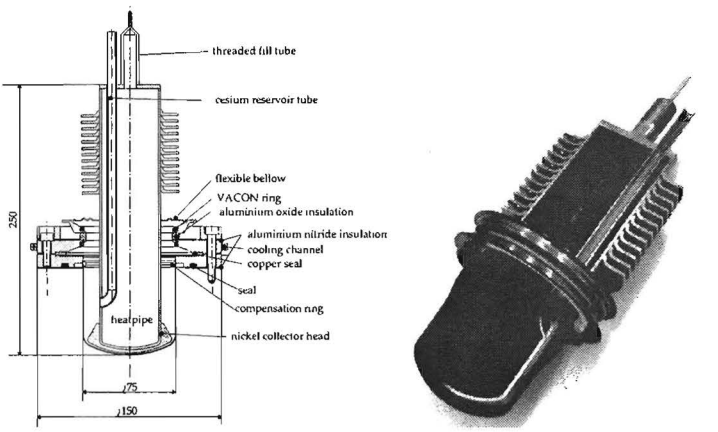

figure 3.8: prototype of the thermionic energy converter

tion in diameter compared to the prototype facilitates the construction of the ceramic seal because the stresses due to the difference in expansion are reduced. In the prototype the aluminium oxide ring is brazed to flexible bellows to allow for adjustments in the interelectrode distance, which is not necessary in a thermionic converter meant for production. The functions of the ceramic seal are to connect the hot shell vacuum tight to the collector, to isolate the hot shell from the collector and to keep the required electrode distance. The most simple solution is to braze the aluminium oxide ring directly to the hot shell and a rigid ring connected with the heat pipe. Another point of attention while constructing the ceramic seal is the brazing of the hot shell. SiC is not wetted by copper based brazing materials and consequently oxygen can diffuse to the molybdenum, causing it to oxidise. Silver based brazing materials cannot be used as they are not cesium resistant. The solution to this problem was sought in decoupling the functions of making a vacuum tight connection and preventing the oxygen from diffusing to the molybdenum. First the molybdenum is brazed to the VACON using a copper brazing material and subsequently a layer of silver based brazing material is added on the outside.

The evaporator area of the heat pipe is already heated close to the working temperature during the first minutes after switching on. Though the heat pipe is not started in this period, the collector temperature is high enough to sustain the thermionic process. The faster the collector temperature is at the working level, the better. The

speed at which the collector heats up is mainly governed by the heat capacity of the evaporator head and hence it is useful to construct the heat pipe as thin as possible based on the pressures in the system. The heat pipe can be made of a standard stainless steel tube welded to a formed evaporation head.

Although it was the aim of the project to design a combustion heated thermionic converter, it was decided to test the TEC electrically heated in a vacuum atmosphere (figure 3.9). The main reason for doing this was that in earlier experiments the hot shell often failed. The measurements were frustrated by the fact that the hot shell could not be replaced quickly as the coating process of the hot shell is costly and time consuming for single products. By testing the TEC in a vacuum environment it is not necessary to coat the hot shell and the molybdenum shell can be made in-house if the need arises. The vessel features double stainless steel walls which are water

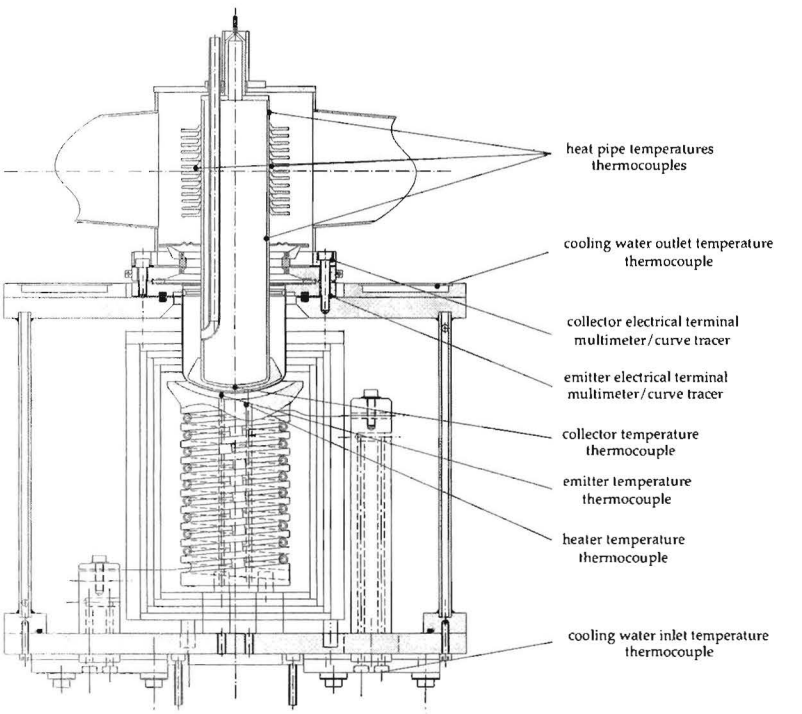

figure 3.9: Experimental set-up

cooled. The TEC is mounted at the top side of the vessel. The heating element is made of graphite with a SiC coating to prevent degassing under operating conditions.

Provisions are made to install thermocouples. The top side of the heating element follows the curvature of the hot shell to achieve a controlled radiative heat transfer. The heating element itself is in turn heated by radiation from a molybdenum wire, isolated by ceramic aluminium oxide rings. The heating wire is connected to copper electrical terminals which are coated with nickel and cooled by water. The heating element is surrounded by five molybdenum radiation shields to reduce heat losses to the walls. Furthermore, the vessel is equipped with a sapphire window to allow optical measurements. The cooling elements are connected in series to allow for an easy measurement of the heat removed by the cooling system. To ascertain that there will be no electrical short through the cooling system, a closed demineralised water loop is used which is cooled through a heat exchanger.

3.2 Compact heat exchangers

The various economic sectors in which thermal equipment plays an important role are heating, refrigeration and air conditioning, electrical power generation, transportation applications (automotive, aerospace), the process industry (chemical, petrochemical, paper, glass, cryogenic). More generally, it concerns the industrial sectors associated with the rational use of energy. During the 1990s, advances in development and understanding of traditional heat exchangers gave rise to new types of heat exchangers that are more compact, more economical and more efficient. While the Compact Heat Exchanger (CHE) technology has been advancing considerably over the last couple of decades, the cost, space and efficiency improvement pressures and significant interest in development of new technologies such as nanotechnology, fuel cell technology, etc. have spurred a significant interest in further development of more compact and enhanced heat exchangers thus reducing mass and volume of the exchanger in such applications. CHEs are characterized by high heat transfer areas per unit volume and per unit mass, usually achieved by construction techniques that result in a large number of small channels, now advancing to mini and microchannels with significant improvement in heat transfer surface area density (meso heat exchangers 3000 m^2/m^3 and a hydraulic diameter D_h= 1 mm; micro heat exchangers 15,000 m^2/m^3 and D_h= 100 mm). The resistance to introducing these technologies in industry is driven by concerns about fouling and cleanability, ruggedness, safety (especially in high temperature, high pressure applications), and designability. However, continuing advances at both the fundamental and equipment-development levels and a growing database of successful plant experiences have demonstrated that significant capital and operating cost savings can be achieved by the reasoned appli-

cation of CHEs, ultra-CHEs and enhanced heat exchangers.

3.3 Design considerations

The heat transferred in a heat exchanger can be found by integrating the following euqation over the length of the heat exchanger:

$$dQ = UdA_w\Delta T \tag{3.1}$$

where Q denotes the heat flux and U the overall heat transfer coefficient. Equation 3.1 can be integrated assuming that physical properties are constant, the heat transfer coefficient is constant over the length of the heat exchanger, no changes in kinetic energy, no heat losses to the environment:

$$dQ = -\dot{m}_h c_{p,h} dT_w = \pm\dot{m}_c c_{p,c} dT_k = UdA_w(T_h - T_c) \tag{3.2}$$

where T_h is the temperature of the hot medium, T_c of the cold medium, k the overall heat transfer coefficient, A_w the heat exchanging surface and c_p the heat capacity. The plus sign in the second term holds for the co-current flow case, the minus sign for counter flow. The combination $\dot{m}c_p$ is often denoted as the heat capacity flow with symbol C. Voor each cross section of the heat exchanger holds that

$$-C_h(T_h - T_{h,in}) = C_c(T_h - T_{c,in}) \tag{3.3}$$

or

$$T_h - T_c = -\left(1 + \frac{C_c}{C_w}\right) T_c + \frac{C_c}{C_w} T_{c,in} + T_{h,in} \tag{3.4}$$

Substitution of 3.4 in 3.2 for co-current flow yields

$$\frac{dT_c}{-\left(1 + \frac{C_c}{C_w}\right) T_c + \frac{C_c}{C_w})T_{c,in} + T_{h,in}} = \frac{UdA}{C_c} \tag{3.5}$$

Integration of equation 3.5 over the length of the heat exchanger leads to

$$\ln\left[\frac{\left(1 + \frac{C_c}{C_w}\right)(T_{c,in} - T_{c,out})}{T_{h,in} - T_{c,in}}\right] = -\left(\frac{1}{C_c} + \frac{1}{C_h}\right) UA \tag{3.6}$$

In general the effectivity of a heat exchanger is defined as the heat transferred defined by the maximum amount of heat that can be transferred:

$$\epsilon = \frac{C_c(T_{c,out} - T_{c,in})}{C_{min}(T_{h,in} - T_{c,in})} = \frac{C_h(T_{h,in} - T_{h,out})}{C_{min}(T_{h,in} - T_{c,in})} \tag{3.7}$$

Substitution of equation (3.7) in (3.6)'leads to

$$\ln\left(1-\epsilon\left(\frac{C_{min}}{C_h}+\frac{C_{min}}{C_c}\right)\right)=-\left(\frac{1}{C_h}+\frac{1}{C_k}\right)UA_w \tag{3.8}$$

so that we can write

$$\epsilon=\frac{1-\exp\left(-\left[1+\frac{C_{min}}{C_{max}}\right]\frac{UA_w}{C_{min}}\right)}{1+C_{min}/C_{max}} \tag{3.9}$$

A similar exercise gives for the counter current case

$$\epsilon=\frac{1-\exp\left(\left[1-\frac{C_{min}}{C_{max}}\right]\frac{-UA_w}{C_{min}}\right)}{1-\frac{C_{min}}{C_{max}}\exp\left(-\left[1+\frac{C_{min}}{C_{max}}\right]\frac{UA_w}{C_{min}}\right)} \tag{3.10}$$

The consequences of these equations are illustrated in figure 3.10 , if the heat exchanger is unbalanced (a large difference between both capacity flows) the configuration of the heat exchanger does not really matter, it is only the heat exchanging area that counts. For balanced heat exchangers however the difference between co- and counter flow can be up to a factor 2.

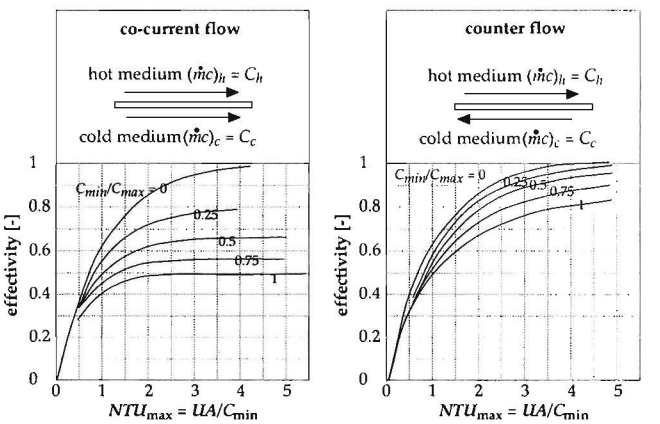

figure 3.10: effectivity as a function of the number of transfer units for co- and counter flow (Kreith 1986)

3.3.1 Thermodynamic analysis

The notion that a heat exchanger consisting of small channels with laminar flow can have a good thermodynamic performance came from a second law analysis following

Bejan(1988). In the case of a balanced heat exchanger, where the capacity flows (mass flow times heat capacity) of both flows are equal, the effectiveness can be expressed as

$$\epsilon = \frac{T_{h,in} - T_{h,out}}{T_{h,in} - T_{c,in}} = \frac{T_{c,out} - T_{c,in}}{T_{h,in} - T_{c,in}} = \frac{kA_w/C}{1 - kA_w/C} \tag{3.11}$$

For ideal gasses the entropy generation can be derived as

$$N_s = \frac{\dot{S}_{gen}}{C} = \ln\left(\frac{T_{h,out}}{T_{h,in}}\right) + \ln\left(\frac{T_{c,out}}{T_{c,in}}\right) - \frac{R}{c_p}\ln\left(\frac{p_{h,out}}{p_{h,in}}\right) - \frac{R}{c_p}\ln\left(\frac{p_{c,out}}{p_{c,in}}\right) \tag{3.12}$$

For heat exchangers with a high efficiency ($(1-\epsilon) \ll 1$) equation(3.12) simplifies to

$$N_s = \frac{\dot{S}_{gen}}{C} = (1-\epsilon)\frac{(T_{h,in} - T_{c,in})^2}{T_{h,in}T_{c,in}} + \frac{R}{c_p}\left[\left(\frac{\Delta p}{p}\right)_h + \left(\frac{\Delta p}{p}\right)_c\right] \tag{3.13}$$

The first right hand term of equation (3.13)is the entropy generation due to heat transfer and the second the entropy generation due to the pressure drop. Proposed design variations have an opposite effect on both contributions and an optimal trade off exists, see Bejan (2001) for examples. As can be seen in figure 3.11 the minimal entropy generation is proportional to the bulk velocity g. The dependance on Reynolds is relatively weak, so it can be stated that entropy generation is governed by the bulk velocity if the channel dimensions are optimised for minimum entropy generation.

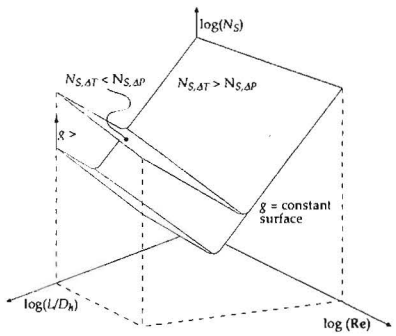

figure 3.11: entropy generation as a function of Reynolds, channel dimensions and bulk velocity

Entropy generation due to friction does not depend on the direction of the flow if we assume constant physical properties. A comparison between the flow configurations can therefore be made by looking at the first term of equation (3.13) only. Figure

3.12 is constructed for a balanced situation, comparing some flow geometries. Nothing is happening for a heat exchanging surface of zero and consequently the entropy production is zero. As soon as there is any heat exchange, the entropy production goes up quickly. For a heat exchanger with an effectivity of 1 the temperature difference before and after the heat exchanger remains the same: the outlet temperature of the hot side equals the inlet temperature of the cold side and the other way around. In that case the entropy generation is zero. co-current flow has the maximum energy production (full mixing) and the other configurations are somewhere in between. The important lesson of figure 3.12 is that the flow configuration only becomes important for NTU numbers larger than 2. To illustrate the influence of the un balance, we look

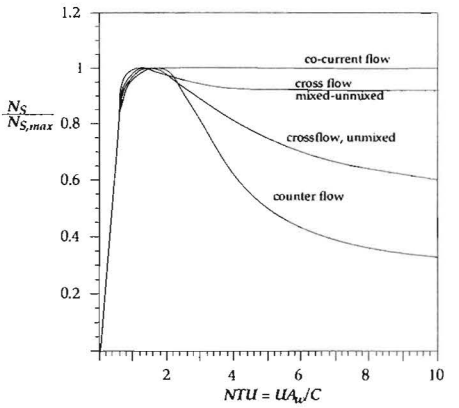

figure 3.12: entropy generation for several flow configurations as a function of the number of transfer units

at an otherwise perfect heat exchanger: $\Delta p = 0$ and $UA_w/C = \infty$. The unbalance ω between both sides of the heat exchanger is defined as $\omega = C_1/C_2, \omega > 1$.The effectivity of the heat exchanger can be written as

$$\epsilon = \frac{1 - \exp\left(\left[1 - \omega^{-1}\right] \frac{-UA_w}{C_{min}}\right)}{1 - \omega^{-1} \exp\left(-\left[1 + \omega^{-1}\right] \frac{UA_w}{C_{min}}\right)} \tag{3.14}$$

if C_2 is the minimum capacity flow. In that case the entropy generation is

$$N_s = \frac{\dot{S}_{gen}}{\dot{m}c_p} = \ln\left(\left(\frac{T_2}{T_1}\right)^{\omega}\left[1 + \left(\frac{T_2}{T_1} - 1\right)\frac{\omega}{1+\omega}\right]^{1+\omega}\right) \tag{3.15}$$

In figure 3.13 this relation is plotted for $T_1/T_2 = 2$. Maximum entropy generation is reached if one of the media does not change in temperature, which is the case

when a phase change occurs in one of the media. The second main conclusion is that although entropy generation in a co current heat exchanger compared to a counter flow heat exchanger, the relative importance is minor when the unbalance ω is larger than 5.

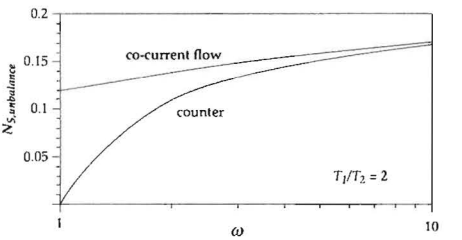

figure 3.13: entropy generation due to unbalance in the capacity flows

The conclusions of the thermodynamic analysis are summarised in figure 3.14. In most cases the unbalance in a given application is given and can not be changed. Entropy generation can not be reduced by the construction of the heat exchanger. If there is a large unbalance ($\omega > 5$) go for the easiest construction. Look at the efficiency needed for the application to assess the minimum NTU number needed for the application. If this value is below 2, optimisation of the heat exchanger is a wasted effort. In other cases an optimisation can be performed for minimum entropy generation by friction and by heat transfer. Using a larger heat exchanger always gives a lower entropy generation, but the reason is that we have neglected the entropy generation associated with the use of material. In practical situations an economic criterion can be used to find the optimum values.

In Veltkamp(1993) several options for the shape of the heat exchanger channels are described. All ducts are surrounded by ducts containing the second medium, so all the wall area is also heat transferring surface (figure 3.15). Headers are integrated to the ducts to provide a means to distribute the media over the ducts and collect them after passing through the ducts. The resulting structure is a counterflow heat exchanger in between two halves of a cross flow heat exchanger. The effectiveness of this heat exchanger is in between cross- and counterflow for a low number of transfer units ($NTU = kA_w/C$) and close to a counterflow heatexchanger for large values of NTU(figure 3.16).

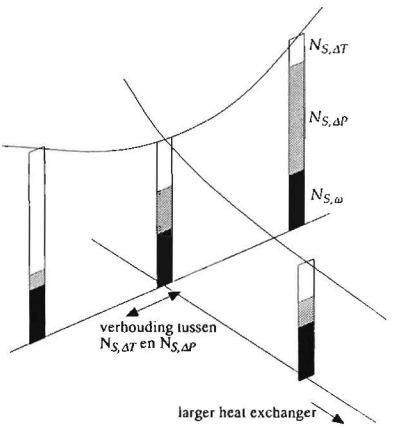

figure 3.14: summary of entropy generation in a heat exchanger

3.3.2 Test rig

One of the more challenging tasks during the development of the recuperator was the experimental verification of the used design tools. The intended production method for the heat exchanger plates was by forming, but fabricating dies was far too expensive for a prototype. The first heat exchanger was therefore manufactured by stereolithography, a process that uses a CAD model to guide a laser through a polymer solution. The laser hardens the solution within the boundary of the part, one thin layer at a time, to produce a real, three-dimensional mockup. Only low temperature measurements could be performed with this prototype

As the effectivity comes near the maximum value small deviations in the measured temperatures have a large impact on the recorded effectiveness (equation 3.11). As the effectiveness is directly related to the capacity of the heat exchanger defined by the overall heat transfer coefficient multiplied by the heat transferring surface, it is an important parameter to compare design alternatives and validate simulation tools. To illustrate what had to be done in order to measure with the required accuracy. figure 3.17 shows a schematic of the test rig build at the TU/e (van Kemenade 1999). In figure 3.18 the dependance of the necessary accuracy for the temperature and flow measurement are given. In order to determine the effectivity, the bulk temperatures of the air flow have to be measured on the locations indicated in figure 3.17. The problem to be solved is how the measure the bulk temperature which is not identical to the mean temperature in a cross section as the velocities may differ. Consequently it

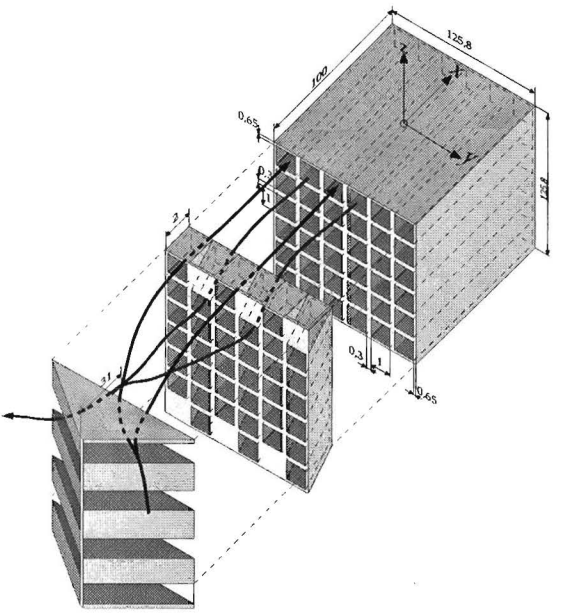

figure 3.15: heat exchanger concept

is necessary to mix the airflow thoroughly before measuring the temperature locally.

Because air hardly radiates, optical temperature sensors are not suitable in this project. As the old mercury thermometer, still being used widely for calibration purposes, shows non-electrical thermometers can be very good. Nevertheless electrical contact sensors are chosen as they allow for a relatively easy data acquisition. Having made that decision, the option for a thermocouple and a resistivity method (plain or with NTC's) remains. Thermocouples, though trusty and widely applied, have a low temperature dependence and a very low voltage output. It is very hard to get a accuracy below 1 K. Although they tend to have a large drift, NTC thermistors where used instead of PT-100 as they have a larger voltage output. NTC thermistors have a negative temperature dependence, the resistance globally varies from -3 to -6 % per Kelvin temperature rise. Most thermistors are produced as spheres or cylinders covered with a protective glass layer. Normally the thermistor are part of a wheatstone bridge, keeping either the current through- or the voltage over the thermistor constant. As a current flows through the thermistor, ohmic heating will occur, which must be accounted for. Also the thermistor has to be connected and is subject to heat

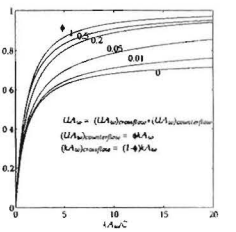

figure 3.16: effectiveness of the heat exchanger as a function of the total number of heat transfer units

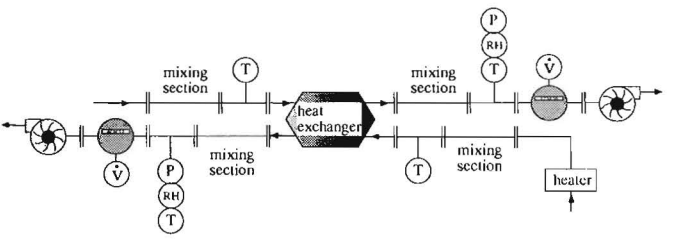

figure 3.17: schematic of the heat exchanger test rig transfer units

conduction through the wires. A third error may occur due to heat exchange with the surroundings. The air flows are thoroughly mixed in the ducts so that in principle one thermistor can be used to measure the bulk temperature. Three thermistors are applied however to be able to detect a faulty thermistor. The design of the temperature measurement units are in figure 3.19. The results are corrected according to a model incorporating the following energy flows:

- ohmic heating of the thermistor
- convection to the thermistor
- radiative heat transfer with the surroundings
- conduction through the support
- convection to the connection wires
- ohmic heating of the connection wires
- conduction through the connection wires

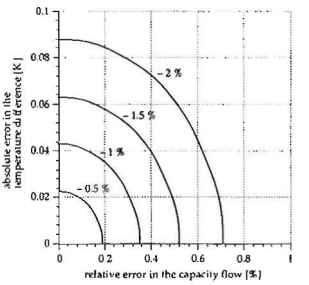

figure 3.18: dependance of the necessary accuracy temperature and flow measurement

The thermistors are mounted within radiation shields consisting of a chromium plated brass tube (15x60 mm) to reduce the radiative heat exchange. The dimensions of the radiation shield are such that a large part of the heat transfer with the surroundings are suppressed with a minimum disturbance of the convective heat transfer to the thermistor. The electrical connection of the thermistor plays a major role in the accuracy of the thermistor. As heat- and electrical conductance are closely related, there exist no materials with a high electrical- and a low thermal conduction. Thermal conduction can be reduced by applying a long thin wire but in that case the electrical resistance also rises which is undesired. Optimisation of both effects resulted in an impractical small diameter or long length of the wire. For that reason another approach is taken. A small wire (0.12 mm) is placed inside the air stream for a certain distance before it is firmly attached to the inner wall. At the inner wall it takes the wall temperature. Optimisation resulted in a wire length of 0.22 m.

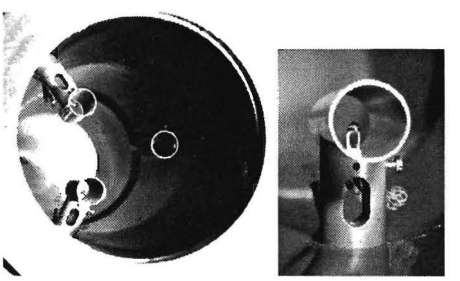

figure 3.19: temperature sensors

In the test rig, the secondary air temperature is heated to accomplish a temperature difference between the primary and secundary flow. The resulting air stream

does not have a homogeneous temperature profile however. For that reason the air stream is mixed to obtain a homogeneous (bulk) temperature. The desired mixing effectivity can be reached by applying static mixers as are manufactured by Sulzer for instance (figure 3.20). Besides the Sulzer static mixer a home made variety, designated by FT-150, was tested. The air stream is stratified by a heater comprising four separate convectors which can be regulated separately. To make sure that a stratified flow develops, a flow straightener is placed behind the heater. The temperature distribution is measured before and after the mixing section with a Cross containing 13 T-type thermocouples (figure 3.21). In the mixing section several static mixers can be placed. For one static mixer the axial velocities were measured behind the static

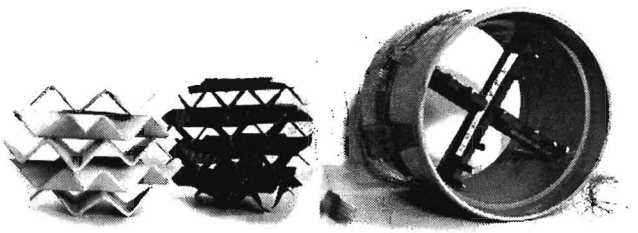

figure 3.20: Sulzer, FT-150 static mixers and temparature measurement unit

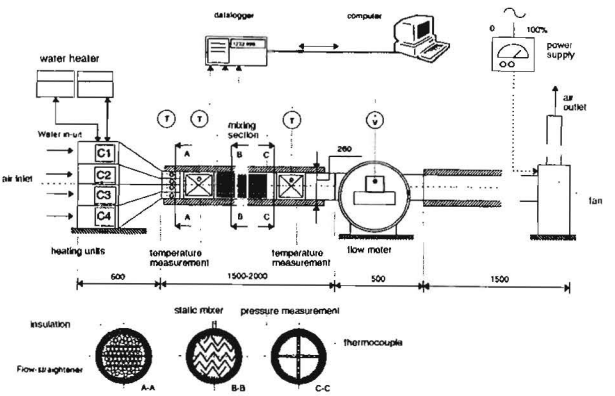

figure 3.21: test rig

mixers using a Pitot tube. Immediately after the static mixer, the profiles are chaotic as can be expected. After a settling length of one diameter (1D) the turbulent velocity

profile starts to develop and after 3D the velocity is almost constant. This distance is taken for the temperature measurements. The measured deviations in the velocity profile are used to calculate the uncertainty in the resulting bulk temperature. In the next experiment two mixers were used at several distances between each other. The Sulzer mixer is not very sensitive to variations in the initial temperature profile, the mixing effectivity is between 95 and 98 % in all cases. The FT-150 mixer is more sensitive to the inlet temperature profile. For both mixer types the best mixing effectivity is reached when the air stream is allowed to settle for 1D between the two mixers. If the distance is less, the chaotic temperature profile hinders the second mixer, if the distance is larger, stratification occurs.

The mass flow can be measured directly (hot wire, Corioli) but these principles cannot meet the demanded accuracy. Volume flow measurement can be done by positive displacement meters and techniques where in a cross section the time and position averaged velocity is measured. Positive displacement meters can reach the best accuracy. An IGA rotary displacement flow meter is used. Measurement errors are mainly due to internal leak as deviations in the counter mechanism can be calibrated.

The measurement results are depicted in figure 3.22. There is a small but persistent deviation in the calculated and measured efficiency of the heat exchanger. The reason was that although the heat exchanger was overall in balance, locally this is not necessary so. A two dimensional model assuming a fully developed laminar pro-

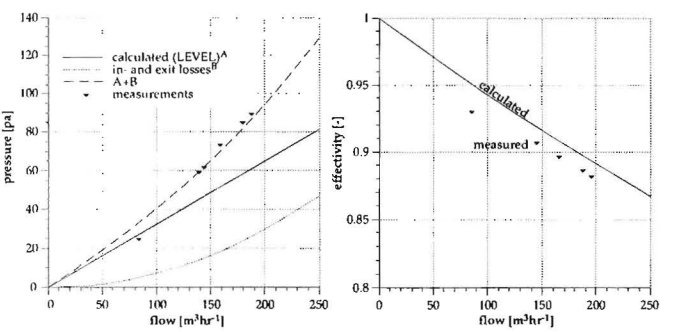

figure 3.22: effectiveness and pressure drop of the heat exchanger

file over the length of the heat exchanger, but incorporating temperature dependent physical properties was developed for further optimisation of the heat exchanger. As shown in figure 3.23 the assumption that the flow through the heat exchanger is symmetrical, made to construct figure 3.16, is reasonable for low temperature differences between the inlets of both media. For larger temperature differences (figure 3.24)the

difference in temperature between the headers causes a non-uniform inlet flow of the counterflow section leading to a local unbalance of the heat exchanger.

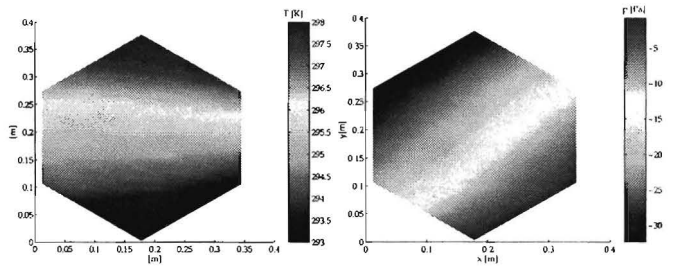

figure 3.23: temperature and pressure difference profile for one medium over the heat exchanger for a temperature difference between the media of 5 K

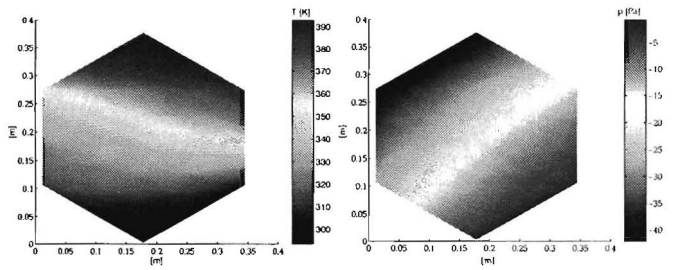

figure 3.24: temperature and pressure difference profile for one medium over the heat exchanger for a temperature difference between the media of 100 K

3.4 Prototypes

In the mean time a search report indicated that the concept of a laminar counterflow heat exchanger was new indeed and the PCT procedure was started. After a national patent was granted. it turned out that a prior Eastern German patent blocked the application for rectangular channels (one of the initial claims). Therefore the patent application had to be limited to triangular channels. Eastern Europe patents from this period were not in the databases in therefore missed in the search report. It was not a big deal as also technical and economical reasons existed to prefer triangular systems. The three basic shapes of the heat exchanger channels: plate, square and triangle (figure 3.25) differ in thermal and hydraulic performance, manufacturability

and mechanical strength. While manufacturing a heat exchanger stack of separate sheets displacements and rotations may occur that can effect the performance of the recuperator. A displacement in triangular channels does not have an effect on performance, while displacement of square channels can lead to a reduction in performance of 50 % (figure 3.26). The reduction in performance due to a rotation of the sheets can be 25% and again has no effect in the triangular case. Further considerations are

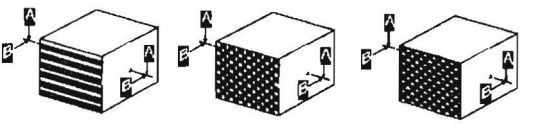

figure 3.25: basic geometries for the heat exchanger channels

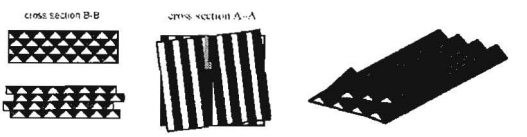

figure 3.26: displacement and rotation of the heat exchanger channels

- triangular channels can be constructed using alternating a formed and an unformed plate with a low degree of deformation so stainless steel can be used
- rectangular channels require a small tolerance and have a degree of deformation in the order of 2
- a triangular shape is stable and allows high internal pressures, plates and to a lesser extend squares do not have this advantage

The production method adopted led to a basic shape of the heat exchanger as shown in figure 3.27.

3.4.1 Recuperative burner

For application by Philips in a glass furnace a recuperative burner was developed as replacement for electrical elements in glass furnaces. Processes where a recuperative burner can be applied range from 200 to 1400 °C. Within Philips most energy is consumed in processes up to 800 °C, in this range efficient burners are required. Above

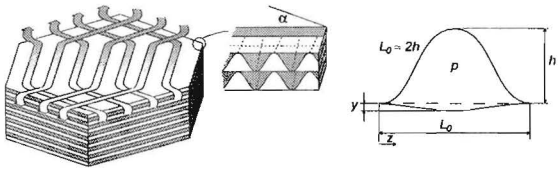

figure 3.27: heat exchanger concept and duct cross section

800 °C the options are limited: existing recuperative burners are sparsely used due to their limited control range and may lead to instabilities in the system. A survey under plant operators indicated that there is a need for modulating burners with a power output of about 20 kW, while most suppliers start at 50 kW. This is not in agreement with the trend that furnaces and heating processes are being segmented requiring more heating elements. As the potential of application in Thermionic systems was judged low, together with Winnox, Royal Schelde and the Gasunie a 20 kW recuperative burner was designed and tested.

3.4.2 Design process

To define the dimensions of the heat exchanger, a sensitivity analysis was performed under the following assumptions:

- constant physical properties
- fully developed laminar flow
- constant mass flow

The 2-D model was used afterwards to check if these assumptions hold in the extremes of the sensitivity analysis. Under these assumptions, the heat transfer coefficient can be derived analytically: $\alpha = 48\lambda/11D_h$ (i.e. Holman 1982), where λ is the heat conductivity of the fluid and D_h the hydraulic diameter of the channels. The heat transferred is inversely proportional with the diameter of the channels, in this case even quadratic as also the number of channels within a given volume increases. The limit is given by the heat resistance of the sheets itself (figure 3.28). Increasing the width or the height of the heat exchanger leads to an increase in the heat transferred (figure 3.29). For a fully developed laminar profile the pressure loss over a triangular channel is given by (i.e. Holman 1982)

$$\Delta p = \frac{48}{Re}\frac{L}{D_h}\frac{1}{2}\rho u_b^2 \tag{3.16}$$

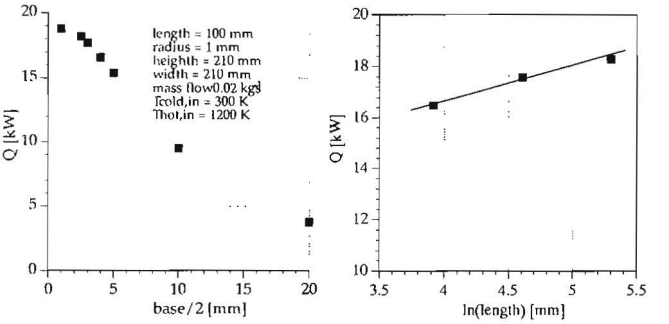

figure 3.28: heat transferred as a function of half the base(left)and the length of the channels (right)

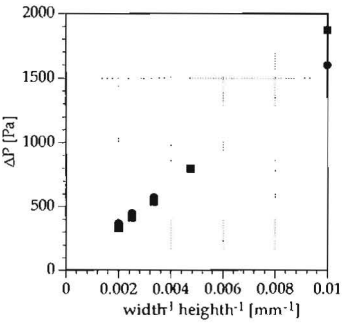

figure 3.29: heat transferred as a function of the width and the height of the recuperator

Under the assumption that the influence of the wall thickness an be neglected and a constant mass flow, the bulk velocity can be written as $u_b = \dot{m}/(2WH\rho)$, W being the width of the recuperator and H the height. Figure 3.30 shows that this approximation is only valid for large channel diameters. For small channel diameters the pressure drop increases fast due to the thickness of the walls (in these calculations 0.2 mm). On increasing the length of the recuperator the temperature profiles and consequently the physical properties will change (figure 3.31), but this influence can hardly be noticed. Figures 3.28 to 3.31 show that optimisation to maximum heat transfer for a minimal pressure drop leads to a very voluminous heat exchanger so economic and technical boundaries have to be applied. The recuperator consists of a multitude of formed sheets. The channels can be pressed one by one requiring low tooling costs but a high positioning tolerance, or a die for the complete shape can be

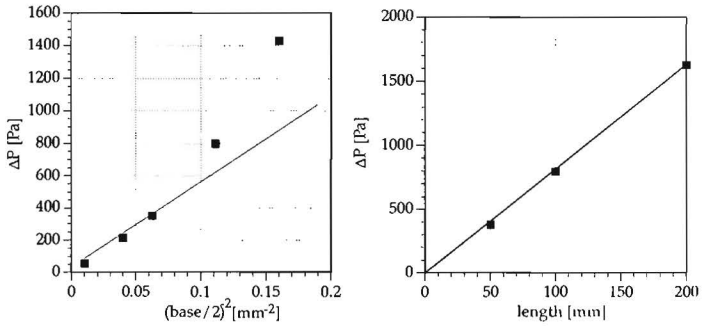

figure 3.30: pressure drop as a function of half the base(left)and the length of the channels (right)

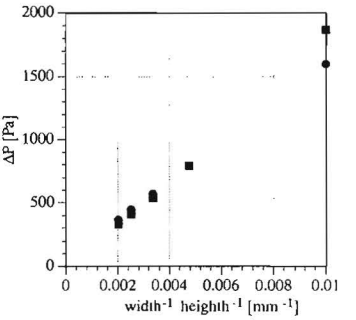

figure 3.31: pressure drop as a function of the width and the height of the recuperator

manufactured. Normally two dies are necessary to press the complicated shape in the metal, but to keep costs down only one die was made, using a rubber on the other side. For the operating conditions in a recuperative burner, the following materials were considered:

- Avesta 253MA
- Inconel 601
- Haynes 214
- Haynes 230

Based on physical and mechanical properties, costs and availability Avesta 253 MA was selected. The elastic limit of this material is 1.4 implying that the top angle of the

triangle can not exceed $\pi/2$. Furthermore plastic instabilities limit the radius of the top angle. Kals (1983) shows based on stability criteria that in most practical cases the limit is given by $R_c r/d_p = 1/n$ where d_p is the plate thickness and n the strain hardening exponent. The minimum radius is also limited by the Youngs modulus of the rubber being used. If the radius is to small the radius will not be completely formed, this effect was determined experimentally.

Another limit is imposed by the maximum pressure drop allowed over the recuperator. In the concept of the recuperative burner are several components with a considerable flow resistance: the heat exchanger, the burner and the radiative tube. All these components become smaller and cheaper if a larger pressure drop over them is allowed, the fan however becomes more expensive. Considering the requirements of the other components it was judged that a pressure drop of 1 kPa over the recuperator is reasonable.

Although it would be preferable to form the connections directly in the sheets this was to expensive for the prototype so separate sealing strips were applied, manufactured by laser cutting. The hot header provided the major pressure drop in this application and was modified so that the flow resistance over each channel is the same to assure balanced conditions in the counterflow part. The resulting design is shown in figure 3.32 and 3.33

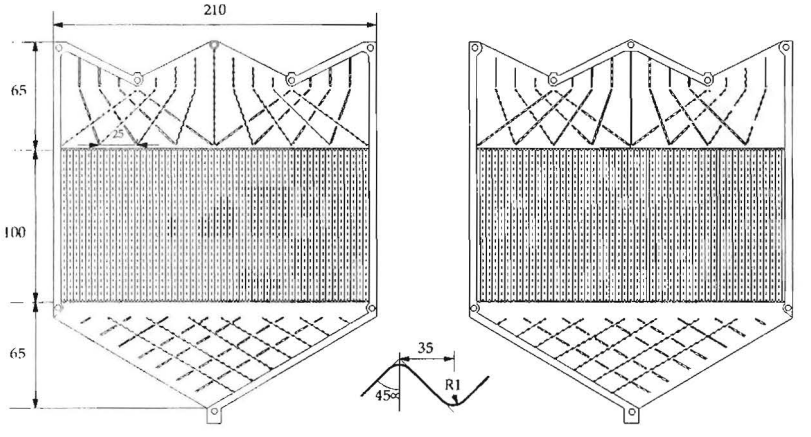

figure 3.32: heat exchanger sheets

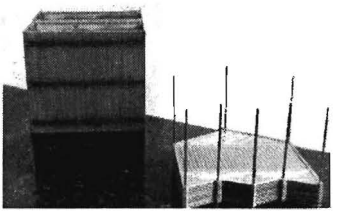

figure 3.33: heat exchanger stack

3.4.3 experiments

Before assembling the recuperative burner, the heat exchanger was tested using the same test rig as used for the plastic protoype. As the sealing strips were point welded to the sheets leakage occurred between the sheets short circuiting 15% of the air from the high to the low pressure side of the heat exchanger so a method to correct the measuring results had to be devised. The efficiency of the total system can sill be measured by looking at the energy content of the flue gasses, divided by the heating value of the gas supplied:

$$\eta_s = 1 - \frac{(\phi + 1)\dot{m}_g Cp_f(T_f, out)T_f, out + (\dot{m}_a - \phi\dot{m}_g)Cp_a(T_f, out)T_f, out}{H_g\dot{m}_g + \dot{m}_a Cp_a T_a, in + \dot{m}_g Cp_g T_g, in} \quad (3.17)$$

ϕ is the stochiometric air ratio, $\dot{m}$ the mass flow, Cp the specific heat capacity and H the heating value. The subscripts a denote air, g the supplied gas and f the flue gas. The first term in the fraction is the energy contained in the flue gasses, the second the energy contained in the air, whether it has gone through the burner or not.

The construction after assembly is shown in figure 3.34. During the first experiments (figure 3.35 and 3.36) the radiant tube was placed open in the environment. Contrary to expectations the tube temperature increases with increasing air ratio indicating that the burner is still heating up and not enough time elapsed between the measuring points. Furthermore the calculated recuperator efficiency is lower than expected, also due to time dependent effects. In the second experiment the burner tube was insulated to obtain higher temperatures of the radiant tube and it was decided to wait longer between the measurements. The consequences are shown in the figures 3.37 to 3.39. The burner was started schochiometrically at 20 kW. After 12 minutes the power was reduced to 10 kW at an air ratio of 2 to obtain a stable operating procedure. This is normal operating procedure for radiant tube burners as the excess air keeps the temperatures low and the operators went for a coffee break. This burner however was equipped with a recuperator and the temperatures continued to

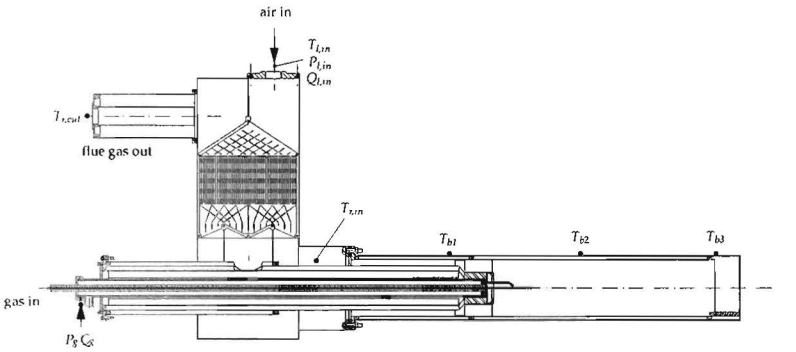

figure 3.34: recuperative burner

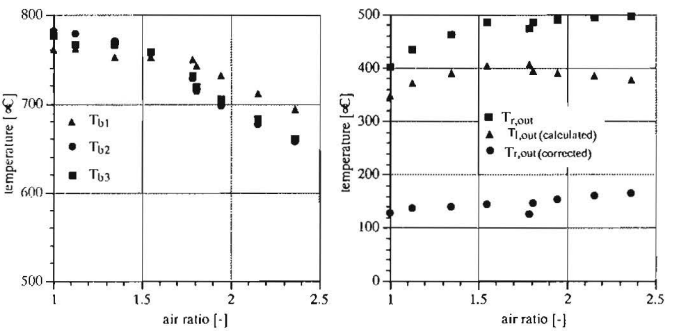

figure 3.35: temperatures of the tube (left) and the recuperator (right) during an experiment at 20 kW gas power

rise till above the melting temperature of the used heat resistant steel. After these experiments further development of the high temperature heat exchanger was put on ice, partly because of the demise of Royal Schelde and partly because developing the plastic recuperator for balanced ventilation units required all resources at LEVEL.

3.4.4 Polymer heat exchanger

The thermionic energy converter was initiated as an energy conversion option for the building environment. Soon it was realised however that a far more interesting option was to use an efficient recuperator polymer for balanced ventilation. Balanced ventilation systems, if properly designed and installed, neither pressurize nor depres-

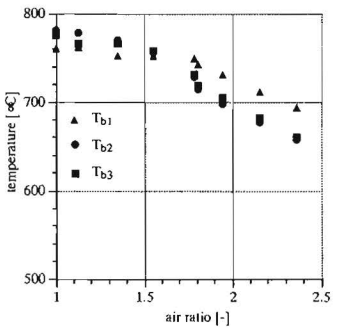

figure 3.36: system and recuperator efficiency during an experiment at 20 kW gas power

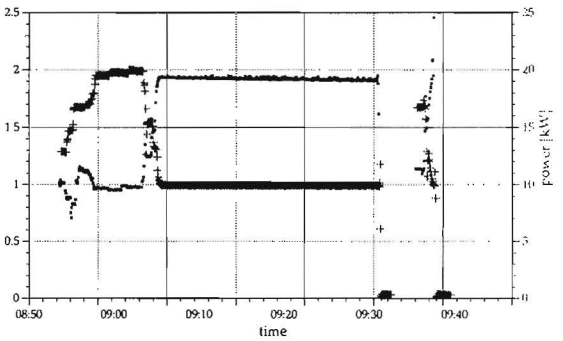

figure 3.37: air ratio and gas power during the second experiment

surize a house. Rather, they introduce and exhaust approximately equal quantities of fresh outside air and polluted inside air, respectively. A balanced ventilation system usually has two fans and two duct systems. It facilitates good distribution of fresh air by placing supply and exhaust vents in appropriate places. Fresh air supply and exhaust vents can be installed in every room. But a typical balanced ventilation system is designed to supply fresh air to bedrooms and living rooms where people spend the most time. It also exhausts air from rooms where moisture and pollutants are most often generated (kitchen, bathrooms, and perhaps the laundry room). Some designs may use a single-point exhaust. Because they directly supply outside air, balanced systems allow the use of filters to remove dust and pollen from outside air before introducing it into the house.

The efficiency of a cross flow heat exchanger is limited to 75% under balanced

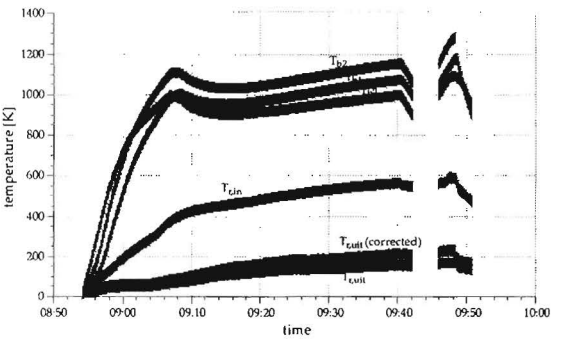

figure 3.38: temperatures during the second experiment

figure 3.39: broken radiant tube

conditions (Kreith 1986) and consequently the difference between the incoming and outgoing air could exceed 5 °C under cold outside conditions introducing an uncomfortable cold natural draught. As a result the use of balanced ventilation systems was not well penetrated and users of the system tended to switch off the system under cold conditions leading to unhealthy indoor conditions. The minimal effectivity of the heat exchanger should exceed 90%, a value easily within reach of the concept of the laminar counterflow recuperator. Furthermore the thin walls allow the use of material which are bad conductors like plastics. As both the cost and manufacturing costs of plastics are lower than metals also an economic advantage was in reach.

Also the building environment market allowed for a relatively "safe" play ground for the development of polymer heat exchangers. Their acceptance in the process industries is not yet widespread. The reasons for this are the lack of awareness of polymer compact heat exchanger benefits and the absence of reliable design methods, along with investigations under actual operating conditions. Perhaps industrial applications are limited only by the imagination of process designers, particularly as

these materials are increasingly used in pumps, valves and other plant ancillaries.

With grants from the Dutch government, the first prototype was developed. An optimisation along the same lines as in the previous paragraph was performed leading to a channel size of 1 mm and a manufacturing method developed to produce plastic sheets as shown in figure 3.40. The sheets are vacuum formed. Vacuum forming is a simplified version of thermoforming, whereby a sheet of plastic is heated to a forming temperature, stretched onto or into a single-surface mold, and held against the mold by applying vacuum between the mold surface and the sheet. Normally vacuum forming is restricted to forming plastic parts that are rather shallow in depth, but relatively deep parts can be formed if the formable sheet is mechanically or pneumatically stretched prior to bringing it in contact with the mold surface and before vacuum is applied (Throne 1999). Suitable materials for use in vacuum forming are conventionally thermoplastics, the most common and easyest being High Impact Polystyrene Sheeting (HIPS) which was used in the end. The major challenge was to keep the product tolerances low as imperfections multiply with the number of sheets. Using this technology a first heat exchanger was produced by glueing the sheets by hand, a rather boring job and the prototype was installed in the LEVEL office in summer. Under dry conditions the recuperator performed fine, but as soon as it became a little colder outside condensation started inside the heat exchanger channels and capillary blockage occurred. A moving bubble on a surface can macroscopically have two different contact angles at the both sides leading to a net force that can equal the fan pressure. Analysis showed that a base of 3 mm is sufficient to prevent capillary blockage.

3.5 Market penetration

At this point there was a concept, a patent, a working prototype and a production process giving a better and cheaper product, success assured it seemed. At first the two leading Dutch manufacturers were contacted and although the idea was well received they both went into a stalling tactic. In retrospect there is some logic to their attitude: a producer wants to produce using his existing production line for as long as possible unless competition forces him to change. Next the idea was picked up by Inatherm b.v., a trading subsidiary of Verhulst b.v. specialising in smaller air treatment units and CCM build a flexible (mechatronic) production machine. After a couple of years the production capacity of 25.000 recuperators a year was reached and a new production was developed by Wees offering less flexibility but a more robust process and a higher capacity. The old machine is now being used to start the

production of new designs and as a backup for the production machine.

For the continuity of the company Recair, which now does the production and sales of the recuperator, it is important to be able to offer new products and applications and to this end LEVEL develops new systems for new application area's like

- (automotive) adiabatic cooling
- condensors for drying processes
- green house climate control

For a small specialised engineering company as LEVEL it is necessary to innovate continuously and guard the innovations using patents. LEVEL focusses on innovations and leaves manufacturability (mainly) to others. Further development of the recuperator can be seen as evolutionary innovation. Radically innovating actions are now taken in other fields like vacuum insulation in the building environment. The experience gained with the metal high temperature heat exchanger together with the condensation phenomena is used again in the aerosol desublimator (chapter 4).

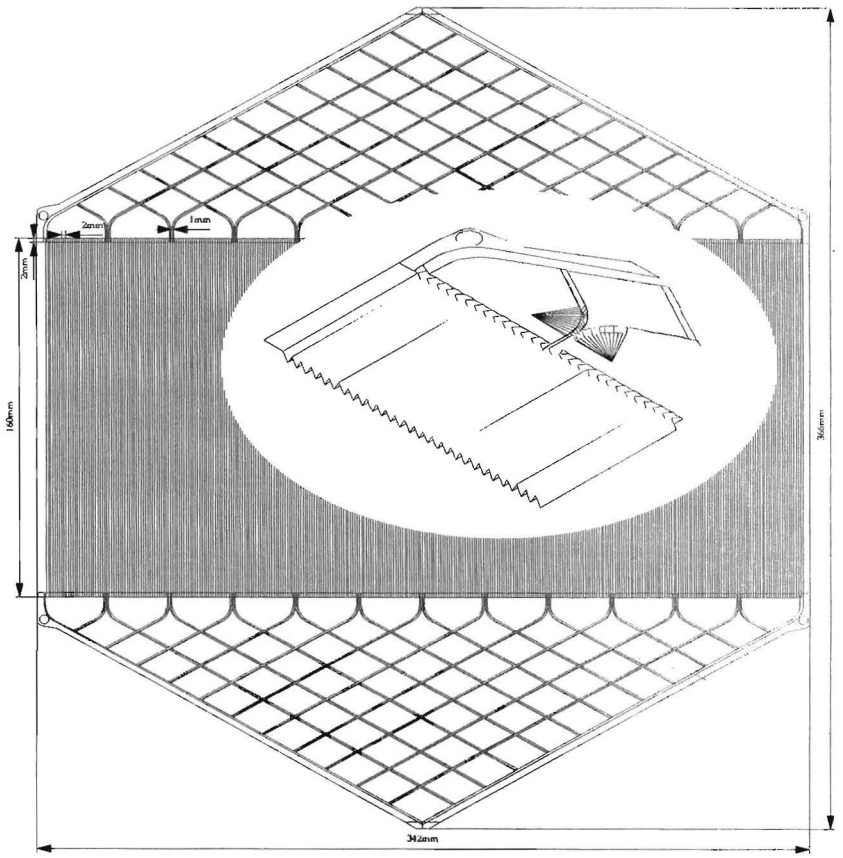

figure 3.40: plastic heat exchanger sheet

4 Rotational phase separator

4.1 Gas centrifuges

Like the laminar counterflow recuperator, the Rotational Phase Separator has its origins in nuclear energy related research. When uranium is mined, it consists of heavy-weight atoms (about 99.3% of the mass), middle-weight atoms (0.7%), and light-weight atoms (< 0.01%). These are the different isotopes of uranium, which means that while they all contain 92 protons in the atom's center (which is what makes it uranium), the heavy-weight atoms contain 146 neutrons, the middle-weight contain 143 neutrons, and the light-weight have just 142 neutrons. To refer to these isotopes, the number of protons and neutrons is added and the total is put after the name: uranium-234 or U-234, uranium-235 or U-235, and uranium-238 or U-238.

The fuel for nuclear reactors has to have a higher concentration of U-235 than exists in natural uranium ore. This is because U-235 is the key ingredient that starts a nuclear reaction and keeps it going. Normally, the amount of the U-235 isotope is enriched from 0.7% of the uranium mass to about 5

In the famous Manhattan project (that produced the atomic bomb) uranium enrichment was achieved by a diffusion process. Gaseous diffusion is still the only process being used in the United States to commercially enrich uranium although the US National Regulatory Commission is conducting licensing activities concerning two planned centrifuge facilities. Gaseous diffusion is based on the separation effect arising from molecular effusion (i.e., the flow of gas through small holes). In a vessel containing a mixture of two gases, molecules of the gas with lower molecular weight (U-235 as opposed to the heavier and more plentiful U-238) travel faster and strike the walls of the vessel more frequently, relative to their concentration, than do molecules with higher molecular weight. Assuming the walls of the vessel are semi-permeable, more of the lighter molecules flow through the wall than the heavier molecules. The gas that escapes the vessel is enriched in the lighter isotope.

Soon after WOII the possibilities of isotope separation by centrifugation was investigated in the Netherlands, especially by the laboratory for fundamental research

on matter (FOM) of prof. Dr. J. Kistemaker. Similar initiatives were taken in England and Germany resulting in a cooperation. The process uses a large number of rotating cylinders interconnected to form cascades. The UF6 gas is placed in the cylinder and rotated at a high speed. The rotation creates a strong centrifugal force that draws the heavier gas molecules (containing the U-238) toward the outside of the cylinder, while the lighter gas molecules (containing the U-235) tend to collect closer to the center. The stream that is slightly enriched in U-235 is withdrawn and fed into the next higher stage, while the slightly depleted stream is recycled back into the next lower stage. Significantly more U-235 enrichment can be obtained from a single gas centrifuge stage than from a single gaseous diffusion stage.

In the general process industry cyclones are commonly used to separate particles or bubbles from a fluid stream. Air flows in a spiral pattern, beginning at the top (wide end) of the cyclone and ending at the bottom (narrow) end before exiting the cyclone in a straight stream through the center of the cyclone and out the top. Larger particles in the rotating air stream have too much inertia to follow the tight curve of the air stream and strike the outside wall, falling then to the bottom of the cyclone where they can be removed. In a conical system, as the rotating air-flow moves towards the narrow end of the cyclone the rotational radius of the air stream is reduced, separating smaller and smaller particles from the air stream. The cyclone geometry, together with air flow rate, defines the cut point of the cyclone. This is the size of particle that will be removed from the air stream with a 50% efficiency. Particles larger than the cut point will be removed with a greater efficiency, and smaller particles with a lower efficiency. A drawback of a cyclone is that it is very hard to separate particles smaller than 10 μm (van Esch 2005).

In the rotational particle separator the priciple of a gas centrifuge, especially the rotating wall is applied to the applications of a cyclone, essentially reducing the cut diameter by one order.

4.2 Working principle

Phase separation by centrifugation in the rotational particle separator involves the application of a separation element which is cylindrical in shape and which rotates around its axial symmetry-axis: figure 4.1 (Brouwers 2002). The element consists of a large number of small channels, typically 1 mm in diameter, which are arranged in parallel to the symmetry and rotation axis. When a fluid is led through the channels, phases and particles entrained in the fluid are driven by the centrifugal force to the walls; to the outer walls if the phases or particles are heavier than the carrier fluid,

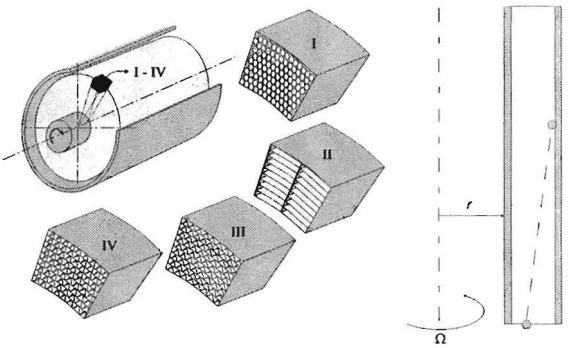

figure 4.1: left: filter element of the rotational particle separator consisting of a multitude of axial channels. Right: while the channels rotate around a common axis, particles entrained in the gas flowing through these channels are centrifuged towards the channel wall.

to the inner walls if lighter. As the radial distances over which phases and particles have to move to arrive at the collecting surfaces of each channel are small, phases and particles of small size are capable of being separated: e.g. solid and liquid particles entrained in gases with sizes of the order of 0.5 μm; hydrocarboneous phases in water with sizes of the order of 10 μm. In case of solid particles in gases the larger sized fraction of such particles will stay at the collecting surface as a result of dry or Coulomb friction apparent under the action of centrifugal forces. The smaller particles (1 μm) adhere at the wall because of Van Der Waals' forces. Under partially humid conditions surface tension causes particles to stick to the walls. It prevents separated material from re-entrainment in the gas.

Separated material collected at the walls can be removed periodically, if necessary, by blowing or flushing fluids through the channels. In case of mists or liquid phases entrained in gases or liquids, the separated material forms films along the collecting surfaces. The liquid films are squeezed out of the channels in the form of droplets being centrifuged in the chambers up- and downstream of the rotating separation element. Under typical conditions pressure drops over the channels of the separation element are limited to some hundred Pascals for gases as carrier fluid and to some thousands of Pascals for liquids as carrier fluid.

Consider a situation where a fluid rotates as a rigid body and flows axially parallel to the rotation axis in a laminar fashion. By design such a situation prevails in the channels of the separation element of the rotational particle separator. As particles

and phases are assumed to be very small in size, inertia forces acting on them are small. Particle or phase concentrations are small so that mutual interactions can be disregarded. Particles and phases follow the streamlines of the fluid except for the radial direction where as a result of centrifugal and buoyancy forces they move relative to the fluid. The radial velocity of the particle or phase follows from a balance between centrifugal and buoyancy forces and the drag force exerted by the fluid in case of relative motion

$$F_c = F_d + F_b \tag{4.1}$$

where centrifugal and buoyancy forces are given by, respectively

$$F_c = \frac{\pi}{6}\rho_p d_p^3 \Omega^2 r, \quad F_b = \frac{\pi}{6}\rho_f d_p^3 \Omega^2 r \tag{4.2}$$

ρ_p being particle or dispersed phase density, ρ_f fluid density, d_p particle or dispersed phase diameter, Ω angular velocity and r radial position. For small-sized particle and phases subject to slow relative motion, the drag force can be described according to Stokes (1850)

$$F_d = 3\pi\mu_f d_p u_p \tag{4.3}$$

μ_f denotes the dynamic viscosity of the fluid. From eq. 4.1 then follows for the radial velocity of particles or phases the expression

$$u_p = \frac{(\rho_p - \rho_f) d_p^2 \Omega^2 r}{18\mu_f} \tag{4.4}$$

Whether particles or phases reach a collecting wall depends on the residence time, their radial velocity and the position they have at entrance. The smallest particle or phase which with 100% probability reaches the wall is the particle or phase which during the available time moves over the entire cross-sectional distance dc between radially placed walls. Assuming a uniform axial velocity profile w_f, the radial velocity of such particles or phases is given by $u_{p,100\%} = d_c / t_r$ where the residence time $t_r = L_c / w_f$, L_c being the axial length of collecting walls. These equations yield for the diameter of the particle or phase which is collected with 100% probability, the equation

$$d_{p,100\%} = \sqrt{\frac{18\mu_f w_f d_c}{|\rho_p - \rho_f| \Omega^2 r L_c}} \tag{4.5}$$

This result applies to a separation unit formed by two adjoining radially placed walls, i.e. a single channel of the rotational particle separator. In case of an assembly of radially placed walls, i.e. a complete filter element consisting of a multitude of channels,

for fixed values of d_c, w_f and L_c the value of $d_{p,100\%}$ increases with decreasing r. This can be avoided by designing an axial velocity which is proportional with r. In that case the smaller centrifugal or buoyancy force at smaller radii is compensated by a larger residence time. In case of the rotational particle separator the appropriate axial velocity profile can be achieved by proper fluid mechanical design of inlet and outlet chambers up- and downstream of the filter element. In that case equation 4.5 can be rewritten as

$$d_{p,100\%} = \sqrt{\frac{27\mu_f Q d_c}{|\rho_p - \rho_f|\Omega^2 L_c (R_o^3 - R_i^3)}} \tag{4.6}$$

where Q is the volume flow, R_o the outer radius and R_i the inner radius of the filter element. In Brouwers (2002) analytical equations for the resulting separation efficiency of filter elements with various channel shapes are derived.

Provided that only r in equation (5.24) is decreased, it follows that $d_{p\,100\%}$ increases due to the fact that the centrifugal force on the particle decreases. This increase of $d_{p\,100\%}$ is avoided by designing the inlet and outlet configuration of the filter element such that the axial fluid velocity increases linearly with r. The decrease of the centrifugal force with decreasing r is then compensated by a longer residence time in the channel. This results in an equal particle separation for all channels. Brouwers (1997) derives an expression, valid for the entire filter element, for the smallest droplet, which is just able to reach the outer wall with 100% probability in case of this optimal distribution of the axial flow

$$d_{p\,100\%} = \sqrt{\frac{27\,\eta_f\,\phi_{fe}\,d_c}{(\rho_p - \rho_f)\,\Omega^2\,L_c\,\pi\,(1-\epsilon)\,(R_{o\,fe}^3 - R_{i\,fe}^3)}} \tag{4.7}$$

where ϕ_{fe} is the fluid volume flow through the filter element, ϵ the reduction of the effective cross-sectional area of the element due to the wall thickness of the channels, $R_{o\,fe}$ the outer radius of the element and $R_{i\,fe}$ is the inner radius. It follows from equation (??) that particles entering a separation channel larger than $d_{p\,100\%}$ will be collected with 100% probability. However, also smaller particles are able to reach the collecting wall provided that the distance of the particle towards the wall is sufficiently small. Brouwers (1997) derived expressions for the particle collection efficiency of an entire filter element for two axial flow distributions; a constant flow distribution over the channels and a flow distribution linearly proportional to r and two channel shapes; concentric rings and triangles. Besides, a parabolic velocity profile inside the channels is assumed. For a filter element composed of triangularly shaped channels and a linear proportional flow distribution $u_f \propto r$, the collection

efficiency of the whole element is given by

$$E = \begin{cases} 1 & x \geq \sqrt{2} \\ 2x^2 \left(1 - \frac{3}{4}\left(\frac{x^2}{2}\right)^{1/3}\right) & x \leq \sqrt{2} \end{cases} \tag{4.8}$$

where $x = d_p / d_{p\,100\%}$.

The smallest fractions, which are separated in the RPS, move with a radial velocity, which is equal to the ratio of the channel height to the channel length times the axial fluid velocity. In practical applications the ratio between the channel height and channel length is very small, in the order of 10^{-2}. Thus the droplets move with a radial velocity, which is only a few percent of the axial fluid velocity u_{fe}. This means that the process of radial migration of the droplets to the channel walls is already disturbed when secondary flows of one percent in magnitude of the axial fluid velocity occur in planes perpendicular to the axial channel axis. To avoid these secondary flows, the flow in the channels of the filter element has to be laminar. It is known that for non-rotating channels such flow only occurs for limited value of the axial Reynolds number

$$\mathrm{Re}_{ax} = \frac{\rho_f u_f d_c}{\eta_f} < 2300 \tag{4.9}$$

For rotating channels a much stronger condition must be fulfilled to satisfy stability, as rotation is an additional destabilization factor. In the case of a tube rotating around its own symmetry axis, not only condition (4.9) must be satisfied but also the rotational Reynolds number, defined as

$$\mathrm{Re}_\Omega = \frac{\rho_f \Omega d_c^2}{\eta_f} \tag{4.10}$$

should not be larger than 108. If however, Re_Ω exceeds 108, the axial Reynolds number should become less than 166, see figure 4.2. Brouwers (1995) shows that these considerations are also valid for tubes rotating around an axis not coinciding with but parallel to their symmetry axis. A further consideration is that tubes should be parallel within a few degrees to prevent secondary flow due to Coriolis forces.

4.3 prototypes

The rotational phase separator has the advantage that it is relatively easy to realise a mock-up of a filter element. A couple of different sized tubes with a lot of drinking straws will do, so quite a number of prototypes have been manufactured and

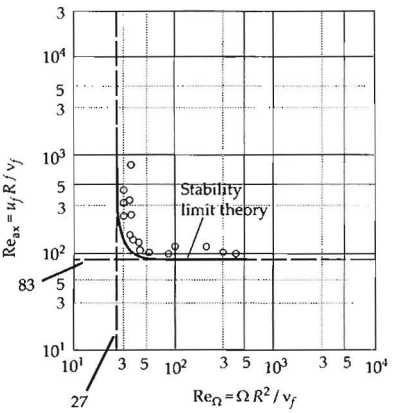

figure 4.2: stability limit of Hagen-Poiseuille flow in a circular pipe with solid-body rotation. Notice that both Reynolds numbers are based on the channel radius R.

tested. In figure 4.3 an overview of the initial experiments is given. The separation efficiency is conservatively predicted by the model. For conventional cyclones having swirling velocities, through flow and external dimensions which are comparable in magnitude to those of the rotating phase separator the particle cut-off diameter will be much larger, by roughly a factor 5 to 10. The underlying reason is the large radial distance over which particles must travel to reach the collecting wall. This distance amounts to R_o in the cyclone. In the rotating element of the rotational particle separator the effective separation distance amounts to the radial gap dc formed by the walls of the separation channels which is much less than R_o. Despite the smallness of this gap the axial pressure losses the fluid is subjected to while flowing in between these walls is limited. Its value can be estimated considering Hagen- Poiseuille flow in a pipe of diameter d_c (Hagen 1839, Poiseuille 1840) $\Delta p = 32\mu_f L_c w_f / d_c^2$ and typically yields pressure drops between 100 and 5000 Pa. More important are the energy losses which occur by bringing the fluid in rotation prior to entry to the rotating configuration and transferring rotation back to static pressure while leaving the rotating configuration. The same losses occur in the cyclone and range between 1000 and 50.000 Pa (Brouwers 2002).

Phase separation in centrifugal fields using the rotational particle separator has found its way to the market in various areas of application (figure 4.4). A multinational electronic consumer goods company has adopted the principle in an air cleaner

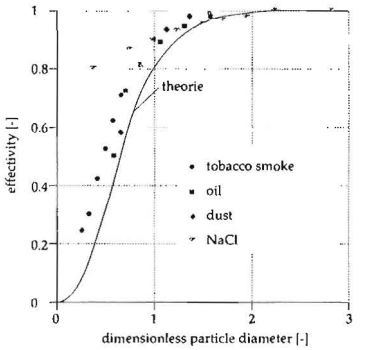

figure 4.3: initial experiments

(4). The device, which is sold world-wide, serves to remove air-borne particles which can cause respiratory allergic reactions to men in houses and offices. For this application the filter element is made from platic by injection moulding. In this case the company obtained a full license from the inventor for application of the product in this specific market.

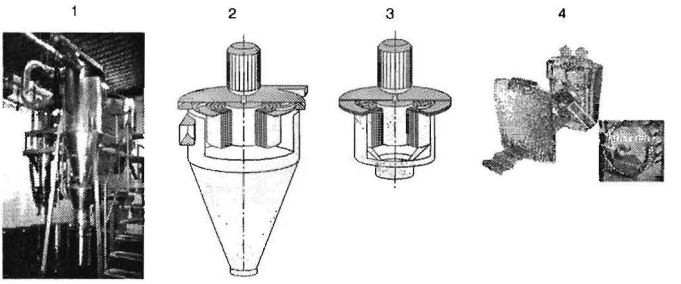

figure 4.4: applications of the rotational particle separator

Another application concerns the collection of powders and particles from gases in food and pharmaceutical processes. A specific advantage in this area is the possibility to fabricate the entire apparatus of stainless steel. It enables to meet strongest conditions on hygiene and cleaning. A design has been shown in figure 4.4 (1) and (2). The rotating element has been integrated in a cyclone. The cyclone acts as a pre-separator in which the gas is filtered from course particles material prior to entrance in the separation element. The cyclone also serves as a pre-swirler within which the gas is brought in rotation before entering the rotating separation element.

An impeller is fitted on the downstream side of the filter element. Here, the gas is brought to the desired pressure. It avoids the necessity of installing a separate fan. This to compensate for the pressure loss incurred in the separation device. Moreover, the over-pressure in the exit chamber ensures that only clean air flows through the gap between rotating filter element and housing from exit chamber to inlet chamber/cyclone, instead of unfiltered air moving vice versa. On top of the device air nozzles are placed by which periodically material collected in the channels is blown towards the cyclone where it is collected in the cyclone outlet. Blowing occurs during normal operation of the filtering process, without stopping flow and rotation.

4.3.1 Cleaning

The nozzle is positioned only a few millimeters above the filter element. The compressed gas comes out of the nozzle with supersonic speed, and recompresses upon entering the channels of the filter element, losing about 20% of its original pressure (brouwers 1996). In the channels a complex pattern of shock waves and expansion waves develops (figure 4.5). The injected compressed air moves downward with an

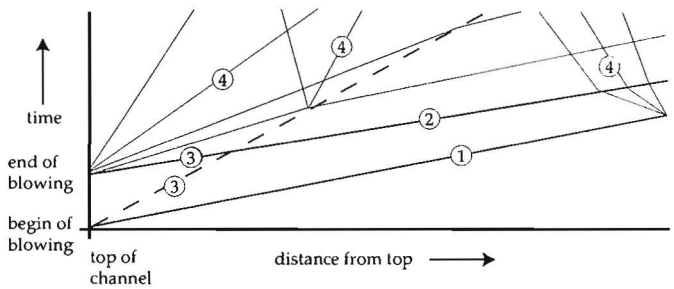

figure 4.5: patern of shock, expansion and reflection waves in a separation channel due to air jet blowing at the top

initial velocity of about 280 m/s. In front of this injected air, a shock wave propagates downwards through the gas of originally 1 bar present in the channel. The propagation speed is initially about 570 m/s and due to channel friction is reduced to about 470 m/s upon arriving at the lower end of the channel. Behind this propagation wave, the gas is compressed to a density about 1.7 times the density of the undisturbed gas, and moves downwards with speeds of initially about 280 m/s and at the bottom end of about 180 m/s. In this region of downward moving compressed air occurring in front of the air injected from the nozzle, particulate material is ripped of the walls and transported downwards. The thickness of the layer of particulate

material which moves downwards can be assessed from a balance between the shear force exerted by the gas and the friction between particles due to centrifugal pressure. It is found to be some tens of micrometers.

Due to filter rotation, a moment will occur when the channel has passed the column of air blown from the nozzle. At this moment expansion waves start to develop from the top of the channel, and the intensity of the axial momentum of the gas begins to decrease. Characteristically for supersonic conditions, the front of the expansion waves propagates faster than the compression wave. As cleaning occurs behind the front of the compression wave, one should avoid a situation where the front of the expansion waves (line 2 in figure 4.5) catches up with the compression wave (line 1 in figure 4.5) before the latter arrives at the lower end of the channel. Therefore the jet should blow sufficiently long. This is achieved by designing the nozzle such that its length in the circumferential direction is sufficiently large.

Under the above conditions, for practical versions of the rotational particle separator it has been established that about 1 kg of fine particles material collected in the channel can be removed by injecting about 1 kg of compressed air at 6 bar. This result is obtained under normal operating conditions with the filter element under full rotation. It compares reasonably well with theoretical predictions based on previously described physics of shock waves and layers of particulate material being moved downwards. Taking account of pre-separation in the cyclone, for a range of practical applications a realistic value for the loading of the filter element is 1 g of fine particles material per unit of gas to be purified. The power consumption of the compressor per unit of purified gas is the assessed as about 300 Jm^{-3}. If required, these values of compressed air consumption and related power consumption can be reduced significantly by adopting a system in which the filter is taken off-line and subsequently cleaned at reduced rotational speed.

As alternative to air (or other gases), cleaning of the filter element may be accomplished by periodically injecting water (or other liquids). In practice it has been established that (hot) water at pressures of 50 to 100 bar can be injected using the same nozzle as the one used for air. It offers the possibility to clean from time to time the filter very thoroughly in addition to regular air cleaning. It is particularly interesting for applications where high standards of hygiene apply.

A third method for removing particles material from the channels of the filter element is to continuously add liquid. This can occur by dispersing a spray of fine liquid particles in the gas upstream of the filter element. The fine liquid particles are centrifuged towards the outer walls of the channels of the filter element. Here they form a liquid film which moves towards and which carries away the other (solid) particles. This technique has been successfully applied to both the axial and the tangential

version of the rotational particle separator.

Another method for permanent wetting of the filter element involves addition of liquid from the top of the filter element. In practice this has been realised by using a small nozzle which moves slowly up and down in radial direction while the filter rotates. The desired amount of liquid (at 5 bar) is injected into the channels and forms a stable film along the outer walls of the channels. In this film centrifuged solid particles are collected, are dissolved or remain floating, and are transported downwards. The advantage of adding liquid from the top of the filter element is that the created liquid film extends over the entire length of the filter element.

The wet version of the rotational; particle separator appears to be an attractive alternative to existing wet scrubbers often employed in chemical and process industry. In contrast to wet scrubbers, in the rotational particle separator water is not injected to separate particles, but only to transport particles material being centrifuged towards the walls. This results in much lower (up to two orders of magnitude) amounts of washing liquids. This is also one of the reasons why the power consumption is much less. For equal separation performance, the power consumption quoted for conventional wet scrubbers (Brouwers 1996) is about five times larger than that established for the rotational particle separator.

4.3.2 Manufacturing and costs

The costs of manufacturing the rotational particle separator are closely related to the kind of application. Costs can be limited as most components are common products: motor, housing, impeller, equipment for cleaning, electronic controls etc. The only item which is not standard is the filter element. The further development of this line of rotational particle separators came to a standstill as in some more demanding situations reliability issues with the filter element arose and the producer of this type of RPS went out of bussiness. The filter element is produced by winding up around a shaft layers of corrugated and uncorrugated sheet material (figure 4.6). Subsequently the sheets were bonded together in a vacuum brazing furnace using an active filler material. The idea was that temperature uniformity is maintained on the work piece when heating in a vacuum, greatly reducing residual stresses because of slow heating and cooling cycles. Radiation however is the only heat transfer mechanism in a vacuum furnace and the filter element acts as a very effective radiation shield. Temperature uniformity is not achieved and the bonding can not be complete throughout the filter element. Normally this is not a problem as the sandwich construction formed by the corrugated and flat sheets is stressed by the outer wall, but the local tensions induced by the cleaning system led to fatigue failure. Recently a welding technique

has been developed to solve this problem and the program is continued now with a pilot project in China and several projects in the Netherlands.

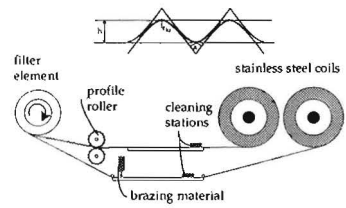

figure 4.6: filter element production

Studies were carried out on the costs of filtering systems based on the rotational particle separator. Considering stainless steel designs suited for industrial applications, the discounted value of annual costs was assessed. These included purchasing costs, utility costs, costs of assembly and replacement, engineering costs and costs of construction and erection. For installations with a total gas flow up to about 100,000 $m^{-3}hr^{-1}$, it was found that the discounted value of annual costs, expressed in dollars per unit of gas flow being purified, were lower than those of existing filtering methods, in particular for installations with lower gas flows. In the case of baghouse filters and electrostatic precipitators, the cost advantage can be ascribed to lower costs for replacement and investment. For wet scrubbers, such as venturi scrubbers, the cost advantage is due to lower utility costs (lower power requirements).

With the development of the RPS for particle-gas separation well under way, the mean research focus shifted to other fields, in particular liquid-liquid or liquid-gas separation. This shift in focus was again triggered by previous experience with oil exploitation and production (Brouwers 1987).

4.4 Naturally driven RPS

With longer exploitation of offshore wells, the amount of liquid, especially water, in the product stream increases. This is mainly due to the fact that water is usually used to keep the well under pressure. The increase in liquid contaminants requires improvement of current separation methods. In commonly used separators gravity is used to separate the dispersed phase. To allow for sufficient settling time, gas velocities in the separators have to be low. As a result these devices are voluminous, heavy and expensive and with increasing liquid amount the capacity is no longer sufficient. More and/or heavier separation devices are needed and sometimes even heavier and

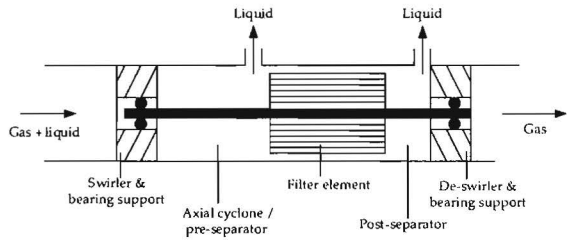

figure 4.7: schematic representation of the RPS-based separator, which is designed to purify natural gas under high pressure.

more expensive supporting structures are required. In some cases, although considerable gas reserves are still present, the exploitation of a well has to be stopped, as current gas treatment techniques are not economically viable. A device which fulfills these requirements is the naturally driven Rotational Phase Separator as depicted in figure 4.7 (van Kemenade 2003, Mondt 2005).

4.4.1 Natural gas production

Natural gas used by consumers is almost entirely composed of methane. However, natural gas extracted from offshore gas deposits, although still composed primarily of methane, is by no means pure. It contains oil, different semi-liquid hydrocarbons, water in the form of reservoir brine and condensate (vapor), sand and other large particle impurities (me 1974). The removal of these contaminants is the most important process step before the gas can be distributed as sales gas. The solid particles have to be removed from the gas because of erosion problems. Water has to be removed for two reasons. First, in the presence of CO_2 and H_2S, two other possible components of natural gas, it forms a highly corrosive mixture. Second, water together with hydrocarbon components can form hydrates, flaky solids, which could cause plugging. Finally, the hydrocarbon condensates are removed from the gas before it is delivered to the customers. To prevent erosion, corrosion and plugging of process equipment, water and the solid particles have to be removed in the earliest stages of production. Hydrocarbon condensates can be removed in a later stage as they form less hazards during processing.

The major transportation pipelines and in particular the compressors, used to transport the gas to shore, impose restrictions on the amount of solid and liquid contaminants. Offshore platforms are therefore built to remove those contaminants from the gas in a number of steps, depending on the composition and quality of the gas

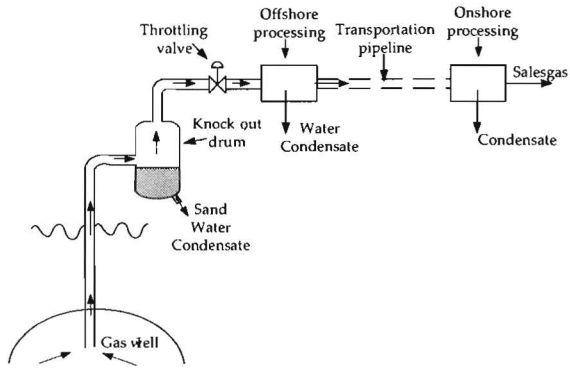

figure 4.8: Simplified schematic offshore separation flow sheet.

extracted. A schematic overview of the separation steps is given in figure 4.8. Natural gas extracted from a reservoir reaches the surface at pressures up to several hundred bar. Subsequently the gas is transported along a high-pressure pipeline into the first separation step, also called wellhead separation. In this stage separation takes place in a conventional separator, a knock-out drum. It consists of a closed tank, where gravity serves to separate the heavier solid contaminants and already condensed liquids, like oil and water under high pressure.

As the pressure of the gas is too high for the transportation pipelines, the pressure must be reduced. This is done in a so-called throttling (Joule-Thomson) valve. In a throttling valve the gas is expanded. Due to this expansion not only the pressure, but also the temperature of the gas is reduced. The reduction in temperature causes condensation of the hydrocarbon vapors and water vapor. When the well pressure is too low for cooling the gas by expansion, the gas is mechanically refrigerated. Besides condensation, sometimes condensable vapors are removed by adding solid or liquid desiccants. These desiccants absorb the liquid phases and are subsequently regenerated. The condensed liquids and/or desiccants are removed in the second separation step. This step usually consists of several interdependent treating steps. In these steps the gas is brought to the required specifications for pipeline transportation to onshore facilities.

Studies on aerosol size distribution in a natural gas stream have identified that significant quantities of droplets below 5 microns are the norm whenever choke valves and other restrictions are present (Regan 1992) or when vapors are at their dew points (Perry 1984). The measurements were performed to determine the concentration of

liquid aerosols in the natural gas stream sampled downstream of vane separators (combination of gravity separator and horizontal filter barrier and equivalent to a mist eliminator pad). Results show that in many cases, large quantities of aerosols can go through this type of separator because the droplets are too small to be trapped by these separation devices. As a result, a liquid/gas coalescer should be the technology of choice whenever high recovery rates are required to protect downstream equipment or to recover valuable liquid products.

4.4.2 State of the art

In a gravity separator or knock-out drum, gravitational forces control separation. The lower the gas velocity and the larger the vessel size, the more efficient the liquid/gas separation. Because of the large vessel size required to achieve settling, gravity separators are rarely designed to remove droplets smaller than 300 microns. A knock-out drum is typically used for bulk separation or as a first stage scrubber. A knock-out drum is also useful when vessel internals are required to be kept to a minimum as in a relief system or in fouling service. Gravity separators are not recommended as the soul source of removal if high separation efficiency is required.

In centrifugal or cyclone separators, centrifugal forces can act on an aerosol at a force several times greater than gravity. Generally, cyclonic separators are used for removing aerosols greater than 100 μm in diameter and a properly sized cyclone can have a reasonable removal efficiency of aerosols as low as 10 μm. A cyclone's removal efficiency is very low on mist particles smaller than 10μm[6] Both cyclones and knock-out drums are recommended for waxy or coking materials.

The separation mechanism for mist eliminator pads is inertial impaction. Typically, mist eliminator pads, consisting of fibers or knitted meshes, can remove droplets down to 1-5 microns but the vessel containing them is relatively large because they must be operated at low velocities to prevent liquid reentrainment.

Vane separators are simply a series of baffles or plates within a vessel. The mechanism controlling separation is inertial impaction. Vane separators are sensitive to mass velocity for removal efficiency, but generally can operate at higher velocities than mist eliminators, mainly because a more effective liquid drainage reduces liquid reentrainment. However, because of the relatively large paths between the plates constituting the tortuous network, vane separator can only remove relatively large droplet sizes (10 microns and above). Often, vane separators are used to retrofit mist eliminator pad vessels when gas velocity exceeds design velocity.

Liquid/gas coalescer cartridges combine features of both mist eliminator pads and vane separators, but are usually not specified for removing bulk liquids. In bulk

liquid systems, a high efficiency coalescer is generally placed downstream of a knock-out drum or impingement separator. Gas flows through a very fine pack of bound fibrous material with a wrap on the outer surface to promote liquid drainage. A coalescer cartridge can trap droplets down to 0.1 micron. When properly designed and sized, drainage of the coalesced droplets from the fibrous pack allows gas velocities much higher than in the case of mist eliminator pads and vane separators with no liquid reentrainment or increase in pressure drop across the assembly. Liquid/gas coalescer cartridges combine features of both mist eliminator pads and vane separators, but are usually not specified for removing bulk liquids. In bulk liquid systems, a high efficiency coalescer is generally placed downstream of a knock-out drum or impingement separator. Gas flows through a very fine pack of bound fibrous material with a wrap on the outer surface to promote liquid drainage. A coalescer cartridge can trap droplets down to 0.1 micron. When properly designed and sized, drainage of the coalesced droplets from the fibrous pack allows gas velocities much higher than in the case of mist eliminator pads and vane separators with no liquid reentrainment or increase in pressure drop across the assembly.

4.4.3 Design considerations

A schematic representation of the naturally driven RPS is given in figure 4.7. After passing the inlet part, which mainly serves as a bearing support, the contaminated fluid (gas/liquid) enters a swirl generator where the fluid is brought in a rotational motion as it passes its static vanes.

After the swirl generator, the mixture enters the pre-separation room, which serves as a kind of axial cyclone. In this separation room large contaminants are swept out of the flow, due to the centrifugal motion of the fluid. The contaminants leave the separator through the pre-separator outlets, which are situated before the filter element at the outside of the separator. The filter element is brought into rotation by the angular momentum of the fluid. Due to the centrifugal force, the droplets in the fluid are driven towards the wall of the channels where a liquid film is formed. This film breaks up at the end of the filter element and larger droplets are formed which can easily be separated in the post-separator (figure 4.9). If the dispersed phase is the lighter medium, as is the case for oil droplets dispersed in water, it is swept to the core of the post-separator. In the case of liquid droplets in a gas flow, the droplets move towards the outer wall. The liquid separated from the fluid flow leaves the separator through the post-separator outlets, which are positioned at the outer radius of the separator. The purified gas leaves the separator axially through the main outlet. Downstream of the post-separator a de-swirler is placed. The stator vanes

convert a large part of the rotational energy of the fluid into static pressure. Without the de-swirler the rotational energy is completely dissipated in heat and thus wasted. Recovering part of the kinetic energy, means that the separation process generates the waste stream at high pressure. This enables re-injection of the contaminants back into the gas reservoir from which they originally came.

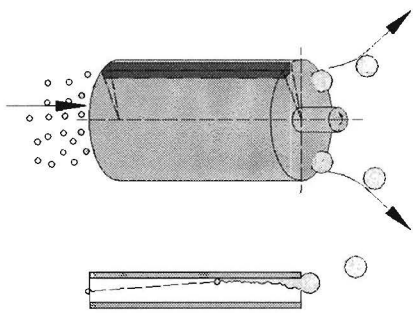

figure 4.9: the filter element operates as a coalescer when separating dispersed liquid phases from gas. Entering droplets are centrifuged towards the outer walls of each channel, creating a liquid film. At the end of each channel the liquid film breaks up in larger droplets. These droplets are collected at the outer wall of the post-separation area.

In the pre-separator coarse particles are removed from the flow. Although the streamlines in the pre-separator partly point to the inner radius, large particles can move, as a result of centrifugal and buoyancy forces, in a radial direction opposite to the fluid stream. Particles, which have a radial velocity that is larger than the average radial velocity of the gas stream are driven towards the outer radius of the pre-separator and can be collected there. The diameter of the particles that can reach the wall can be determined analogous to equation (4.6).

$$d_{p\,pre} = \sqrt{\frac{18\,\eta_f\,v_{pre}r}{(\rho_p - \rho_f)\,w_p^2}} \tag{4.11}$$

where v_{pre} is the average radial gas velocity in the pre-separator and w_p is the tangential velocity of the particle at radius r.

The pre-separator can be considered as an axial cyclone. In the core of a cyclone the tangential velocity component can be approximated by a solid body rotation (w/r = constant). While at the outside of a cyclone the tangential velocity component comes close to a free vortex ($w\,r$ = constant).

The general expression for the tangential velocity component in case of a solid body rotation is $w = \Omega r$. Substituting this expression in equation (4.11) gives the smallest droplet or particle diameter, which is separated in case the fluid flow in the pre-separator is regarded as a solid body rotation

$$d_{p\,pre} = \sqrt{\frac{18\,\eta_f\,v_{pre}}{(\rho_p - \rho_f)\,\Omega^2\,r}} \tag{4.12}$$

In case of a free vortex, the tangential velocity component is given by $w = C_\Gamma / r$ with $C_\Gamma = \Gamma / 2\pi$ and Γ is the magnitude of the circulation. Substituting this expression in equation (4.11) gives the relation for the smallest droplet or particle diameter, which is separated in case of a free vortex

$$d_{p\,pre} = \sqrt{\frac{72\,\pi^2\,\eta_f\,v_{pre}\,r^3}{(\rho_p - \rho_f)\,\Gamma^2}} \tag{4.13}$$

Besides that the pre-separator prevents blockage of the filter element channels, the pre-separator is also designed such that the desired axial fluid velocity profile at the inlet of the filter element is created.

The post-separator is a tubular section located after the filter element (figure 4.7). It receives flows from all the individual filter element channels. The droplets, which reach the walls of the filter element, coalesce and form a liquid film. At the exit of the channels this liquid film breaks up into relatively large droplets. In the post-separation area the rotational motion of the gas forces these droplets towards the outer wall, where they are separated from the main flow. However, before the droplets reach the outer collecting wall, they may break-up into smaller droplets as a result of centrifugal forces and/or forces due to the turbulent motion of the fluid. As a result these small droplets may leave the separator together with the gas stream and this deteriorates the separation performance. Therefore, the minimum diameter of the droplets present in the post-separator area is an important quantity for the design of the post-separator.

The droplets that can reach the walls of the filter element form a liquid film. At the exit of the channels the film breaks up due to centrifugal forces and/or turbulence. According to Hinze (1955) the maximum stable droplet diameter in an isotropic, homogeneous turbulent flow can be expressed by

$$d_{max} = C \left(\frac{\rho_f}{\sigma}\right)^{-\frac{3}{5}} \epsilon^{-\frac{2}{5}} \tag{4.14}$$

if the shear forces on the droplets can be neglected. This is the case if the viscous forces inside the droplet are small compared to other forces. C is a constant and σ

denotes the interfacial tension. The energy dissipation per unit mass can be estimated by

$$\epsilon = \frac{2f u_{mean}^3}{d_{pipe}} \tag{4.15}$$

where f is the friction factor, u_{mean} the mean velocity in the pipe and d_{pipe} the pipe diameter. It is assumed that the minimum droplet diameter equals half the maximum stable droplet diameter.

Droplets are also generated due to centrifugal forces. The interfacial tension gives rise to a surface force that counteracts this deformation process. The droplet size at which break-up occurs can be found by equalling these forces

$$d_{p,breakup} = \sqrt{\frac{6\sigma}{(\rho_1 - \rho_2)\Omega^2 R_0}} \tag{4.16}$$

The length necessary for the post-separator is found analogous to equation (4.6). The post-separator is an open space receiving flows from individual filter element channels. The angular momentum ensures further phase separation takes place.

In the swirl generator the angular momentum required to drive the filter element is generated. The angular momentum equals the momentum losses in other parts of the separator. The parts that contribute the most to these losses are the filter element, the pre-separator, the gap between the filter element and the static housing and the bearings

$$G_{\theta,swirl} = G_{\theta,fe} + G_{\theta,gap} + G_{\theta,decay-pre} + G_{\theta,bearings} \tag{4.17}$$

The general definition of angular momentum is

$$G_\theta = \int_S \rho_f u_f w_f r \, dS \tag{4.18}$$

where S is the cross sectional area. The angular momentum of the flow leaving the filter element is given by Hendriks (2000)

$$G_{\theta,fe} = \int_{R_i}^{R_o} \rho_f u_f u_f 2\pi r(1-\epsilon)\, dr = 2\pi\rho_f\Omega(1-\epsilon)\int_{R_i}^{R_o} u_f r^3\, dr \tag{4.19}$$

For a linear axial velocity distribution $u_f = br$, with b a constant, as desired for an optimal performance, it follows that the axial fluid velocity is given by

$$u_f = \frac{3Q}{2\pi(1-\epsilon)(R_o^3 - R_i^3)} r \tag{4.20}$$

Substitution of equation (4.20) in (4.19) gives the loss of angular momentum in the filter element

$$G_{\theta,fe} = \frac{3\rho_f \Omega Q}{5} \frac{R_o^5 - R_i^5}{R_o e^3 - R_i e^3} \tag{4.21}$$

where the subscript e denotes the entrance. In Li and Tomata (1994) a relation is given for the axial decay of angular momentum in a hydraulically smooth tube. With this relation the loss of momentum in the pre-separator can be described as

$$G_{\theta,decay-pre} = G_{\theta,swirl}(1 - 10^{-0.01605(x^*)^{0.8}}) \tag{4.22}$$

where x^* denotes the ratio between the pipe length and hydraulic diameter of the tube. The momentum required to turn a cylinder in a static housing is given by Schlichting (1979)

$$G_{\theta,gap} = C_m \frac{1}{2} \pi \rho \Omega^2 R_o^4 L \tag{4.23}$$

For a turbulent flow the torque coefficient C_m is given by $C_m = 0.019886\mathbf{Ta}^{-0.2}$. The Taylor number **Ta** can be written as

$$\mathbf{Ta} = \frac{\rho_f \Omega}{\mu_f} R_o^{\frac{1}{2}} s_g^{\frac{3}{2}} \tag{4.24}$$

where s_g denotes the gap size between the rotating filter element and the static housing. The loss of angular momentum in the bearings due to friction is dependent on the type of bearing chosen.

The pressure drop over the filter element is due to friction at the channel walls and the development of a free vortex in the pre-separator to a solid body rotation in the filter element. The pressure loss due to friction in the channels is given by (Schlichting 1979)

$$\Delta P_{friction,fe} = \left(f \frac{L_c}{d_c} + 1.16 \right) \frac{1}{2} \rho_f u^2 \tag{4.25}$$

This equation is corrected for entrance effects. In a laminar pipe flow the friction coefficient f equals $64/\mathbf{Re}$. The pressure loss due to a difference between the tangential velocity component prior to and in the filter element can be estimated from the conservation of mass and momentum over the filter element. The pressure drop due to different tangential velocities can be written as

$$\Delta P_{veldiff} = \rho_f \left(< \overline{w}_1^2 > - < \overline{w}_2^2 > \right) \tag{4.26}$$

$< \overline{w}_1^2 >$ and $< \overline{w}_2^2 >$ denote the mean tangential velocities at the filter in- and outlet respectively. The tangential velocity of a free vortex is given by $w = C_\Gamma / r$ with $C_\Gamma = \Gamma/(2\pi)$, Γ is the magnitude of the circulation. The tangential velocity in a solid body rotation is . Integration over the cross sections and substitution in equation (4.26) leads to

$$\Delta P_{veldiff} = \rho \left[\frac{2C_\Gamma^2 \ln(R_o/R_i)}{R_o^2 - R_i^2} - \frac{1}{2}\Omega^2(R_o^2 + R_i^2) \right] \tag{4.27}$$

The unknown C_Γ can be calculated by considering conservation of mass over the control volume

$$C_\Gamma = \frac{\Omega(R_o^3 - R_i^3)}{3(R_o - R_i} \tag{4.28}$$

The pressure drop over the swirl generator is due to friction in the small annulus and the introduction of a tangential velocity component. The flow relations of a fluid with viscous effects in a duct of constant cross-sectional area give the pressure drop due to friction in case a compressible flow is considered (Owczarek 1964). In case of an incompressible flow equation (4.25) gives the pressure drop due to friction. The pressure drop caused by introducing a swirl component in the flow can be estimated by

$$\Delta P_{swirl} = \frac{1}{2}\rho w_f^2 = \frac{1}{2}\rho(u_f \tan\alpha)^2 \tag{4.29}$$

where a is the blade angle of the vanes.

4.4.4 Experiments

A full scale prototype was build for separating water droplets from naural gas., capable to handle the volume flow of one typical wellhead under high pressure (80 bar) and which separates droplets down to 2 micron (table 4.1).

The performance of the separator was measured in two test facilities. In one test facility the separation performance and the hydrodynamic performance of the prototype at low (atmospheric) pressure was measured. In the second test facility hydrodynamic performance of the separator was simulated at elevated pressures. A schematic overview of the low pressure test facility is shown in figure 4.10. In this test loop air is used as the working fluid. The pressure and temperature inside the test loop are respectively about 1.2 bar and 283 K. The measuring equipment is listed in table 4.2.

The pressure drop over the filter element is measured by using the 4 equally spaced pressure holes situated at the circumference of the housing upstream as well

tabel 4.1: Desired operating characteristics for the RPS-based natural gas – water separator

	Value
$d_{p\,100\%}$	2 μm
D_o	0.6 m
L	0.36 m
Volume flow gas	0.65 $m^3\,s^{-1}$ ($\rho_g \simeq 50$ kg m^{-3})
Volume fraction contaminants	0.1 – 1%
Pressure	80 bar
Temperature	340 K
Pressure drop	$<$ 1 bar

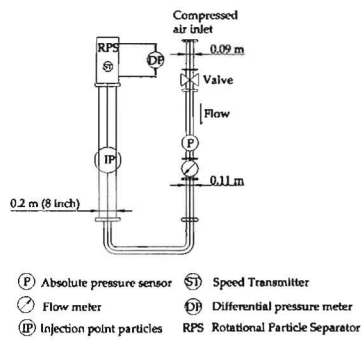

figure 4.10: schematic representation of the low pressure test facility.

as downstream of the filter element (figure 4.11). The 4 holes were interconnected such that, before as well as behind the element, the average pressure is measured. Besides one pressure hole is located upstream of the swirl generator. By using this pressure hole the total pressure drop over the separator can be measured.

The high pressure loop is filled with Sulfur Hexafluoride (SF6). SF6 is a high density gas, with a density of 5 to 6 times the density of natural gas. This means that at relatively low pressures, high fluid density flows can be simulated. Measurements were performed at 3 different absolute mean pressures: 1.9 bar, 2.9 bar and 3.6 bar, corresponding to fluid densities of respectively: 11.2, 17.5 and 22.2 kg m^{-3}

The separation efficiency of the prototype was determined by injecting calcium hydroxide ($Ca(OH)_2$), also called chalk hydrate or slaked lime (supplied by Carmeuse)

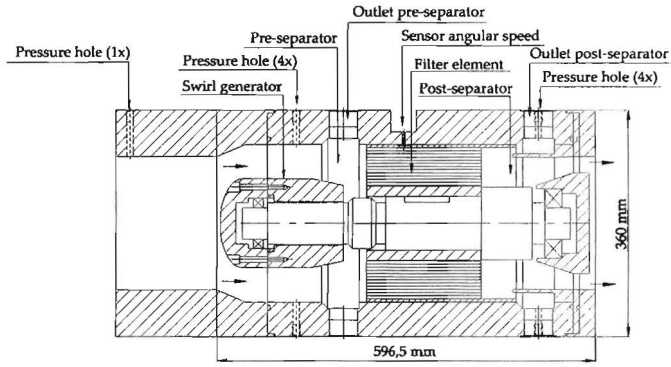

figure 4.11: location of the pressure holes and angular speed sensor on the prototype of the natural gas – water separator.

tabel 4.2: operating conditions of the measuring devices in the low pressure test loop.

	Flow meter[a]	**Abs. pres. sensor**[b]	**Diff. pres. sensor**[c]	**Inductive sensor**[d]
Operating range	0.0042 – 0.55 $m^3\ s^{-1}$	0 – 21 bar[e]	0 – 0.2 bar	0 – 100 Hz
Temp. medium	255 – 473 K	227 – 394 K	227 – 394 K	not applicable
Ambient temp.	233 – 358 K	233 – 358 K	233 – 358 K	248 – 343 K
Static pressure rating	100 bar	150 bar	150 bar	not applicable
Accuracy	Re $<$ 20000: 2% Re $>$ 20000: 1%	$<$ 0.075%	0.2%	$\leq$ 2%

[a]Invensys vortex flow meter, type 83F
[b]Invensys I/A series absolute pressure sensor, type 1GP10
[c]Invensys I/A series differential pressure sensor, type 1DP10
[d]Turck inductive sensor, type Bi1-EG05-AP6X
[e]absolute or gauge units

into the low pressure setup at the injection point (IP in figure 4.10). The particle size distributions both up- and downstream of the separator were determined by sampling the flow isokinetically with an eight stage Andersen impactor type Mark II.

In figure 4.13 the rotational speed n is depicted as a function of the flow rate through the separator for air at 1.2 bar. The solid line represents the model, the circles, crosses and dots each represent one measurement series. It can be seen that the

measurements are well reproducible. Comparing the measurement results with the theoretical model shows good agreement, except for a slight deviation at low flow rates. For flow rates smaller than about 0.06 $m^3 s^{-1}$ the filter element does not rotate. This is mainly due to the static bearing friction. The model also predicts the onset of rotation well. The small bend in the model at small flow rates is due to the fact that the relation for the dynamic bearing friction at low angular speeds differs from the one at higher speeds (SKF 1990).

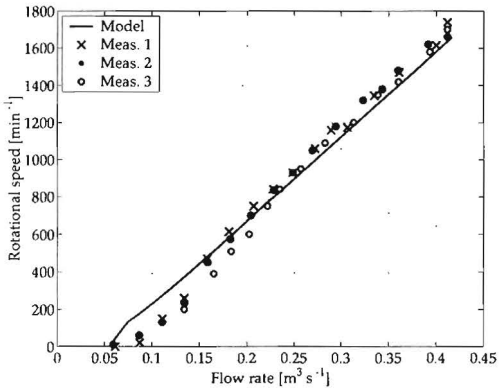

figure 4.12: rotational speed of the filter element as a function of flow rate for air at 1.2 bar.

In figure 4.14 the rotational speed at elevated fluid densities is depicted as a function of the flow rate through the separator. The solid line represents the model, while the crosses represent the measurement data. As the temperature and absolute pressure in the test setup varied during one measurement cycle, the mean temperature and pressure values of one measurement cycle are used to calculate the theoretical hydrodynamic performance of the separator. The density and viscosity of SF6 are interpolated from the measured data of Wilhelm (2005).

For the two lowest fluid densities the models predict a slightly lower rotational speed than measured. Comparing the three measurement results at elevated pressures shows that the rotational speed of the filter element hardly depends on the fluid density. This is expected as both the generated momentum and the loss of angular momentum in the filter element, which has the highest contribution to the total dissipated momentum, are linearly dependent on the gas density. In figure 4.15 the pressure drop over the filter element for air as the working fluid is depicted. The crosses and dots each represent one measurement series, while the lines represent the

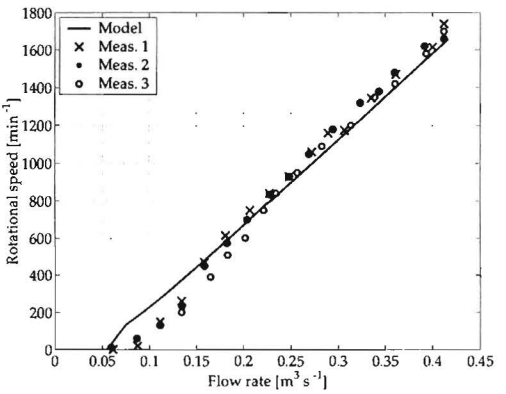

figure 4.13: rotational speed of the filter element as a function of flow rate for air at 1.2 bar.

model. Losses are calculated for the two types of channel shapes: triangular and sinusoidal. It follows that the pressure loss over the filter element is best represented by the model, assuming sinusoidal channels. This is also expected, as the filter element channels of the prototype have a more or less sinusoidal shape. The model assumes a fully developed flow in the channels of the filter element. In reality this is not true, as the dynamic entrance length, L_{hy} for the channels is rather large. The dynamic entrance length is defined as the required duct length to achieve a maximal duct velocity of 99% of that for fully developed flow when the entering fluid velocity profile is uniform (Shah 1978). For example, for sinusoids channels for which the width is much larger than the height, Shah and London give a dimensionless entrance length L_{hy}^{+} (=$L_{hy}/(D_h\,\mathrm{Re})$) of 0.0648. The hydraulic diameter of the channels is $1{\cdot}10^{-3}$ m and the Reynolds number in the channels during the measurements is of the order $1{\cdot}10^{3}$. This means that the dynamic entrance length is about 0.0648 m, which is about one third of the total channel length (L_c=0.18 m). Although the model neglects the entrance length, there is a good agreement between the measurements and the model.

In figure 4.16 the total pressure loss over the separator together the pressure loss over the filter element is given. It follows that total pressure loss is well predicted by the theoretical model. The pressure loss in the pre- and post-separator and pressure drop in the pipe before the swirl generator are not included in the model, as they are negligible compared to the other losses. It can also be seen that pressure loss over the filter element is the main contributor to the total pressure loss over the separator. In

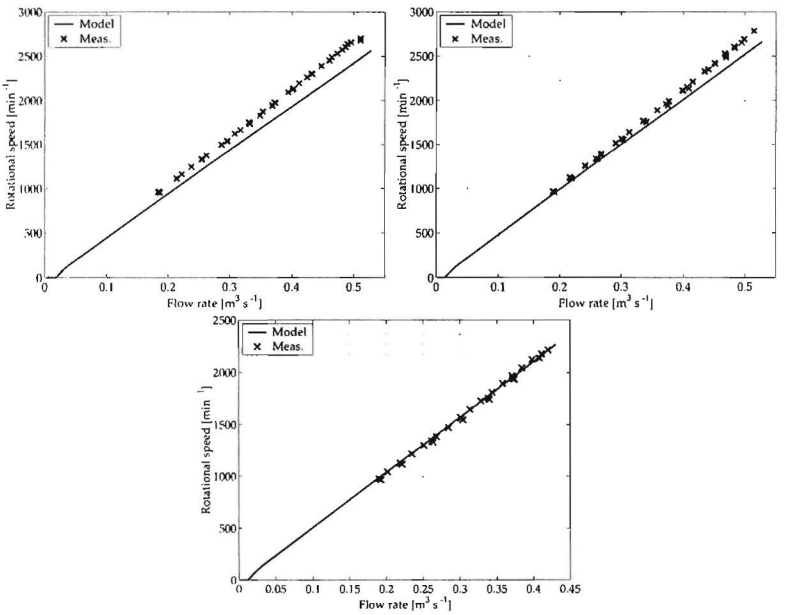

figure 4.14: rotational speed of the filter element as a function of the SF6 flow rate. From left to right the density of SF6 is respectively 11.2, 17.5 and 22.2 kg m^{-3}.

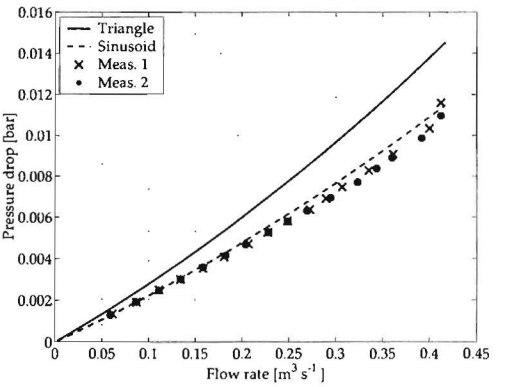

figure 4.15: pressure drop over the filter element as a function of flow rate for air at 1.2 bar.

the second place follows the pressure loss due to the generated swirl.

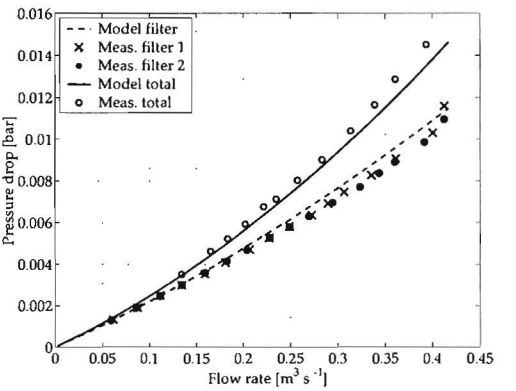

figure 4.16: pressure drop over the filter element and the whole separator as a function of flow rate for air at 1.2 bar.

In figure 4.17 the pressure loss over the filter element and the total pressure loss over the prototype are given as a function of the flow rate for the SF6 test loop. The lines represent the theoretical calculations, while the crosses, dots and circles represent the measurement data. Opposite to the measurements in the low pressure test setup during which the flow in the channels of the filter element was laminar, the

channel flow during the high pressure measurements was turbulent (the Reynolds number in the channels varied between $9{\cdot}10^3$ and $2{\cdot}10^4$). For calculating the pressure drop over the filter element due to friction, the Blasius (1907) relation is used. A value of 2 is assumed for the factor ζ, which represents the additional pressure drop at the entrance region of the duct.

All measurement series show a gradual increase of the pressure loss with increasing flow rate. The filter element has again the highest contribution to the total pressure loss. The measurement data of the pressure loss over the filter element are slightly below the predicted pressure loss. The measurement data for the total pressure loss on the other hand are somewhat higher than predicted. This can be attributed to the fact that in the model some flow phenomena in the swirl generator which contribute to an additional pressure loss are neglected. One of these phenomena is the fact that the angle of incidence of the fluid at the inlet of the vanes differs from the angle of the vanes itself. Furthermore, there will be an additional pressure loss due to the acceleration of the fluid as it enters the vanes (decrease in cross-sectional area due to thickness of the vanes). Besides, wakes may occur at the trailing edges of the vanes, which cause an extra pressure loss. Furthermore, it can be seen that for increasing fluid density, the pressure losses increase. This is also predicted by the model as all pressure loss contributions increase for increasing fluid density.

In an ideal situation the total particle concentration upstream the separator C_{us} measured with the impactor equals the injected particle concentration. In practice, however, the impactor concentration was 2 to 3 times less than the injected concentration due to the loss of lime from the injection point to the impactor.

The total particle concentration downstream of the separator can be determined with an absolute filter. Measurements performed at the University of Twente, however, showed that the total particle concentration downstream of an RPS-based separator is approximately equal to the total particle concentration on the impactor plates when measuring downstream of the separator. In these experiments also calcium hydroxide and the same Anderson impactor were used. Equal concentrations can be expected, as the impactor works as a kind of absolute filter. Therefore, in processing the measurement results the concentration downstream of the separator C_{ds} is assumed equal to the total impactor concentration of the downstream measurements.

When the total injected concentration and the total impactor concentration downstream of the separator are known, the total efficiency E_{total} follows from

$$E_{total} = \left(1 - \frac{C_{ds}}{C_{us}}\right) 100\% \tag{4.30}$$

In figure 4.18 the results of the measurements are shown together with two analyt-

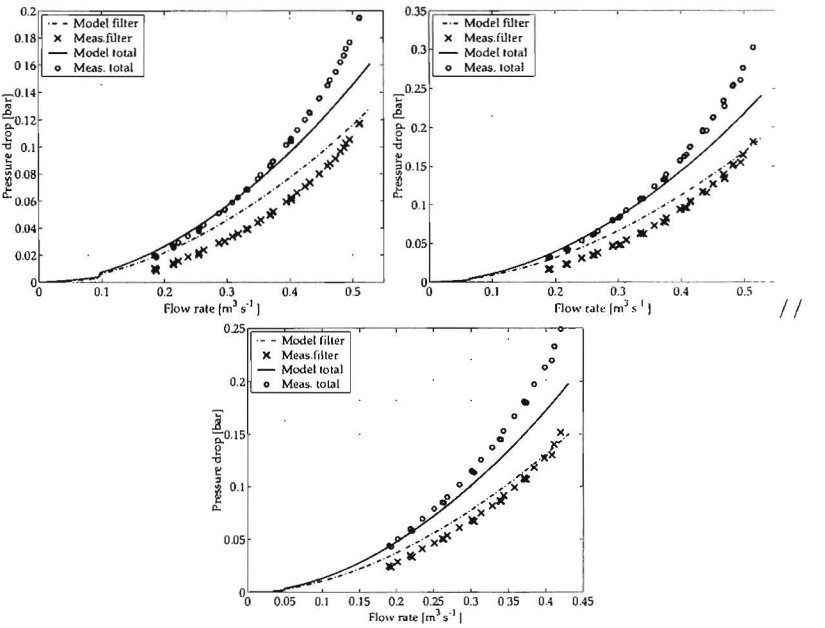

figure 4.17: pressure loss over the filter element, the swirl generator and the total pressure loss over the prototype as a function of SF6 flow rate. From left to right the density of SF6 is respectively 11.2, 17.5 and 22.2 kg m^{-3}.

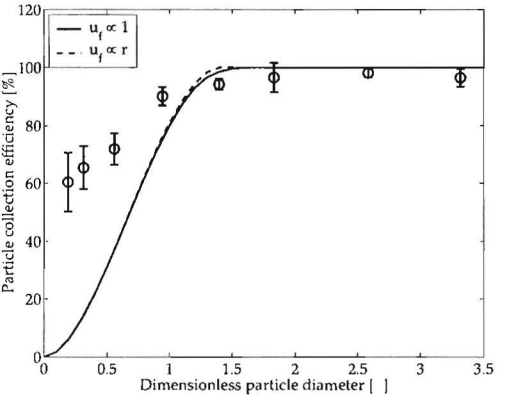

figure 4.18: separation efficiency as a function of particle size. The solid line represents the theoretical efficiency prediction for a constant axial flow distribution, the dotted line represents the theoretical efficiency prediction for an axial flow distribution, which is linearly proportional to r and the circles represent the measurement data (vertical bar denotes the standard deviation).

ical predictions of the filter separation efficiency. The circles represent the mean separation efficiencies per size class obtained from the measurements, while the vertical lines through the circles represent the standard deviation. In the figure eight measurement points are depicted. These represent all collection plates of the impactor, except the pre-separator and the back-up filter. The pre-separator is not accounted for as it only serves to remove coarse particles from the flow. The back-up filter is not regarded because, after the measurements upstream of the separator, no weight increase of the back-up filter could be measured. The filter efficiency is given as a function of the dimensionless particle diameter x. This diameter represents the mean particle diameter per size class divided by the diameter of the smallest particle which is separated with 100% probability in the filter element (Brouwers 2002).

Analytical expressions for the separation efficiency of the filter element were derived by Brouwers (1997). In figure 4.18 the dotted line represents the theoretical separation efficiency for triangularly shaped channels, which have a flow distribution linearly proportional to radial distance r, while the solid line represents the efficiency for triangular channels in which the axial flow distribution is constant over the channels, $u_f \propto 1$. In both models a parabolic velocity profile in the channels is assumed (in reality this is not valid, as the dynamic entrance length, L_{hy} for the channels is rather large). Theoretical expressions for triangular channels are used, as they are

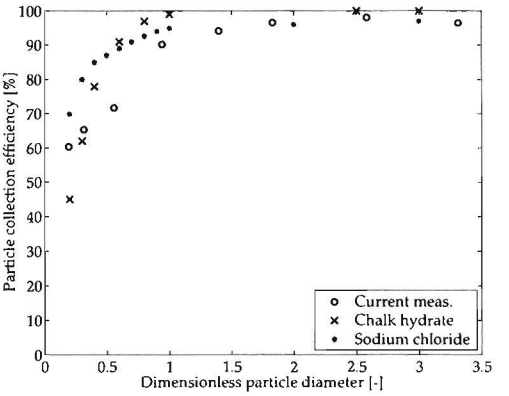

figure 4.19: separation efficiency as a function of particle size. Comparison of current measurements (circles) with previously performed measurements (asterisks and triangles).

easier to derive than expressions for sinusoidally shaped channels. Besides, the theoretical results for triangularly shaped channels are a good approximation to those of sinusoidally shaped channels. Furthermore, in practice the channel shape is quite irregular and also the sinusoidal shape is only an approximation of the actual channel shape.

It can be seen that the standard deviation increases for smaller particle sizes. This is expected as the measurement errors are larger in these size ranges, due to a smaller weight difference between the impactor plates prior to and after the measurements. For particle sizes around $x = 1$ and larger, the agreement between theory and experiments is reasonable. However, for particle sizes smaller than x=1 a large difference between the models and the experiments is observed. Previously performed measurements with an electrical driven RPS, using the same Anderson cascade impactor to measure efficiency, showed similar results (Brouwers 1996), see figure 4.19. It can therefore be concluded that the naturally driven RPS has the same particle separation efficiency as an externally driven RPS.

4.5 Further developments

At this stage the naturally driven RPS was proven as a technique for the removal water droplets in oil (with the help of Royal Dutch Shell) and to remove liquid droplets

from natural gas (with the help of CDS engineering b.v.). The main application is offshore oil/gas production where the production life of existing platforms can be elongated by using these techniques as retrofitting large settling tanks to the platforms is not an option. A further step would be to bypass the platform altogether and use the RPS for down-hole separation (figure 4.20 thus eliminating the need to bring the water up. To that end the design is such that all fits inline in standard sized pipes.

Further development of this design is now taken over by the cooperating industries as actual demonstration on a platform requires a large coordinated effort to guarantee safety and production. Independent manufacturing and marketing as in the case of the heat exchanger and the cyclone type heat exchanger is not an option here. Nevertheless the inventor has still an influence on the process through licensing the original and subsequent patents.

During the research of the naturally driven RPS, contacts with industry (Royal Dutch Shell in particular) led to a new research area: combining phase transition with separation to remove unwanted components in natural gas, opening up yet another field of applications for the RPS.

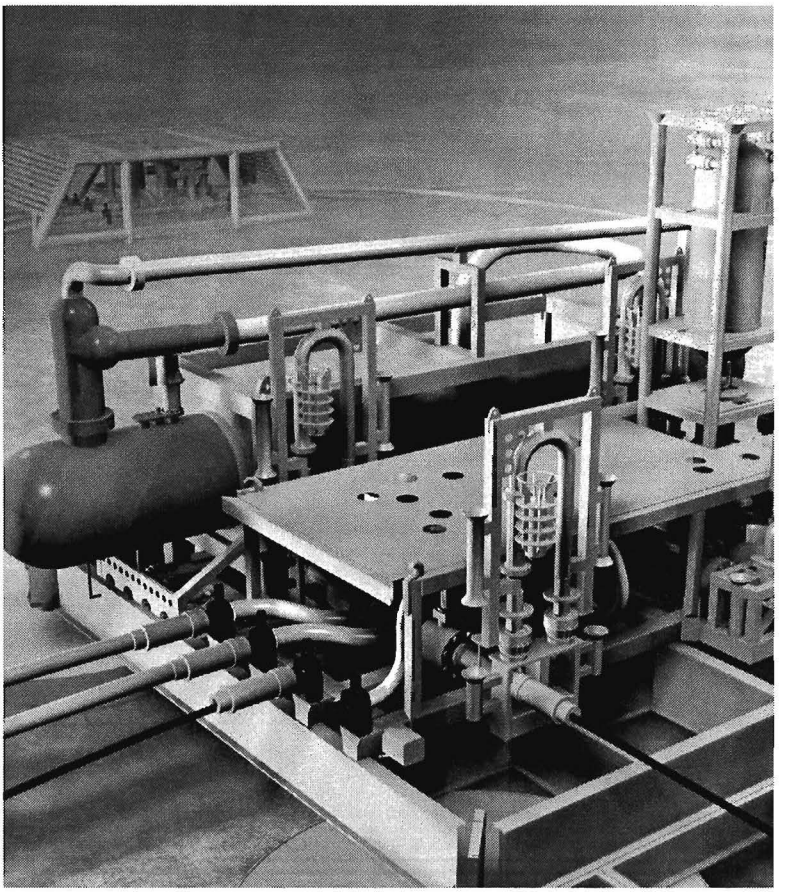

figure 4.20: Statoil subsea facilities

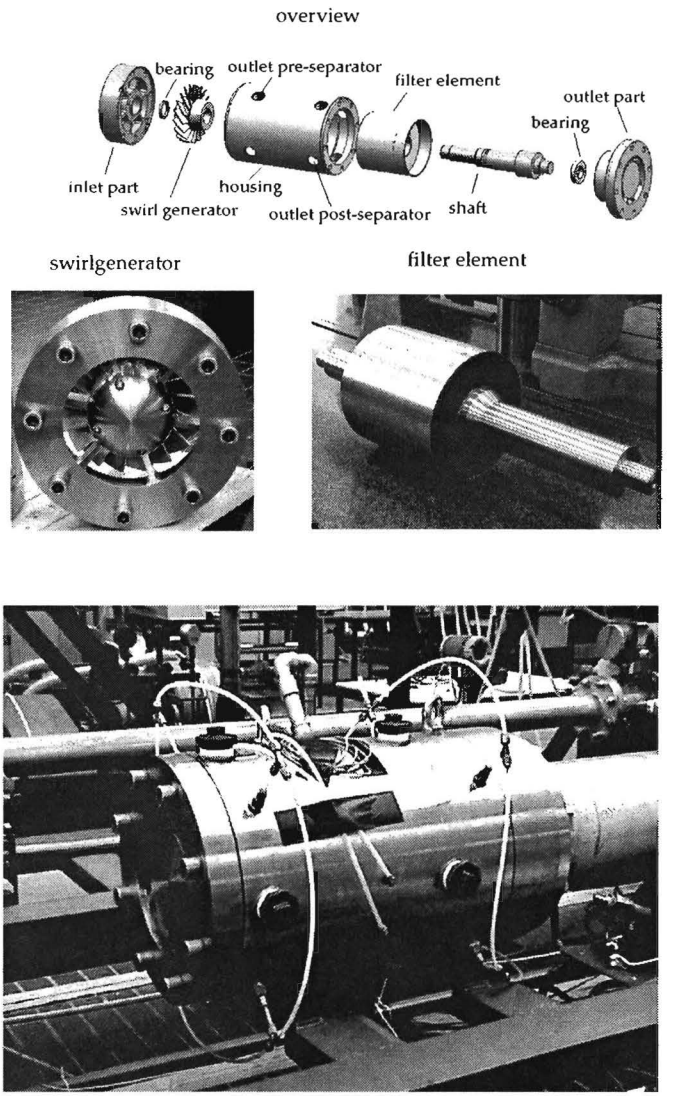

figure 4.21: overview of the naturally driven RPS

5 Separation by phase transition

In this chapter two innovations are discussed that are based on a new combination of existing elements, specifically the combination of the high temperature heat exchanger and the naturally driven rotational phase separator with phase transition. These inventions serve as an example how seemingly independent lines of research may lead to a patentable innovation when combined.

5.1 Aerosol emissions in biomass combustion

One of the limiting factors preventing large scale introduction of small biomass combustion units are the associated particulate emissions. Large combustion units in general are equipped with electrostatic precipitators and can achieve very low particulate matter emissions (<50 $mgNm^{-3}$), while small scale units (in the order of 1 Mw) have at most a cyclone. Micro scale (< 100 kW) units are not equipped with gas cleaning devices apart from the heat exchanger. At the end of the previous century it turned out to be difficult to meet the lower emission standards for medium scale units, even with cyclones as particles below 10 μm are hard to catch devices of this type. While investigating potential application of the RPS, measurements showed that the particle matter emissions of a biomass combustion plant exhibit a bi-modal distribution (5.1).

The particle size of the coarse fly ash fraction can vary between some few μm up to about 200 μm. The second fraction consists of aerosols, formed during the cooling of the flue gas in the heat exchanger section. If the concentration of ash-forming vapours in the flue gas and the cooling rate in the heat exchanger are both high, supersaturation of these vapours could occur, causing formation of new formed particles by nucleation. The aerosol-forming vapours are mainly chlorides and sulfates of alkali components. The particles formed by nucleation are very small in size, about 5 to 10 *nm*, but on their way in the flue gas, these particles are able to grow by coagulation, agglomeration and condensation of ash-forming vapours (Obernberger 2001, Brunner 1998, Joller 2005, Valmari 1998, Christiansen 2000, van Loo 2002). These particles

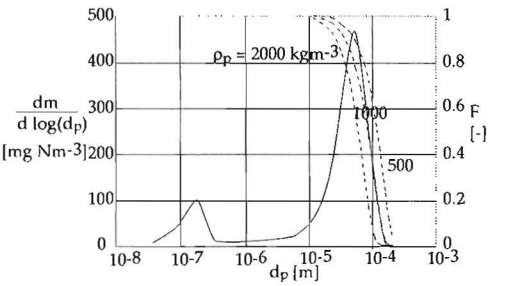

figure 5.1: bi-modal distribution of biomass combustion emissions

form the basis of the aerosol fraction, characterised by a particle size $< 1\ \mu$m.

The coarse particles are not affected by the turbulent eddies and are deposited by inertial forces. In that case the equation of motion is given by

$$\frac{dv}{dt} = \frac{u - v}{\tau} + g \tag{5.1}$$

u being the velocity of the fluid and v the velocity of the particle while g denotes the gravitational acceleration. In the test furnace the particle laden flue gas flow reverses direction twice. Assuming a potential flow model for the fluid the particle trajectories were calculated whereby it was assumed that particles that enter the swirling area, always end up at the wall (van Kemenade 2005). The results of these calculations are compared with the measured results. The density ρ should be interpreted as the density including the porosity of the particle and is not exactly known. The cut-off at the right side of the graph coincides well with the calculated distribution and can easily be predicted.

In He (1998) particle deposition in turbulent duct flows in the presence of a large temperature gradient is studied. One of their main conclusions are far away from the wall, far beyond the viscous sub layer the turbulence is the dominating dispersion mechanism, a result already obtained by Prandtl and Taylor. When particles are very close to the wall, Brownian motion is the dominating mechanism of diffusion for particles. Thermophoresis, the transport under influence of a temperature gradient, has a strong effect on the deposition and transport of particles smaller than a few micrometers and the thermal drift decreases as particle size increases for particles larger than 0.1 μm. A simple empirical equation for the non dimensional deposition velocity suggested by Wood (1983) is given as

$$u_d^+ = \frac{u_d}{u^*} = 0.057\mathrm{Sc}^{-2/3} + 4.5{\cdot}10^{-4}\tau^{+2} + u_{th}^+ \tag{5.2}$$

where u_d is the deposition velocity, u^* is the shear velocity, Sc$= \mu/\rho_g D_p$ is the Schmidt number, D_p is the particle diffusivity, u_{th}^+ is the nondimensional thermophoretic sedimentation velocity and. The non-dimensional particle relaxation time is given by

$$\tau^+ = \tau \frac{\rho_g u^{*2}}{\mu_g} = \frac{\rho_p d_p^2 C_c}{18\mu_g} \frac{\rho_g u^{*2}}{\mu_g} \tag{5.3}$$

The correction factor C_c is due to Cunningham (1910) describing the deviation from continuum behaviour when the particle diameter is comparable to the molecular mean free path.

$$C_c = 1 + 2Kn\left(1.257 + 0.4\exp\left(-1.1\frac{1}{Kn}\right)\right) \tag{5.4}$$

The Knudsen number is defined as $Kn = \lambda/d_p$, where λ is the mean free path in the gas. The mean free path is defined as the average distance travelled by a molecule between successive collisions and can be described by

$$\lambda = \frac{1}{\sqrt{2}n\pi d_m^2} \tag{5.5}$$

n is the density of the gas and d_m the molecular diameter. For air at 20 ^{o}C and atmospheric pressure the molecular diameter is 0.00037 mm and the mean free path is 0.066 mm.

The first term in equation 5.2 is the particle deposition rate due to Brownian motion and eddy diffusion, the second term is particle deposition induced by eddy diffusion-impactation and the third term is due to thermophoresis. Various functions are available to describe the experimentally observed velocity profile for fully developed turbulent pipe flow. One such function which accurately describes the time averaged streamwise velocity sufficiently far from the wall over a broad range of Reynolds numbers is given by Bird (1960)

$$\frac{u}{u_{max}} = \left(1 - \frac{r}{R}\right)^{1/7} \quad \frac{u_{avg}}{u_{max}} = \frac{4}{5} \tag{5.6}$$

When a temperature gradient is established in a gas, the aerosol particles in that gas experience a force in the direction of decreasing temperature. The motion of the particle resulting from this force is called thermophoresis. The magnitude of this force depends on gas and particle properties and the thermal gradient. The relation between the shear velocity can be found as $u^* = u_{avg}(f/8)^{1/2}$ where f is the Darcy friction factor (Tandon 1998). The theoretical thermal force on a particle is (Waldmann 1966)

$$F_{th} = \frac{-p\lambda d_p^2 \nabla T}{T} \quad d_p < \lambda \tag{5.7}$$

where p is the gas pressure and λ the mean free path. For large particles the mechanism is more complicated due to the presence of a temperature gradient in the particle. Particle Brownian rotation does not prevent the establishment of a temperature gradient inside the particle because the time required for significant rotation is greater than the time for temperature adjustment (Fuchs 1964). In that case the thermal force is given by (He 1998)

$$F_{th} = \frac{-9\pi\mu^2 d_p H \nabla T}{2\rho_g T} \quad d_p > \lambda \tag{5.8}$$

ρ_g is the gas density and the coefficient H includes the effect of the temperature gradient

$$H = \left(\frac{1}{1+6\lambda/d_p}\right)\left(\frac{k_g/k_p + 4.4\lambda/d_p}{1+2k_g/k_p + 8.8\lambda/d_p}\right) \tag{5.9}$$

where k_g is the gas conductivity and k_p the particle conductivity. The nondimensional thermophoretic velocity can subsequently be calculated as

$$u_{th}^{+} = \frac{F_{th}}{u^* m}\tau = \frac{6F_{th}}{u^*(\rho_p - \rho_g)\pi d_p^3}\tau \tag{5.10}$$

In figure 5.2 an example is given of the contribution of the terms in equation (5.2) to the total deposition velocity in the test furnace. The results compare well with measurements, however it was noted that also some direct wall condensation occurred, reducing aerosol emissions by about 10 to 20 %.

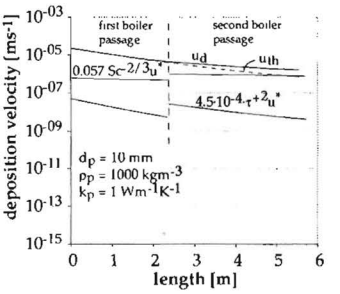

figure 5.2: deposition velocities in the Mawera experimental furnace

5.2 Condensing heat exchanger

Separation of the fly ash fraction could easily established by using cyclones or multi cyclones (Brouwers 1997, Brunner 1998). For the removal of aerosols, bag house filters

or electro statistic precipitators can be used, however, due to the high investment cost, these techniques are only cost effective in large scale combustion plants (Ebert 2001). In virtue of this reason a new, cost efficient precipitation technique for small scale biomass combustion plants has to be developed in order to precipitate aerosols from the flue gas.

During the combustion of chemical untreated wood chips, ash is entrained from the fuel bed. However, also a fraction of the ash-forming compounds in the fuel is volatilised and released to the flue gas. Depending on the cooling rate and the concentration of ash-forming vapours in the flue gas, these volatilised compounds nucleate or condense on the surface of pre-existing ash particles in the flue gas as well as on cold surfaces of the heat exchanger. Consequently it may be possible to reduce aerosol emission by enhancing wall condensation, contrary to the goal of current heat exchanger designs. If the reduction of the total emitted mass by stimulated wall condensation is high enough to eliminate the need for an expensive flue gas treatment system the additional costs of a heat exchanger cleaning system may be justified.

5.2.1 Model

As soon as the flue gas temperature equals the condensation temperature of aerosol-forming species, condensation on pre-existing particles as well as on heat exchanger walls take place as competing processes (figure 5.3). Removal of particles in the flue

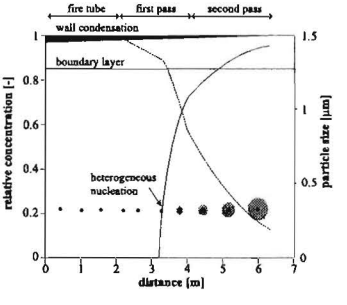

figure 5.3: competing condensation processes

gas due to thermophoresis and homogeneous nucleation is not taken into account. Furthermore it is assumed that the flue gas already contains a constant number of particles in the nanometre range. This assumption is reasonable as a constant particle number concentration is observed during the combustion of bio fuels and nucleation of new particles is suppressed when the initial particle number concentration is

within the same range as the final particle number concentration Obernberger 2001, Jensen 2000).

Besides assumptions regarding removal mechanisms and particle formation processes, also assumptions with respect to the flow behaviour are made. For the model, a laminar flow in a axis-symmetric heat exchanger tube is assumed, which is characterised by a Reynolds number lower than 2300 (Bird 1960):

$$Re = \frac{D_h \rho_g u_g}{\mu_g} < 2300 \tag{5.11}$$

In Eq. 5.11, D_h represents the hydraulic diameter of one heat exchanger tube, which is defined as $\frac{4A}{O}$, where A represents the cross section of the conduit and O is the wetted perimeter. ρ_g and μ_g represent the density and the dynamic viscosity of the flue gas, whereas u_g represents the axial bulk velocity of the flue gas. Since a fully developed laminar flow is assumed, also the distribution of the aerosol-forming vapours exhibits a parabolic profile over the radius r of a heat exchanger tube and can be written as:

$$\rho_\alpha(r) = 2\rho_{\alpha,0}\left(1 - \left(\frac{r}{R_h}\right)^2\right) \tag{5.12}$$

where $\rho_\alpha(r)$ is the mass concentration of the aerosol-forming species as function of the radius r, whereas R_h represents the hydraulic radius of one heat exchanger tube, which is equal to $\frac{1}{2}D_h$. The initial mass concentration is expressed by $\rho_{\alpha,0}$. A general description of the mass fraction of the aerosol-forming species ω_α is given by (Bird 2002)

$$\omega_\alpha = \frac{\rho_\alpha}{\rho_{tot}} \tag{5.13}$$

where ρ_{tot} represents the total mass density of the flue gas. Fick's law of diffusion is applied, which describes how the mass of species α in a binary mixture is transported by means of molecular motions (Bird 2002)

$$j_\alpha = -\rho_{tot}\mathbb{D}\nabla\omega_\alpha \tag{5.14}$$

In Eq. 5.14, j_α represents the mass flux, whereas $\mathbb{D}$ represents the diffusion coefficient. Axial diffusion is neglected in order to calculate the mass flux towards the wall. Furthermore it is assumed that the total mass density ρ_{tot} remains constant, which is acceptable due to the fact that $\rho_{tot} >> \rho_{\alpha,0}$. Now, the mass flux per unit length to

the wall $j'_{\alpha,w}$ can be described by applying these assumptions and combining Eq. 5.14 and a wall surface area per unit length of $2\pi R_{eq}$:

$$j'_{\alpha,w} = -2\pi R_{eq}\rho_{tot}\mathbb{D}\nabla\omega_{\alpha}\Big|_{r=R_{eq}} = 8\pi\mathbb{D}\rho_{\alpha,0} \tag{5.15}$$

As the particles follow the streamlines, the number concentration N also exhibits a parabolic profile:

$$N(r) = 2N_0\left(1-\left(\frac{r}{R_{eq}}\right)^2\right) \tag{5.16}$$

where N_0 denotes the initial number concentration. Equation 5.17 describes the mass vapour density profile around a particle with diameter d_p:

$$\rho_{\alpha}(r^*) = \rho_{\alpha}(r)\left(1-\frac{\frac{1}{2}d_p}{r^*}\right) \tag{5.17}$$

The spherical coordinate originating at the centre of the particle is represented by r^*. For the sake of brevity, $\rho_{\alpha}(r^*)$ is denoted as ρ^*_{α}. Now, the mass vapour concentration around a particle ω^*_{α} is defined as:

$$\omega^*_{\alpha} = \frac{\rho^*_{\alpha}}{\rho_{tot}} \tag{5.18}$$

The mass vapour flux of the aerosol-forming species towards the particle at the same axial position in a heat exchanger passage can be written as:

$$j''_{\alpha,p} = \pi d_p^2\overline{\phi}\rho_{tot}\mathbb{D}\nabla\omega^*_{\alpha}\Big|_{r^*=\frac{1}{2}d_p} = -2\pi\overline{\phi}d_p\rho_{\alpha}(r)\,\mathbb{D} \tag{5.19}$$

where $\overline{\phi}$ is an average correction factor for diffusion outside the continuum limit. Equation 5.19 is based on diffusion of molecules to the surface of the particle. However when particles are within the mean free path regime, transport is controlled by kinetic processes. The effect of the correction factor ϕ results in a slowing down of the growth rate and is defined as (Davies 1978)

$$\phi = \frac{2\lambda + d_p}{d_p + 5.33\left(\lambda^2/d_p\right) + 3.42\lambda} \tag{5.20}$$

In Eq. 5.20, λ represents the mean free path in the flue gas. In this research the mean free path mainly depends on the temperature of the flue gas and is evaluated at the saturation temperature of the aerosol-forming species. The average value for the correction factor $\overline{\phi}$ as described in Eq. 5.19, during the growth process is calculated by integrating Eq. 5.20 with respect to d_p from 0 to d_p and dividing the whole integral by d_p. The total vapour flux towards the particles can subsequently be found by:

$$j'_{\alpha,p} = -8\pi\overline{\phi}d_p\mathbb{D}\rho_{\alpha,0}N_0\int_0^{R_{eq}}\left(1-\left(\frac{r}{R_{eq}}\right)^2\right)^2 2\pi r dr = -\frac{8}{3}\pi^2\overline{\phi}d_p\mathbb{D}R_H^2\rho_{\alpha,0}N_0 \quad (5.21)$$

If wall condensation as well as heterogeneous condensation take place at the same moment, the absolute wall condensation rate η_{abs} can be expressed as the ratio of the vapour flux towards the walls compared to the total vapour flux:

$$\eta_{abs} = \frac{j'_{\alpha,w}}{j'_{\alpha,w} + j'_{\alpha,p}} \quad (5.22)$$

Using the fact that R_{eq} is equal to $\frac{1}{2}D_{eq}$, now the absolute wall condensation rate can be found by substituting Eq. 5.15 and Eq. 5.21 into Eq 5.22:

$$\eta_{abs} = \frac{12}{12 + \overline{\phi}N_0\pi D_{eq}^2 d_p} \quad (5.23)$$

The particle diameter d_p in Eq. 5.23 is related to the initial mass density of aerosol-forming species $\rho_{\alpha,0}$ as well as to the mass density of the condensate ρ_p. Conservation of mass is applied in order to calculate the mean particle size under assumption of a constant number concentration N_0:

$$d_p = \left(\frac{6\rho_{\alpha,0}}{N_0\rho_p\pi\left(1-\eta_{abs}\right)}\right)^{\frac{1}{3}} \quad (5.24)$$

Due to the fact that Eq. 5.23 is coupled with Eq. 5.24 via the particle diameter d_p, an iterative method is used in order to determine the absolute wall condensation rate η_{abs} and the corresponding final particle diameter d_p.

Experiments performed at a biomass combustion plant with a horizontally moving grate showed that the concentration of aerosols in the flue gas increases from spruce (about 20 mg/Nm^3 related to dry flue gas and 13 vol.% O_2) to bark (up to 60 mg/Nm^3) (Obernberger 2001) These aerosol concentrations, in combination with the

fact that almost all volatilised components are transferred into aerosol particles allows us to use a typical initial aerosol-forming vapour density $\rho_{\alpha,0}$ of 50 mg/Nm^3. Several independent measurements show that the final number concentration of aerosols after the heat exchanger is typically $1 \cdot 10^{13}\ Nm^{-3}$ (Johansson 2001, Christiansen 2000, Jensen 2000). Combining these properties with the fact that a large amount of the aerosol-forming vapours consists of potassium sulfate, K_2SO_4, results in a wall condensation rate as a function of the radius of the tube R_{eq}, depicted in Fig. 5.4. The density of the condensed phase ρ_p, in this case solid K_2SO_4, is 2662 kg/m^3 (Janz 1967)

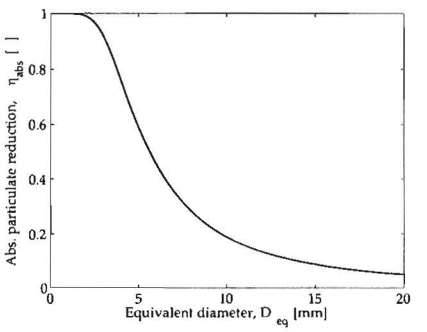

figure 5.4: The effect of varying the tube radius on the absolute wall condensation efficiency, η_{abs}. Initial conditions: $\rho_{\alpha,0}$ = 50 mg/Nm^3, N_0 = $1 \cdot 10^{13}$ and ρ_p = 2662 kg/m^3

From Fig. 5.4 it can be seen that decreasing the tube diameter up to typically 2 mm results in a significant increase of the wall condensation rate. Applying conservation of mass, subsequently decreasing the tube diameter results in a significant decrease of the particulate emission at the outlet of the heat exchanger, which is a desirable result. Theoretically, a wall condensation rate of almost 100 % could be achieved applying a tube diameter smaller than 2 mm. Increasing the diameter results that condensation of aerosol-forming vapours on pre-existing surfaces becomes rapidly the dominating process. Consequently, the assumption having a laminar flow, stated in the beginning of this section, is valid due to the small dimensions of the tubes of the heat exchanger. A suitable candidate to test this hypothesis is the high temperature laminar counterflow heat exchanger.

5.2.2 Heat exchangers

The most common types of fire tube boilers for biomass combustion plants require high turbulence intensity. The Reynolds number, as denoted in Eq. 5.11, is a mea-

sure for the turbulence intensity; the higher the Reynolds number, the higher the turbulence intensity. Increasing the Reynolds number results in an increase of the convective heat transfer between the walls of the heat exchanger and the bulk of the flow, but causes a high pressure drop and consequently requires a lot of energy. [?] Contrary to turbulent flow heat exchangers, laminar flow heat exchangers are based on conductive heat transfer and causes a lower pressure drop, but require a higher number of small channels. The flow inside the heat exchanger is laminar when then Reynolds number is below 2300.

Reducing the tube diameter automatically results in a laminar flow behaviour. Based on this theory, three laminar flow heat exchangers with different dimensions were designed in order to measure the influence of the tube diameter on the particulate reduction. The boundary conditions, with respect to the design of these exchangers were caused due to physical and practical limitations:

- The Reynolds number based on the flue gas velocity inside the heat exchanger should always below 2300 in order to achieve a laminar flow.
- The flue gas temperature after the heat exchanger should be less than 200 ^{o}C in order to make sure that the condensation process of all volatilised species in the flue gas is fully completed. It this way comparison of the particulate reduction with common boiler designs is permitted. Furthermore, a large flue gas temperature difference is required in order to achieve a reasonable heat transfer efficiency, the main essence of a heat exchanger.
- The pressure drop over the heat exchanger should be less than 350 Pa and therefore be comparable with usually applied boiler designs.
- A minimum flue gas velocity of 6 m/s in the measurement section is required in order to perform accurate BLPI measurements.

Two laminar flow shell and tube water cooled heat exchanger and the compact laminar counterflow gas-gas heat exchanger of chapter 3 are used for the experiments. A shell and tube heat exchanger with variable inner tube diameter was developed based on the boundary conditions described in Sec. 5.2.2, see Fig. 5.5. Water flows around the circular tubes. Five and fifteen tubes for respectively tube diameters of 12.50 and 6.20 mm were used for the experiments. A thermostatic valve near the cooling water outlet was used to control the water temperature by flow regulation. The tubes inside the heat exchanger have a fixed length of one metre which and could easily be exchanged by other diameters. The side of the heat exchanger which is directly in contact with the flue gas is covered with a heat resistance insulation plate.

This isolation plate minimises the temperature drop of the flue gas in front of the inlet of the heat exchanger due to radiation. When the inlet temperature of the flue gas is below the condensation temperature of the aerosol forming species, condensation can already occur in front of the heat exchanger, instead of inside the heat exchanger which is an undesirable result.

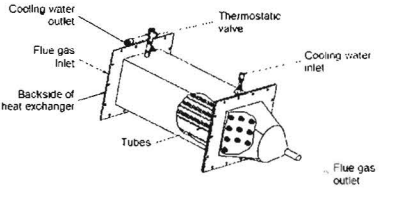

figure 5.5: Schematic picture of shell and tube heat exchanger.

For the calculations, the wall temperature was kept constant at 70 ^{o}C. An adapted equation for the heat transfer coefficient for a thermally and hydrodynamically developing entrance region was applied in order to calculate the temperature profile. Figure 5.6 shows the calculated bulk flow temperature profile inside one heat exchanger tube, using an inlet temperature of 1000 ^{o}C. The inlet velocity, necessary for calculating the heat transfer coefficient in one heat exchanger tube, was calculated in such a way that the velocity in the measurement section was constant at 6 m/s. From Fig. 5.6 can be observed that the calculated outlet temperatures for both tube diameters are below 200 ^{o}C, which satisfied the boundary conditions described in Sec. 5.2.2. Conservation of mass, in combination with temperature dependent physical properties were applied in order to calculate the Reynolds number. From Fig. 5.7, an increasing Reynolds number can be observed while decreasing the flue gas temperature, however the flow is always laminar, indicated by a Reynolds number < 2300. The pressure drop over the heat exchanger is depicted in Fig. 5.8. For both tube diameters, the maximum pressure drop was always below 350 Pa.

5.2.3 Experiments

High quality, chemical untreated wood chips with a typical dimension of a couple of centimetres are chosen as a fuel for the experiments. The composition of this fuel is depicted in Tab. 5.1.

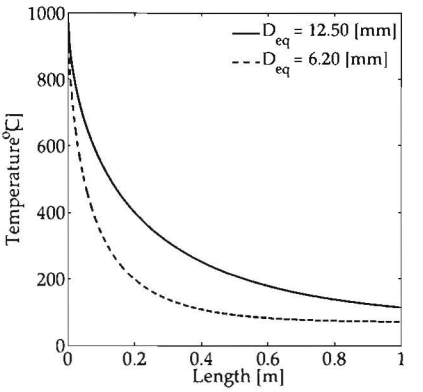

figure 5.6: Calculated flue gas temperature for two different tube dimensions as a function of the length using the water cooled heat exchanger

The biomass combustion plant itself consists of a furnace equipped with a horizontally moving grate, staged air injection, a secondary combustion zone and a flame tube boiler consisting of a fire tube and two ducts of flame tubes with an inner diameter of $1\frac{1}{2}$", see Fig. 5.9. The first and second duct of the flame tube boiler was equipped with respectively 30 and 16 tubes. Combustion temperatures were sampled continuously and controlled by flue gas recirculation below and above the grate. The nominal boiler capacity was 180 kW_{th}.

The heat exchanger was connected with the secondary combustion zone via a slip stream (see Fig. 5.9). The flow through the special designed test heat exchanger and measurement section was established by a flue gas fan. The measurement section after the test heat exchanger consists of a $1\frac{1}{4}$" tube. Measuring devices for measuring the flue gas temperature, velocity, oxygen content and the particulate emissions were installed in this section, denoted with respectively (T), (V), (O_2) and $(BLPI)$ (see Fig. 5.9). The same measurement devices were also mounted in the chimney after the ordinary boiler (see Fig. 5.9). Type K thermocouples were used to measure the temperatures, whereas Prandtl tubes were used for measuring the flue gas velocities. Nine stage Berner-type low pressure impactors (BLPI) and upstream nozzles for iso-kinetic sampling were used for measuring the particulate emissions downstream the test heat exchangers as well as downstream the ordinary boiler. In contradiction to the previous mentioned measuring devices, these impactor measurements are not continuous measurement devices.

A steady state temperature distribution inside the furnace was required for the

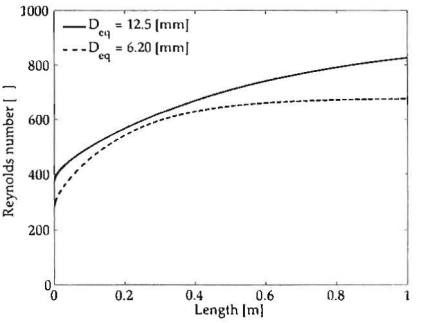

figure 5.7: Calculated Reynolds number for two different tube dimensions as a function of the length using the water cooled heat exchanger

experiments. The flue gas temperatures in the secondary combustion zone were 956.6 ^oC and 949.8 ^oC during the impactor measurements after respectively the heat exchanger and the boiler. The oxygen content was measured in order to normalise the particulate emissions related to dry flue gas with an oxygen content of 13 $vol\%$. The oxygen content after both the test heat exchanger and the boiler for each coupled set of measurements did not change very much, indicated by the low fluctuations. The mean oxygen content after the test heat exchanger and the boiler were equal within the statistical accuracy, as were the normalised particulate emissions. The particulate reductions obtained with the special designed heat exchangers $\eta_{rel,exp}$ are calculated according to the following relation:

$$\eta_{rel,exp} = \left(1 - \frac{M_{test}}{M_{boiler}}\right) \tag{5.25}$$

In Eq. 5.25, M_{test} and M_{boiler} represent the normalised particulate concentration expressed in mg/Nm^3 related to dry flue gas (13 $vol\%$ O_2) after respectively the test heat exchanger and the ordinary boiler. Despite the use of high quality, chemical untreated wood chips, fluctuations of the aerosol-forming species concentration and inhomogeneity of the fuel cannot be avoided. Therefore, several coupled sets of measurements were required in order to determine a statistically proven particulate reduction. The average relative particulate reduction $\overline{\eta_{rel,exp}}$ is depicted in Tab. 5.2 and is calculated according to the following relation:

$$\overline{\eta_{rel,exp}} = \frac{1}{n}\sum_{i=1}^{n} \eta_{rel,exp} \tag{5.26}$$

where $\eta_{rel,exp}$ represents the particulate reduction for one coupled set of impactor

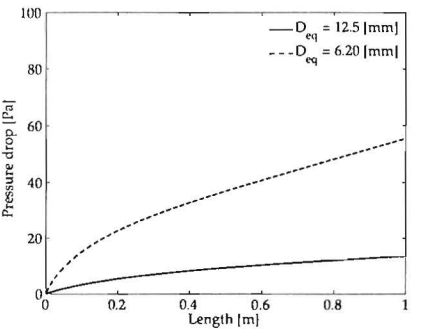

figure 5.8: Calculated pressure drop for two different tube dimensions as a function of the length using the water cooled heat exchanger

measurements and n represents the number of coupled set of measurements. It is noticed that average particulate reduction is nonlinear in the input parameters yields that the calculated average relative particulate reductions, $\overline{\eta_{rel,exp}}\left(M_{test}, M_{boiler}\right)$, is not equal to $\eta_{rel,exp}\left(\overline{M_{test}}, \overline{M_{boiler}}\right)$.

From the experiments is observed that the particulate emissions after the ordinary boiler fluctuates between respectively 19.7 and 60.0 mg/Nm^3. Due to these large deviations, simulations in order to calculate the absolute particulate reductions, η_{abs}, after the aerosol reducing heat exchanger are performed for the minimum and maximum amount of particulate forming species. These minimum and maximum amounts of particulate forming species are calculated from the particulate emissions after the boiler, in combination with the absolute amount of aerosol forming species which ends up in the fire tube and the boiler. The resulting minimum and maximum amount of aerosol forming species in the flue gas for the simulations of the absolute particulate reductions were respectively 22 and 75 mg/Nm^3. The initial number concentration, N_0, for the simulations was always constant at $1 \cdot 10^{13}\ Nm^{-3}$, whereas the particle density, ρ_p, was 2662 kg/Nm^3.

Now the theoretical relative particulate reduction can be described as,

$$\eta_{rel,theo} = \left(\frac{\eta_{abs} - \eta_{boiler}}{1 - \eta_{boiler}}\right) \cdot 100\%, \tag{5.27}$$

where $\eta_{rel,theo}$ represents the theoretical relative particulate reduction. The absolute amount of aerosol forming species which end up in the fire tube and the boiler is represented by, η_{boiler}, and is 12% of the total amount of aerosol forming species in

tabel 5.1: Composition of chemical untreated wood chips used for the experiments determined with a confidential interval of 95 %

parameter	unit	average value
Moisture content	wt. % (w.b.)	20.89 ± 0.83
Ash content	wt. % (d.b.)	0.39 ± 0.04
S	mg/kg (d.b.)	160.8 ± 1.3
Cl	mg/kg (d.b.)	108.0 ± 22.2
Si	mg/kg (d.b.)	53.8 ± 16.6
Na	mg/kg (d.b.)	6.7 ± 0.9
Mg	mg/kg (d.b.)	83.3 ± 7.9
K	mg/kg (d.b.)	822.0 ± 42.3
Ca	mg/kg (d.b.)	815.8 ± 154.3
Zn	mg/kg (d.b.)	2.0 ± 0.7
Pb	mg/kg (d.b.)	10.0 ± 0[a]

d.b. ... dry base; w.b. ... wet base

[a] not detectable

the flue gas. The theoretical calculated and experimental obtained relative particulate reductions are depicted in Fig. 5.10.

Figure 5.10 shows the theoretical determined and the measured particulate reductions. Deviations between the theoretical approach and the experimental results are caused due to several effects which are not taken into account. In the theoretical approach it is assumed that the mass of the initial particulate concentration is negligible compared to the total amount of aerosol forming species. However in reality, homogeneous nucleation and condensation of aerosol forming species on nuclei also occur at temperatures above 1000 ^{o}C. Nevertheless these particulate concentrations are relatively small, but not negligible. This makes that a theoretical calculated particulate reduction of approximately 100 % for hydraulic tube radii in the order of 1 mm cannot be achieved. Another important reason for the shortcoming of the model can be found by the assumption that for the calculation both the nuclei and the wall are below the condensation temperature of the aerosol forming species. However, in reality the wall are always faster below the condensation temperature of the aerosol forming species compared to the bulk temperature. This deviation between wall temperature and bulk temperature increases for increasing tube radii. This effect causes the difference between the theoretical and experimental determined particulate reduction for

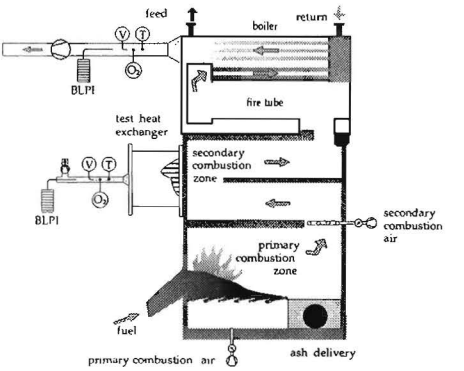

figure 5.9: Experimental set-up of the biomass combustion plant with measurement points after both the test heat exchanger and the boiler

tabel 5.2: Overview of the average particulate reduction, related to dry flue gas, 13 $vol\%$ O_2, determined with 95 % confidential interval. The equivalent tube diameter of the boiler was always 38.8 [mm]

run [-]	D_{eq} [mm]	$\overline{\eta_{rel,exp}}$ [-]
1	2.22	0.72 ± 0.021
2	6.20	0.36 ± 0.055
3	12.50	0.23 ± 0.064

tube radii larger then 5 mm, see Fig. 5.10.

5.2.4 Current status

The conclusion to be drawn from the experiments is that the concept of an aerosol condensor might work and is especially applicable in small (domestic) biomass combustion combustion plants by exchanging the current heat exchanger and an added cleaning system keeping the costs approximately equal.

Current state of the art for domestic biomass fired heating systems are finned steel heat exchangers comparable to the heat exchangers used in oil fired heating systems. By changing to a design as being used in high efficient gas fired heaters a considerable material reduction and thus cost reduction can be achieved while maintaining the desired distance to the wall for desublimation.

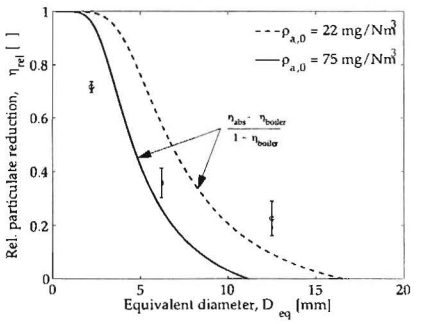

figure 5.10: Theoretical (continuous and dashed line) and measured (o = gas-gas heat exchanger, □ = water cooled heat exchanger) particulate reductions compared to the ordinary boiler design (η_{boiler} = 12%). Measured particulate reductions are determined with a 95 % confidential interval, related to 13 *vol*% O_2 in dry flue gas.

As the pitfalls in the development of this type of heat exchanger are known from the high temperature laminar counterflow recuperator and the condensing heat exchangers in both gas-fired heaters and balanced ventilation units, further development of the aerosol condensor is done in-house. The main issues here are thermal design to minimise temperature induced stresses in combination with the material selection and production methods.

5.3 Centrifugal gas cleaning

Increasing shortages in world natural gas supply over the next few decades could be mitigated if existing large but contaminated gas fields could be utilised in an environmentally responsible manner (Wissen 2006). Current large throughput gas cleaning processes are not able to deal with highly contaminated gas .elds. Amine treatment is typically used for removing these contaminants - CO_2 and H_2S - from gas, but is not economic or practicable for highly contaminated gas, that is, where the concentrations of CO_2 and H_2S are above ca. 10 and 5 % respectively. Together with Royal Dutch Shell a gas centrifuge was investigated as an alternative process (Wissen 2005) drawing on previous experience with uranium enrichment and the RPS, but a purely gaseous is too slow for practical application.

Previously established analytical approximations are not applicable for natural gas decontamination. Numerical simulations based on the batch case show that al-

though the separative strength of the centrifuge is quite good, its throughput is very limited. Both enrichment and throughput are only a function of length and peripheral velocity. A centrifuge with a length of 5m and a peripheral velocity of approximately 800 m/s would have a throughput of 0.57 mol/s and a product flow of 0.17 mol/s. These numbers are calculated with the assumption that the centrifuge is refilled and spun up instantaneously. The results for the countercurrent centrifuge show how the production rate varies as a function of internal circulation, product-feed ratio, peripheral velocity and centrifuge length and radius. Under conditions similar to those of the batch case the production is approximately half compared to the batch case, i.e., 0.08 mol/s. Optimization can yield a higher production at the cost of lower enrichment. Considering the current natural gas prices and the low production rate of the centrifuge, it is certain that the gas centrifuge will not generate enough revenue to make up for the high investment costs.

Increasing the pressure is not that helpful for component separation in the gas phase, because to a first approximation the product of diffusion and pressure pD is constant, that is, at higher pressure the diffusion constant decreases (Golombok 2004). However, at the higher pressures generated in a centrifuge, there is a second much more dominant mechanism which will also cause separation, namely condensation due to wall condensation.

5.3.1 Centrifugation with wall condensation

Figure 5.11 shows the condensation curves at different temperatures for various mixtures of methane as a function of the concentration of CO_2 in the mixture.

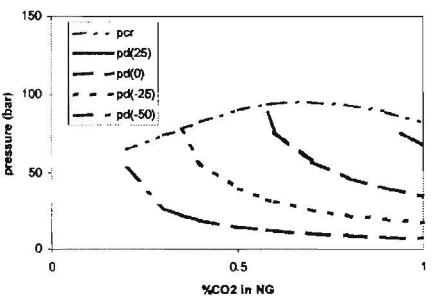

figure 5.11: condensation curves at different temperatures as a function of percentage CO_2 in gas

There are, in the case of a condensing centrifuge, two mechanisms for condensa-

tion. Pure compression work corresponds to moving up the vertical pressure line: for example, with a 50/50 CO_2/CH_4 mixture at 25 °C, if we increase the pressure (for example, along the radius of the centrifuge rotor) then around 40 bar, condensation of a CO_2 rich waste liquid starts to occur. Pure enrichment work corresponds to moving horizontally to the right whereby the local concentration of CO_2 at any point is increased as a result of centrifugally induced diffusion. For example, if we started with a 25 bar 50/50 mixture of CO_2/CH_4 and allowed CO_2 enrichment to proceed near the rotor wall, then around $x_d = 0.6$, condensation will occur.

The core idea is to operate the centrifuge with a sufficiently high feed pressure that the when the centrifuge is spinning, condensation will occur (figure 5.12). Initially the process runs identically to the gas-gas centrifuge. However, at one point along the radius, at $r = r_d$, the pressure is sufficient that the condensing pressure is reached. Initially, when the pressure profile is (almost instantaneously) established, we still have a uniform composition throughout the cylinder, because the diffusion process concentrating CO_2 near the wall occurs more slowly than the fast pressure generation profile - at this point rd is determined purely by the partial pressure. Subsequently, centrifugally driven mass transfer occurs of CO_2 from the center to the outer region of the centrifuge. This net transport of CO_2 has the effect of shifting condensation closer to the center to the equilibrium value.

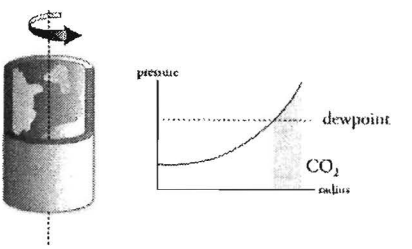

figure 5.12: principle of operation for condensing centrifuge

The region where condensation occurs is shown in Figure 2 by the shaded area, where the pressure exceeds that required for condensation of liquid (referred to as the "dewpoint"). The condensing separation is faster than pure gas-phase separation because CO_2 is removed from the gas phase. This will act to further drive the mass transport of CO_2 from the center to the outer radial annulus.

In a gas centrifuge, the dimensionless partial differential equation describing the

time-dependent mole fraction distribution of one component is (Cohen 1951)

$$\frac{\rho r_0^2}{\rho D}\frac{\partial x_i}{\partial t} = \frac{1}{r^*}\frac{\partial}{\partial r^*}\left(r^*\frac{\partial x_i}{\partial r^*} + (A_2 - A_1)x_1(1-x_1)(r_0 r^*)\right)^2 \tag{5.28}$$

where D is the diffusion coefficient, ρ the mixture mass density, r_0 the wall radius, r^* the dimensionless radial coordinate, defined as $r^* = r/r_0$, t denotes time, x_i the mole fraction of component i. Whereas for a centrifuge where only gas-gas separation occurs, the boundary conditions are constant, in a condensing centrifuge these vary continually and are a function of composition. Condensation occurs, resulting in liquid, which because of its higher density and the large centrifugal forces, is pushed to the wall, where it is extracted. This removal of mass from the system results in new boundary conditions, those for the gas/gas case are no longer valid. The feed concentration is equal to the condensation concentration for the wall pressure at $t = 0$

$$x_{feed}(r^*, t = 0) = x_{dewpoint}(p_{wall}(t = 0)) \tag{5.29}$$

Any liquid that is formed by condensation is considered to be removed instantaneously. Since this will only occur at the wall, it is sufficient to correct the boundary conditions at the wall

$$\text{if } p_{wall} \geq p_{sat} \text{ then } x(r_0, t) = (P_{wall}(t)), \quad \text{for } 0 < z^* < 1 \tag{5.30}$$

Figure 5.13 shows that condensation processes yield a product flow that is approximately twice that of the gas/gas centrifuge. The doubling of the removal rate due to condensation of a centrifugally enriched mixture is still small compared to the pure compression work which removes a large amount of the CO_2. For pure centrifugal condensation, the rate is still dependent on the CO_2 molecules diffusing to the wall where they concentrate sufficiently to decrease the local condensing pressure below the local quasi-stationary pressure. The process, thus, still depends on diffusion, but over a smaller distance. Experiments (Golombok 2005) indicate that an improvement of several orders of magnitude is required to make gas/ gas centrifugation a viable option for removing contaminating gases from natural gas streams. Condensation by compression has more potential, since it is not a diffusion dominated process. However, since the gas centrifuge is not a dedicated compression device, and the benefits of the centrifugal enrichment are limited, it is better to seek for other means to optimize this process.

5.3.2 Cooling and separating

A way to accelerate the process is by employing phase change: changing the thermodynamic state of the mixture such that the CO_2 is transformed to the liquid state.

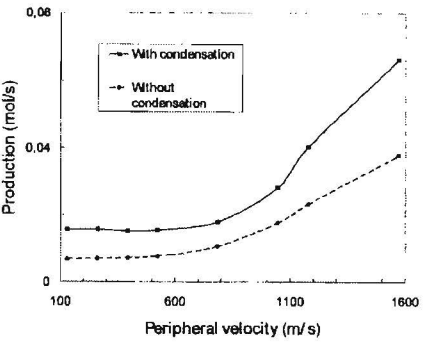

figure 5.13: principle of operation for condensing centrifuge

This idea resulted in the novel process shown in figure 5.14 and consists of two steps:

- Cooling the gas to a temperature whereby the gaseous contaminant becomes liquid in the form of micron sized droplets.
- Separating the mist from the gas by the rotational particle separator, this is the core innovation in the process

To achieve feasible gas/gas separation in an economically attractive manner, one of the components has to be transformed into a phase capable of forming particles. This can be achieved by cooling and condensation. Since gas in reservoirs is already compressed (130-450 bars is typical), then expansion can be used to attain the necessary cooling for contaminant condensation. Even the reduced pressures available top hole (80-130 bar) are still sufficient to drive expansion cooling. An expansion turbine is in most cases preferred to techniques employing expansion by acceleration such as the Joule-Thomson process. The turbine can be used to drive a compressor to bring the gas back to system pressure. In addition, after the turbine the velocity of the gas can be kept relatively small, cooling occurs by withdrawing power from the gas rather than from gas-speed. This avoids the risk of heating up by internal friction of the gas - the ultra-fine condensed droplets could easily evaporate. The separation of components using condensation to form a phase boundary is well established (Buonicore 1984) The method used is invariably reduction of temperature, although usually by heat exchange rather than the direct expansion method which we apply. The latter is standard in preparation of for example cryogenic gases or LNG. However the main problem which we address here is the spatial separation of the two phases which are often intimately dispersed and difficult to split into apart streams.

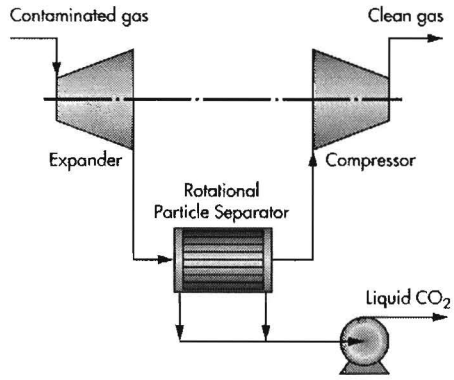

figure 5.14: schematic of condensed contaminant centrifugal separation

The low pressure side of the expansion refers to a condition which is sufficient to lead to cooling so that two separate phases form. The product phase is gaseous and enriched in methane (and thus depleted in CO_2). The waste phase is liquid and is enriched in CO_2 and depleted in methane. Of course this process does not spontaneously lead to a nicely separated liquid and gas phase - a mixture of fine CO_2 rich droplets in a methane riched gas forms. Between the expansion and separation steps the microdroplets have to grow to a sufficient size that they can be separated. This so-called "induction" process is known for knock-out vessels of for example, condensate components using cyclones. However these devices can only be used at high volume throughputs for droplet sizes greater than around 15 micrometer and with much lower mass loadings than are present in contaminated gases. (Removal of smaller droplets is possible but only for extremely low throughputs, so-called micro-cyclones.) In our case droplet sizes will be smaller than this with mass loading much higher than condensate in gases.

Consider a feed flow(Q_f) of contaminated gas which is split into a cleaned-up stream (Q_c) and a waste stream (Q_w) of CO_2 rich liquid. Conservation of mass requires that input is the same as output

$$Q_f = Q_c + Q_w \tag{5.31}$$

a mass balance on the methane component yields

$$x_f Q_f = x_c Q_c + x_w Q_w \tag{5.32}$$

The most obvious condition is that we wish to have the highest concentration x_p of methane possible in the product stream. Simultaneously we need to minimise the

loss of incoming feed methane into the waste stream so that the maximum number of molecules of methane in the feed end up in the product stream. This corresponds to maximising the recovery r given by

$$r = \frac{x_c Q_c}{x_f Q_f} = \frac{x_c(x_f - x_w)}{x_f(x_c - x_w)} \tag{5.33}$$

The recovery is purely a function of the methane concentrations x_i: this can be seen by dividing eq. 5.31 and 5.32 by Q_f and solving for the two variables Q_c/Q_f and Q_w/Q_f. Since we specify the input concentration, the recovery is then purely a function of the product and waste concentrations derived from the thermodynamics. We calculate the methane content in the clean and waste streams (x_c and x_w) from the pressure and temperature p, T however there are a large range of feasible p, T conditions with corresponding solutions for x_C and x_w. We need to find realistic values which also optimise the recovery r, at the same time.

Consider a 50/50 mixture of CH_4/CO_2, which is representative for contaminated gas and which we use as a basis of design. We wish to ascertain the optimum values of product concentration x_c and methane recovery r for a variety of pressures and temperatures (Shavit 1995). The lower bound for these conditions can be obtained from an evaluation of the phase boundary for pure carbon dioxide as shown in fig. 5.15 which shows the freeze-out curve. Most materials have a triple point below atmospheric pressure with normal melting and boiling points corresponding to the temperature points at 1 atm. (i.e. ca. 1 bar) where solid-liquid and liquid-gas transitions occur respectively. However for CO_2 the triple point is actually above atmospheric pressure. For CO_2 p_t=5.1 bar and T_t=-56.6 °C, the subscript t referring to triple point conditions. Fig. 5.15 shows that operation in the liquid regime requires that we be above 5 bar and -56 °C and this forms the minimum value for our thermodynamic conditions. The maximum value is set by reasonable pressures for the expansion and bearing in mind that this will be after the cooling expansion phase.

Fig. 5.16 shows the methane recovery r plotted against methane product concentration x_c for a range of pressures and temperatures. This was obtained from an extended cubic equation of state simulation based on the Soave-Redlich-Kwong model. This shows that in a single separation step it is possible to get high methane recoveries however the problem is maximising the methane concentration in the product stream. At the ideal point $x_c \approx r \approx 0.85$, the turbine inlet pressure would be 600 bar which is clearly unrealistic. In general, given the restrictions for pipe wall thickness and corresponding safety and handling considerations, we would wish to be below 200 bar at the inlet.

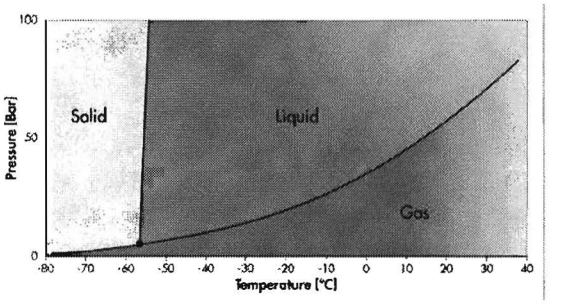

figure 5.15: Phase diagram for CO_2 showing triple point at 5 bar and -58 °C

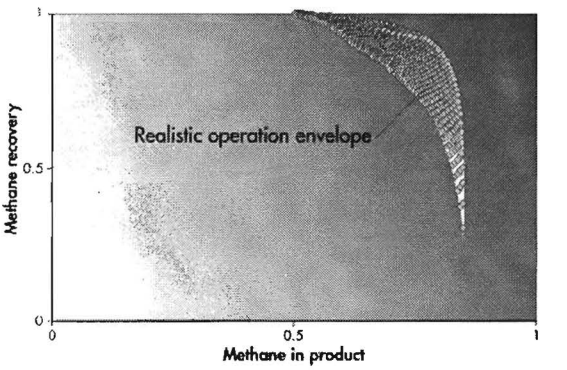

figure 5.16: Methane recovery as a function of methane concentration in product stream, displayed for a variety of pressure and temperature separation conditions

The question then is to choose the optimal realistic p, T values for the operation of the separator. If there is too much expansion, the temperature may be sufficiently low but the pressure will be too low for liquefaction to take place. If we restrict the expansion process we may have sufficient pressure but not enough cooling and hence insufficient yield. An examination of the various p, T conditions coupled to the parameters above shows that an expansion to around the regime 25-30 bar providing the inlet pressure is above 100 bar gives significant phase separation.

From a practical engineering standpoint, an inlet pressure of 102 bar to the expander is sufficient to recover ca. 95 % of the methane into the product gas stream with a concentration of around 67 %. Note that phase separation is only initiated by the expansion and is only complete by the end of the induction period - here the liquid state is materialised in droplets of a few microns in size. Subsequently, the spatial separation of the dispersed waste and purified product takes place in the rotational particle separator. The foregoing analysis assumes that the CO_2 rich liquid is already in the dispersed waste material of flow rate W which will be spatially concentrated and separated to the waste stream in the rps.

The droplet removal needs to occur within a very short time and for very small droplet sizes. In principle a standard cyclone would be capable of doing this, however for very small droplet sizes a long residence time is required and this is difficult to attain when the throughput is very high. The main advantage of the rotational particle separator (rps) is that it enables this to happen much more quickly (i.e. at much higher throughputs) and for much smaller droplets than is the case with other centrifugal methods such as the cyclone or the gas centrifuge as is shown in the next section.

5.4 RPS versus Cyclone

The axial cyclone, also known as vortex tube or uniflow cyclone, consists of a stationary cylindrical pipe which contains at the entrance stationary vanes or blades: figure 5.17 (Wissen 2006). Fluid which enters the pipe and passes through these blades obtains a swirling motion. Dispersed phase entrained in the fluid obtains this swirling motion as well. Having a density which is higher than the density of the carrier fluid, the dispersed phase will be subjected to a centrifugal force which causes it to move radially towards the cylindrical wall. It leaves the device via outlets so situated at the end of the pipe constituting the axial cyclone. Detailed investigations of swirling flows in pipes (Svarovsky 1984) have shown that the tangential velocity vt changes its radial shape with axial distance from the point where the swirl is initiated. While

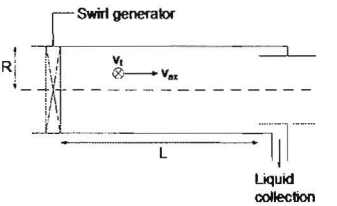

figure 5.17: schematic drawing of the axial cyclone

initially the radial profile may be more like that of a free vortex, with axial distance tangential velocity profiles evolve more towards that of solid-body rotation. At the same time the strength of the swirling motion decays as a result of wall friction. In the present analysis we shall assume that v_t is constant with respect to r. This is some kind of compromise between solid body rotation and the free vortex. The axial decay is described by an exponential function in accordance with experimental observations.

$$v_t = v_{t0} \exp\left(-\frac{z}{R}\beta\right) \tag{5.34}$$

where z is axial distance, R radius of cyclone wall and β an empirical factor which for conditions existing in cyclones is about 0.05. Furthermore, it is assumed that the axial velocity of the carrier fluid in the cyclone is constant with respect to radius, $v_a = v_{a0}$. Again this is a reasonable compromise for the various profiles encountered in measurements. Tangential and axial velocity of dispersed profiles are to first order equal to those of the carrier fluid. The axial position of a particle is thus given by $dz/dt = v_{a0}$, which upon integration yields $z = v_{a0}t$, where it is assumed that at time $t = 0$ the particle is at the entrance of the cyclone, i.e. $z = 0$. While a particle follows to first order the gas in axial and tangential direction, it will migrate in radial direction according to equation (4.4). Noting that its radial position r is given by $(d/dt)r = v_m$, implementing (4.4) and (5.34), and using $z = v_{a0}t$ to eliminate z, gives:

$$r\frac{dr}{dt} = \frac{(\rho_p - \rho_f)d_p^2 v_{t0}^2}{18\mu} \exp\left(-\beta\frac{v_{a0}}{R}t\right) \tag{5.35}$$

Upon integrating one obtains

$$r^2(t) = \frac{2(\rho_p - \rho_f)d_p^2 v_{t0}^2}{18\mu}\left(\frac{R}{\beta v_{a0}}\left(-\exp\left(-\beta\frac{v_{a0}}{R}t\right)+1\right)\right) + r^2(0) \tag{5.36}$$

where $r(0)$ is the radial position of the particle at the entrance of the cyclone. The axial velocity of carrier fluid and particles is taken constant with respect to radius.

It implies that 50 % of particle which enter the cyclone will be present in the area $r > R/\sqrt{2}$, 50 % in the area $r < R/\sqrt{(2)}$. The diameter of the particles which has a probability of 50 % of reaching the collecting wall in a cyclone of length L can therefore be calculated from (5.36) by taking for $r(t) = R, r(0) = R/\sqrt{2}$ and $t = L/v_{a)}$. It results in

$$d_{p50\%} = \sqrt{\frac{18\mu R}{4(\rho_p - \rho_g)v_{t0}^2} \frac{\beta v_{a0}}{1 - \exp\left(-\frac{\beta L}{R}\right)}} \tag{5.37}$$

Energy consumption occurs through the pressure drop the fluid undergoes when flowing through the cyclone. One can assume that the kinetic energy use of the swirl which is induced at the entrance and all radial pressure build-up by swirl is eventually lost: the irreversible pressure loss can be taken equal to ρv_{t0}^2. The total energy loss can be calculated by integrating over all radial positions:

$$\dot{E} = \int_0^{2\pi} \int_0^R \rho v_t^2 v_{ax} r dr d\theta \tag{5.38}$$

For v_{t0} and v_a constant with respect to r, the result is: $\dot{E} = \rho v_{t0}^2 Q$, where Q is volume flow through the cyclone: $Q = v_a \pi R^2$. Energy consumption per unit mass flow $\epsilon = \dot{E}/(\rho_f Q)$ then reads as: $\epsilon = v_{t0}^2$. The pressure drop over the cyclone relates to ϵ as $\Delta p = \epsilon \rho_f$.

The degree of swirl imposed at the inlet of the cyclone is in general limited. For large values of the ratio of swirl velocity to axial velocity a reverse flow in the centre of the cyclone will appear which leads to mixing of separated material. To avoid this, the swirl velocity is limited to a magnitude which is twice the axial velocity: $v_{t0} = 2v_{a0}$. The residence time of the fluid in the cyclone is given by $\tau = L/v_{a0}$. It is now possible to express $d_{p50\%}$ as a function of the volume flow of carrier fluid, Q, which is to be filtered:

$$d_{p50\%}^2 = \frac{9\mu}{(\rho_p - \rho_f)\pi} \frac{Q}{\tau \epsilon^{3/2}} \frac{\gamma}{1 - e^{-\gamma}} \tag{5.39}$$

where

$$\gamma = \beta \left(\frac{\pi}{8}\right)^{1/2} \frac{\tau \epsilon^{3/4}}{Q^{1/2}} \tag{5.40}$$

In the above relation two important design parameters occur: the residence time τ which is a measure for the size of the device and thereby for the investment costs, and the energy consumption ϵ which determines to a large extent the operating costs.

The separation process taking place in the channels of the RPS is equal to that in the cyclone. The diameter of the particle which is collected with 50 % probability can

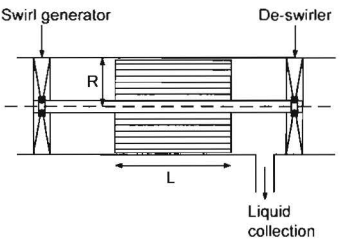

figure 5.18: schematic drawing of the RPS

be calculated by considering the radial position of the channel $R_{50\%}$ at which a cut of 50 % of the throughput occurs. The filter element has an inner radius of δR, in which case $R_{50\%} = \sqrt{1+\delta^2}/\sqrt{R/2}$. Now $d_{p50\%}$ can be calculated by considering the path of the particle which enters the channel halfway its radial height d_c, the channel itself being located at $r = R_{50\%}$. Tangential velocity equals Ωr where Ω is the angular speed of the rotating element; axial velocity v_a is constant with respect to r so that $v_a = Q(\pi R^2(1-\delta^2))^{-1}$. One then obtains

$$d_{p50\%} = \frac{9\sqrt{2}\mu d_c}{(\rho_p - \rho_f)\sqrt{1+\delta^2}(1-\delta^2)} \frac{Q}{\pi\Omega^2 L R^3} \tag{5.41}$$

The energy consumption of the RPS consists of two parts. First there is the energy loss because of rotation. Downstream of the filter element a stationary de-swirler is installed (figure 5.18) which recovers about half of the energy associated with swirl. Therefore the irreversible pressure drop along each stream line passing through the rotating filter element is taken equal to half of that of the cyclone: $1/2\rho v_t^2$, where $v_t = \Omega r$. The second source of energy consumption is pressure drop in the small-sized channels of the RPS. Total energy consumption per unit volume flow, or irreversible pressure drop, can be expressed as $\Delta p_{RPS} = \Delta p_t + \Delta p_{ch}$, where $\Delta p_t = 1/4\rho(\Omega R)^2(1+\delta^2)$ is irreversible pressure drop because of swirl evaluated over the whole filter element according to equation (5.38 taking $v_t = \Omega r$ and $v_a = v_a 0$. Irreversible pressure drop over the channels can be described according to $\Delta p_{ch} = \rho v_a^2 f L/(2d_c)$, where f is friction factor. Here we disregard the extra pressure losses due to entrance effects as well as blockage of channels - in practice these amount to $< 1\%$ of the channel pressure drop. However even when allowing for partial restrictions due to liquid formation in the channels, we show below that such terms contribute less than 15% of the total pressure drop which has its origin predominantly in the swirl term. The correction due to entrance and possible blockage is therefore extremely small and we therefore restrict our channel losses to the friction factor which

depends on Reynolds number of the flow (Bird 1960). For Re$< 10^5$ one can take the Blasius formula: $f = 0.316Re^{-0.25}$.

With the presented formulae we can transform equation (5.41, depending on L, R, v_{a0} and Ω, to a new equation in which $d_{p50\%}$ depends on Δp_l, Δp_c, τ, and Q:

$$d_{p50\%} = \sqrt{\frac{9\mu d_c^{5/6}(1+\delta^2)^{1/2} f^{1/6}\rho^{7/6}}{2^{5/3}(\rho_p - \rho_g)\pi^{1/2}(1-\delta^2)^{1/2}\Delta p_{ch}^{1/6}\Delta p_l} Q^{1/2}\tau^{5/6}} \tag{5.42}$$

It is seen that $d_{p50\%}$ becomes smaller (better separation performance) with increasing dissipations Δp_l and Δp_{ch}. The best situation is one were the ratio of both dissipations, $x = \Delta p_{ch}/\Delta p_l$, has a value such that the total dissipation is a maximum and the value $d_{p50\%}$ is a minimum as well (maximum separation performance). To calculate this ratio it is noted that $d_{p50\%} \sim ((\Delta p_{ch})^{1/6}\Delta p_l)^{-1} = ((\Delta p_{RPS})^{7/6}x^{1/6}(1-x))^{-1}$, which reaches a minimum for $x = 1/7$, so that $\Delta p_{ch} = 1/7\Delta p_{RPS}$, and $\Delta p_l = 6/7\Delta p_{RPS}$. It is noted that the minimum value op $d_{p50\%}$ is only slightly sensitive to deviations of x from its optimum value of $1/7$. For example a deviation of x of 20 % from its optimum value leads to an increase of $d_{p50\%}$ of 0.2 %. The expression for $d_{p50\%}$ now becomes

$$d_{p50\%} = \sqrt{\frac{9\mu d_c^{5/6} f^{1/6}}{2^{5/3}(\rho_p - \rho_g)\pi^{1/2}} \left(\frac{1+\delta^2}{1-\delta^2}\right)^{1/2} \epsilon^{-7/6} Q^{1/2}\tau^{-5/6}} \tag{5.43}$$

where $\epsilon = \Delta p_{RPS}/\rho_f$ and

$$f = \left[0.316\left(\frac{2}{7}\right)^{-\frac{1}{12}} \rho_f^{-\frac{3}{12}} d_c^{-\frac{1}{3}} \mu^{\frac{1}{4}} \epsilon^{-\frac{1}{12}} \tau^{\frac{1}{12}}\right] \tag{5.44}$$

From equation 5.43 it is seen that $d_{p50\%}$ of the RPS becomes smaller with d_c. In practice, however, d_c is limited by fabrication and operational requirements to about 1 mm. It is further seen that $d_{p50\%}$ decreases with δ. But the dependence is weak; in practice the inner radius of the filter element is taken about $1/2$ to $1/3$ of the outer radius. For given values of d_c and δ, equation 5.43 specifies $d_{p50\%}$ of the RPS versus flow Q with residence time τ and specific energy consumption ϵ as parameters.

Equations (5.39 and (5.43) can be used to compare the separative performance of the cyclone and RPS as a function of volume flow Q at equal values of specific energy consumption ϵ and residence time τ (=building volume). The result for separation of water droplets ($\rho \approx 1000$ kgm^{-3}) from air at ambient conditions ($P = 1$ bar, $T = 20^o$C, and $\rho = 1.2$ kgm^{-3}) is shown in figure 5.19, which displays $d_{p50\%}$ for both units as a function of flow in actual cubic meters per second. Residence time and specific

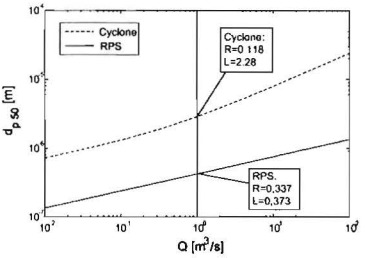

figure 5.19: $d_{p50\%}$ as a function of volume flow

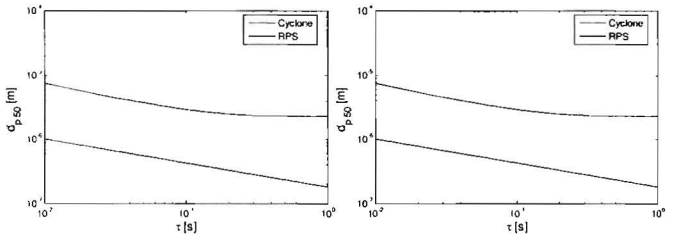

figure 5.20: $d_{p50\%}$ as a function of residence time and energy consumption

energy consumption are set at values commonly found in practice of $\tau = 0.1$ s and $\epsilon = 2$ kJkg^{-1} which corresponds to $P \sim 2500$ Pa at $P = 1$ bar and $T = 20^{o}$C. The RPS channel diameter and inner/outer radius ratio are taken equal to the standard production values of $d_c = 1.5$ mm and $\delta = 0.5$.

As can be seen, the smallest particles collected by the RPS are an order of magnitude smaller than those collected by the axial cyclone. To resolve such small particles, a conventional cyclone would require extremely fast supersonic peripheral gas velocities. This is associated with very high energy consumption - however note that we have specifically excluded this regime: we have restricted the specific energy consumption and limited the swirl number to 2 - this ensures that tangential velocities stay an order of magnitude smaller than acoustic velocities. In fact, the RPS can take a throughput 10000 times higher than a cyclone when it comes to collecting 1μm sized droplets. Figure 5.20 shows the results for varying values of residence time and energy consumption respectively. Throughput is fixed here at a moderate value of 1 m^{3}s^{-1}. The results for the RPS are in both cases again an order of magnitude better than that of the axial cyclone. Both units show a large increase in performance for higher residence time and energy consumption. Although figures 5.19 and 5.20 are plotted using the properties of air at ambient conditions, they are approximately

valid for all gases at a large pressure range, since the properties of the carrier fluid are of minor influence as follows from eq. 5.39 and 5.43. The influence of pressure is seen in both cases to be inversely proportional to the difference between the particles and gaseous phases i.e. $\rho_p - \rho_g$. For a carrier gas pressure of 100 bar the density difference term in these equations still has approx. 90 % of the value it has for a carrier gas at ambient pressure, i.e. $\Delta\rho = 900$ kgm^{-3} instead of 1000 kgm^{-3}3. Using eqs. 5.39 and 5.43 one can see that in this case this would lead to an increase in $d_{p50\%}$ of about 6%, which is only marginal. When the carrier fluid is a gas, then this inverse density term is at best a second order correction for the range of pressure conditions normally encountered in practice - the justification for this is the range of surface facility inlet manifold pressures - these are typically in the range 70-130 bar. Thus the performance of the separator at 1 m^{3}s^{-1} can correspond to either a gas flow at 1 bar or at 100 bar equivalent to 100 normal m^{3}s^{-1}. (The latter corresponds in imperial production units to 300 MMscfd - a good sized gas well.)

The only situation where the inverse term is important, is when the carrier fluid is a liquid instead of gas at ambient pressure. An example is the application of oil-water separation when decrease of the pressure difference term is of course substantial. This leads to a shift upwards, i.e. larger $d_{p50\%}$, for the results in fig. 5.19- 5.20 which remain universally applicable. This effect is equally large for both the cyclone and the RPS as follows from eqs. 5.39 and 5.43.

In addition we note that for application to contaminated gas, that condensed hydrocarbon fluid droplets are significantly more compressible than water. This compressibility actually means that it is favourable to carry out the processes at higher pressure because any increase in the density gas is more than offset by the significant increase in the fluid density in eq. 5.43. This all the more so for contaminated gas since the condensed waste liquid CO2 contains typically ca. 10% methane gas which makes the liquid phase even more compressible. The relative advantage of using the RPS system for cleaning gas is seen in fig. 6 where the effect of pressure is seen to be large at the levels of flow associated with gas well production. For this example of industrial relevance the units of flow are the gas production industry norm: MMscfd (millions of standard cubic feet per day -for SI conversion 1 MMscfd=0.33 norm m3/s.)

The results for both units are a function of volume flow and not of mass flow. This means that an increase in pressure will not only lead to a smaller unit, at constant residence time, but also to a better separation performance at equal mass flow. For instance, from fig. 5.19 it can be seen that for air at ambient pressure carrying water droplets the $d_{p50\%}$ of a well designed RPS with a throughput of 1 m^{3}s^{-1} is equal to . Increasing the pressure to 10 bar leads, at equal mass flow and for an ideal gas, to

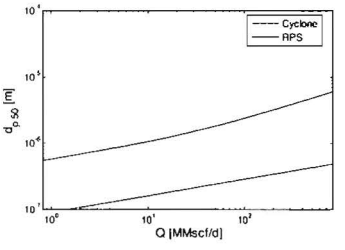

figure 5.21: $d_{p50\%}$ as a function of normal (i.e. molar) flow for a 50/50 CH4/CO2 separation system at p=27 bar, T=-47 C

a volume flow of 0.1 m^3s^{-1}. Fig. 5.19 shows that for this flow the $d_{p50\%}$ for an RPS reduces to 0.2 μm. At the same time the volume of the RPS has decreased equally with the volume flow, to 0.1 times the original size. If the original separation performance, before the pressure increase, was satisfactory, then one could also, by increasing the pressure, reduce the residence time or energy consumption, without affecting the separation performance. This leads to an even smaller device or to lower operational costs.

Application of the RPS implies the introduction of rotating equipment. Complications involved with rotation, however, are limited. Peripheral speeds of the rotating body are limited, typically to 50 m/s which is far below the speeds where structural integrity might become problematic. In fact, the speeds are limited because of constrains on energy consumption (value of ϵ). Sealing problems of shafts penetrating through stationary walls do not exist either. The RPS is internally driven by the swirl of the gas entering the rotating body. External drive by a motor is not necessary. In summary, the complexities involved with rotation are rather modest; they are outweighed by the advantages being the possibility to collect micron-seized particles in a device of limited dimension.

5.5 Current status

The processes discussed here part of a joint development by Royal Dutch Shell and the university. Currently a demonstration set-up is being constructed by Shell. The prototype RPS was designed and tested by the EUT (figure 5.22 drawing on the experience gained in the development of the naturally driven RPS for gas cleaning sec. As the economic impact of the process can potentially be high, i.e. exploitation of the large but contaminated gas reservoirs near Indonesia might become economically viable, subsequent development of the basic idea is largely kept out of open literature.

As the initial notion of cooling and subsequent separating was already indicated in one of the first patents regarding the RPS, the inventor took out a subsequent, more detailed patent on the process thus being able to influence further development to a certain extend.

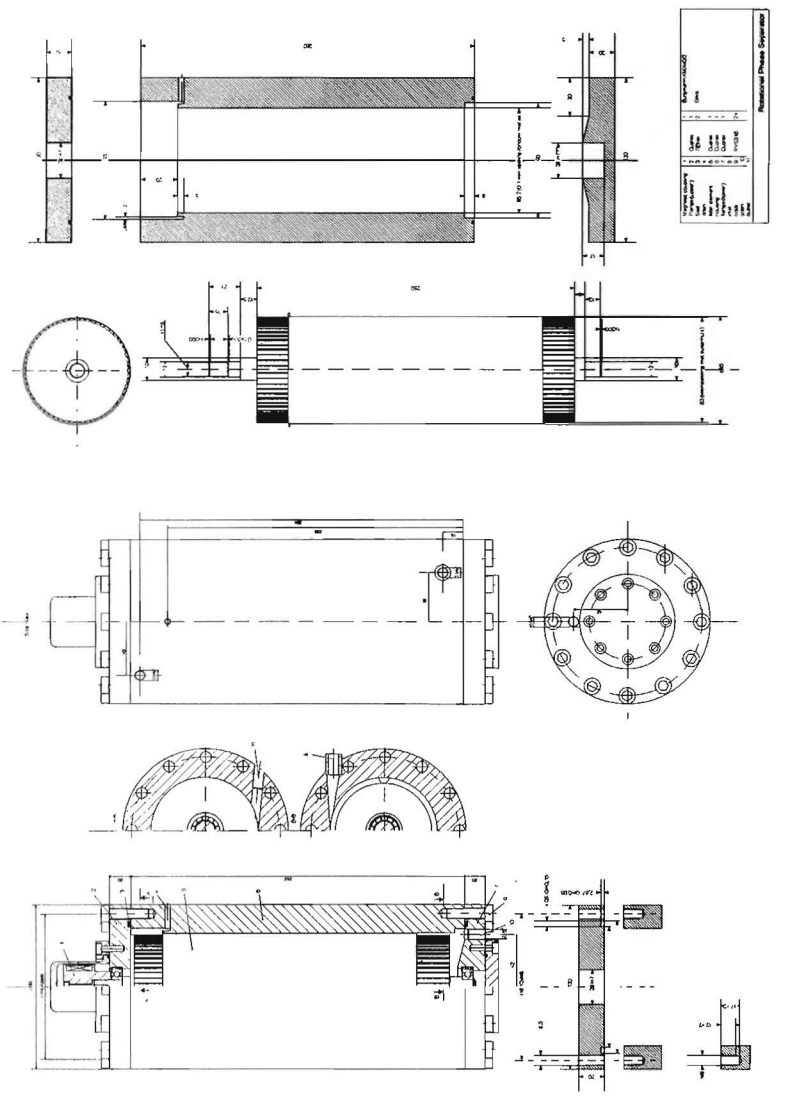

figure 5.22: Protoype RPS for natural gas cleaning

6 Closure

The cases discussed illustrate that although science plays a critical role in in innovations, it is not necessarily the driver of new products, processes, and services. New ideas for innovation can stem from many sources, including new manufacturing capabilities and recognition of new market needs, as well as scientific and technological discoveries. Innovation does not necessarily proceed linearly from basic scientific research to product development; it is an iterative process of both matching market needs to technological capabilities and conducting research to fill gaps in knowledge, whether during product conception, product design, manufacturing, marketing, or other phases of the innovation process. Innovation is an iterative process that responds to both demand and supply side forces. Successful innovations tend to undergo extensive modification during development. This is due to changes in perceptions of user requirements and of producers' abilities to offer the product, process, or service with the necessary features at an acceptable cost. Innovators continually try to find new applications for science and technology and ways of satisfying market demands, but not until technology push and market pull are combined do innovations find market success.

Research activities can be distinguished in those to explore and develop a new body of knowledge and those pursued to solve particular problems in the development process. In the former case, the goals of the research are often diffuse and the benefits are difficult for any one company or institution to monopolize. In the latter case, research results are more targeted and the results easier to appropriate. Researchers, therefore, tend to collaborate more widely on the former type of R&D and to share information more freely. In the latter case, researchers will usually try to solve the R&D problem with internal resources or with limited use of outside capabilities.

Technology is not merely the application of knowledge generated by scientific activity; it is a body of knowledge about certain classes of events and activities. It is a knowledge of techniques, methods, and designs that work, and that work in certain ways and with certain consequences, even when one cannot explain exactly why.

Science and technology are best thought of as two parallel streams of cumulative knowledge that have many interdependencies and cross relations, but whose internal connections are much stronger than their cross connections. As a result, technological progress is not necessarily dependent on scientific progress or the other way around.

Though all the innovations presented here, have their origins in basic scientific research in the field of heat and mass transfer, exploitation of the ideas have only been possible as the researchers had direct access to the technology used in the field of energy technology. Consequently the major applications of the discussions are to be found in that field and less so in related areas as for instance food processing or the fine chemical industry. This can be attributed to the background of the inventors: when introducing a new technology, it is imperative to introduce only one new element at the time. Thorough (inside) knowledge of the state of the art in a specific field of application is required to make this assessment.

Translating new science into new products is typically a slow, laborious process. Much of the difficulty in commercializing scientific breakthroughs is in determining suitable applications and understanding the engineering limitations of new devices. In many cases, the science is still not sufficiently understood for scientists and engineers to select the application with the highest probability of successor the most favorable financial return. New technology often finds its greatest success in products that were not even conceived of at the time of discovery. Considerable time and effort must be allocated to applied research in which the capabilities of the new technology in different applications are evaluated. This process often requires considerable trial and error because performance cannot be predicted with accurate models. New technologies often have difficulty dislodging an entrenched technology because of resistance from potential users of the new product. Customers must be convinced that the new technology offers superior performance in their particular application and is reliable-characteristics a new technology cannot always achieve at first. Similarly, manufacturers of the existing technology often have a strong disincentive to invest in new technologies. By their very nature, new technologies tend to destroy the competencies that firms have developed in certain technical areas; they often require capabilities and skills different from those used in manufacturing the entrenched technology.

Succesfull commercialisation is not a simple matter of getting to the market first. A competitive advantage in the marketplace must be found by by staking out and protecting a proprietary position through patents, trade secrets, or market barriers, and by securing the complementary assets and skills needed to ensure proper manufacturing, marketing, and support. Often the most difficult stage is that of converting a prototype into a salable product.The profitability of innovation depends on the

costs of commercialisation. In some industries or technologies, the sheer size of the investment required is the largest single hurdle to commercialisation. Uncertainties regarding cost also enter the decisionmaking process. Especially in new industries that are expected to demonstrate strong learningcurve effects, decisionmakers often cannot determine how quickly production costs will drop to a desired level. For first movers, rapid cost reduction is important to building barriers to entry and to expanding markets. For imitators trying to catch up with a market leader, uncertainties over cost make it difficult to determine the period of time required to become a competitive player in a market.

Innovators have several mechanisms for protecting their innovations from competitors. They can use patents and software copyrights to legally bar other firms from copying their invention without an explicit license; they can keep their innovation secret from potential imitators; or they can take advantage of other barriers to market entry. The choice of method is, in many ways, determined by the nature of the technology itself.

Patents arguably offer the strongest form of protection, but are highly effective for only a limited number of product types, in a limited number of industries. Patents allow innovators the rights to their inventions for 20 years after the patent application is filed, allowing them a period of exclusivity during which they can attempt to earn monopolistic returns on their innovation. Patenting requires innovators to publicly disclose the details of their innovation; in some fields, competitors can then invent around the patent by devising a somewhat different way to provide the same functionality. The elements of a product's design and manufacture can be gleaned through careful analysis, and similar products can be manufactured that perform almost identically. This capability makes it more difficult for innovators to capture or appropriate the returns from a new innovation because they cannot maintain their monopoly positions for long.

In cases in which patent protection is not effective, innovators may instead opt to keep the workings of their inventions secret, to the extent possible. The law provides only partial protection for trade secrets. Firms can attempt to restrain former employees from competing with them by using knowledge gained during their employment. Similarly, they can sue firms that illegally gain access to trade secrets. But the law normally permits competitors to analyze products, figure out how they work, and find ways to produce similar products.

Many firms must, therefore, rely on other barriers to entry to protect their innovations. In industries characterised by significant economies of scale or steep learning curves, innovators can often gain protection by being first to market and rapidly expanding production. Although this strategy may often require large up-front invest-

ments in plant and equipment, it can enable companies to rapidly reduce their production costs by spreading the capital investment over a larger number of products and by allowing them to rapidly gain experience with the manufacturing process. Such experience frequently translates into lower manufacturing costs over time, as workers and managers begin to understand the subtle interactions between components of a system or the effects of changes in manufacturing conditions on product performance. Experiential knowledge of this sort, often referred to as tacit knowledge, is not easily codified and conveyed; therefore, it cannot easily be acquired by a competitor who does not make a similar investment in production.

Firms can also erect barriers to entry through superior strategies for product development, sales, or service. Rapid product development, for example, can allow an innovator to put new, im proved products on the market more quickly than its competitors, thereby incorporating newer technology and responding to more recent changes in market demand.

The innovations discussed here use a combination of methods. The first concepts are protected by patents to enable open scientific discussion about the underlying physical phenomena and encourage further understanding and development of general design rules. To secure a lead over possible imitators, advancements in for instance manufacturing technology or details of the designs, which often have taken years to achieve, are kept out of the open literature. In all cases the designs are as close as possible to existing technology to avoid pitfalls as the "not invented here" syndrome and/or reliability issues. Keeping the detailed information about both the scientific background and the used technology within a limited group of people allows for quick decisions about the commercialisation of the inventions in a specific application in accordance with the needs and conventions of that specific market.

7 Literature

1839 Hagen, G., *Über die Bewegung des Wassers in engen cylindrischen Rohren*, Poggendorfs Ann. Phys. Chem. 46:423-442.

1840 Poiseuille, J. L. M. *Recherches expérimentales sur le mouvement des liquides dans les tubes de tres-petits diametres*. CR Acad. Sci. Paris. 11:961-967

1850 Stokes, G.G., *On the Effect of the Internal Friction of Fluids on the Motion of Pendulums*, Transactions of the Cambridge Philosophical Society, Vol. IX., p.8

1885 Preece, W.H., *On peculiar behaviour of glow-lamps when raised to high incandence*, Proc. Roy. Soc, series A, vol. 38, p. 219

1907 Blasius, H. (1908) *Grenzschichten in Flüssigkeiten mit kleiner Reibung. Zeitschrift für Mathematik und Physik* 56, 1-37

1915 Schlichter, W., *Die spontane Electronenemission glühender Metalle und das glühelektrische element*, Ann. Physic, vol. 47, p. 573-640

1923 Langmuir, I, *The collected works of Irving Langmuir*, Volumes 3 and 5, Pergamon press, New York, 1961

1941 Gurtovoy, M.Y. and G.I. Kovalenko, *A study of the operation of a diode in cesium vapour*, Fizichni Zapiski, vol. 9, p. 240

1951 Cohen, K.P., *The Theory of Isotope Separation as Applied to the Large- Scale Production of U-235*, McGraw-Hill Book Company, New York

1955 Hinze, J.O., AIChE. J., 1, (1955), No.3, pp. 289-295.

1960 Bird, R.B., Stewart, W.E., Lightfoot, E.N., *Transport Phenomena*, John Wiley & Sons, New York, 1960, 2002

1963 Martini, W.R., Internal flame-heated thermionic converters, Thermionic specialist conference, Oct 7-9 1963, Gatlinborg, Tennessee, p. 356

1964 Fuchs, N.A., *The mechanics of Aerosols*, Pergamon press

1964 Owczarek, J.A., *Fundamentals of gas dynamics*, International Textbook Company, Scranton Pennsylvania

1966 Waldmann, L. K.H. Schmidt, *Thermophoresis and diffusiophoresis of aerosols* , in: Aerosol Science, Academic Press, London - New York

1967 Janz, G.J. *Molten Salts Handbook*; London Accadamic Press: London

1969 Shefsiek, P.K. and J.P. Angello, *Test results from an improved flame fired thermionic diode*, IEEE TCSC Oct 21-23 1969, p. 521

1978 Davies, C.N.; In *Fundamental of Aerosol Science*; Shaw, D.T., Ed.; Wiley, New York

1978 Shah, R.K., London, A.L., *Laminar Flow Forced Convection in Ducts*: a Source Book for Compact Heat Exchanger Analytical Data, Academic Press, London

1979 Schlichting, H., *Boundary-layer theory*, McGraw-Hill, London

1982 Holman, J.P., Heat Transfer, McGraw Hill, London

1983 Kals, J.A.G., J.H. Dautzenberg and J.A.H. Ramaekers, Bewerkingstechnologie, Eindhoven University of Technology, lecture notes no. 4558

1983 Wood, N.B., *The Mass transfer of Particles and Acid Vapour to Cooled Surfaces*, Journal Institute of Energy, Vol. 76, pp. 76-93

1984 Buonicore, A.J., L. Theodore and G. Tchobanoglous, *Waste Management* in Perry's Chemical Engineers' Handbook (McGraw-Hill, New York, 1984)

1984 Perry's *Chemical Engineers Handbook*, 6th Edition, McGraw-Hill, New York, 1984, Chap. 18, pp.48-56.

1984 3. Svarovsky L. *Hydrocyclones*. London: Holt;

1986 Kreith, F., M.S. Bohm, Principles of Heat Transfer, Thomson Learning College

1987 Brouwers, J.J.H., P.H.J. Verbeek, W.R. Thomson, *Analytical System Availability Techniques*, Reliability Eng., 17, 9-22, (1987)

1988 Bejan, A. "*A Second Look at the Second Law*," Mechanical Engineering, Vol. 110, No. 5, May 1988, pp. 58-65.

1989 Veltkamp, W.B., et al., *Design and testing of a heatpipe cooled thermionic energy converter*, proc. 25th IECEC, p. 1171

1989 Wolff, L.R., *Performance of terrestrial thermionic converters*, Thermionic Energy Conversion short course, Eindhoven

1990 SKF Hoofdcatalogus, Veenendaal: Svenska Kullagerfabriken Nederland

1992 Regan, C.A.G., *A Novel Separator/Scrubber Design Program - The Impact of Upstream and Downstream Equipment on Separation Performance*, Paper presented at the 9th Continental Meeting of the Gas Processing Association, European Chapter, May 14-15, 1992

1994 Li, H., Tomita, Y., J. Fluids Eng., 116 (1994), pp. 370-373

1995 Brouwers, J.J.H., Appl. Sci. Res. (1995), pp. 95-105

1995 Kemenade, H.P. van, *The design of a combustion heated thermionic converter*, PhD thesis, Eindhoven University of Technology

1995 Shavit, C. Gutfinger, *Thermodynamics: from concepts to applications*, (Prentice Hall, London

1996 Brouwers, J.J.H., *Rotating Particle Separator: a New Method for Separating Fine Particles and Mists from Gases*, Chem. Eng. Techn., 19, pp. 1-10

1996 Laagland, G.H.M., J.J.H. Brouwers, J. Poorting, *The rotating air filter for gasturbines*, Proc. Power-Gen. Europe 96 2 (1996) 413-439.

1997 Brouwers, *Particle Collection Efficiency of the Rotational Particle Separator*, Powder Techn., 92, pp. 89-99

1997 Obernberger, I.; Biedermann, F.; Widmann, W.; Riedi, R. *Biomass & Bioenergy*, **1997**, 12 (3), pp. 211–234

1998 Brunner T., I. Obernberger, J.J.H. Brouwers, Z. Preveden, *Efficient and economic dust separation from flue gas by the rotational particle separator as an innovative technology for biomass combustion and gasification plants*, Proceedings of the Tenth European Bioenergy Conferеence, 1998, pp. 1630-1633.

1998 Hasler, Ph, Th. Nussbaumer, H.P. Scharner, J.J.H. Brouwers, *Reduction of aerosol particles in flue gases from biomass combustion in a rotating particle separator RPS*, Proceedings of the Tenth European Bioenergy Conference, 1998, pp. 1353-1355.

1998 He, C., G. Ahmadi, *Particle Deposition with Thermophoresis in Laminar and Turbulent Duct Flows*, Aerosol science and technology, Vol. 29. pp. 525-546

1998 Tandon, P., M.A. Adewumi, *Particle deposition from turbulent flow in a pipe*, , Aerosol Science, Vol. 29, pp 141-156

1998 Valmari, T.; Kaupinnen, E.I.; Kurkela, J.; Jokiniemi, J.K.; Sfiris, G.; Revitzer, H.; *J. Aerosol Sci.*, **1998**, 29 (4), pp. 445–459

1999 Kemenade, H.P. van, *Heat Exchanger test rig*, Eindhoven University of Technology

2000 Aart, F. van, N. Bolt, B. de Boer, J.J.H. Brouwers, W. Niggeschmidt, A. Strehlow, *Operational experiences with the rotating air inlet filter at the 3.6 Megawatt industrial gasturbine of kappa*, Proc. Power-Gen Europe 2000

2000 Christensen, K.A.; Stenholm, M.; Livbjerg, H. *J. Aerosol Sci.*, **1998**, 29 (4), pp. 421–444

2000 Hendriks, A.J.A.M., Graduation thesis, Eindhoven University of Technology, Department of Mechanical Engineering

2000 Jensen, J.R.; Nielsen, L.B.; Schultz-Møller, C.; Wedel, S.; Livbjerg, H. *Aerosol Sci. and Tech.*, **2000**, 33, pp. 490–509

2000 Jensen, P.A.; Frandsen, F.J.; Dam-Johansen, K.; Sander, B. *Energy & Fuels*, **2000**, 14, pp. 1280–1285

2001 Bejan A., *Thermodynamic Optimization of Geometry in Engineering Flow Systems*", Exergy, an International Journal, Vol. 1, No. 4, 2001, pp. 269-277

2001 Braun-Fahrländer, C. In *Proceedings of the IEA Seminar "Aerosols from Biomass Combustion"*, Zürich, Switserland; Nussbaumer, T., Ed.; Verenum: Zürich, 2001; pp 11–18.

2001 Ebert, F.; In *Proceedings of the IEA Seminar "Aerosols from Biomass Combustion"*, Zürich, Switserland; Nussbaumer, T., Ed.; Verenum: Zürich, 2001; pp 41–46

2001 Johansson, L.; Tullin, C.; Leckner, B.; In *Proceedings of the IEA Seminar "Aerosols from Biomass Combustion"*, Zürich, Switserland; Nussbaumer, T., Ed.; Verenum: Zürich, 2001; pp 87–92

2001 Obernberger, I.; Brunner, T.; Jöller, M. In *Proceedings of the IEA Seminar "Aerosols from Biomass Combustion"*, Zürich, Switserland; Nussbaumer, T., Ed.; Verenum: Zürich, 2001; pp 69–74

2002 Bird, R.B.; Steward, W.E.; Lightfoot, E.N. *Transport Phenomena, second edition*; John Wiley & Sons Inc.: New York

2002 Brouwers, J.J.H., *Phase Separation in Centrifugal Fields with Emphasis on the Rotational Particle Separator*, Exp. Thermal Fluid Science, 26, pp. 325-334

2002 Brunner, T.; Jöller, M.; Obernberger, I.; Frandsen, F. In *12th European Conference and Technology Exhibition on Biomass for Energy, Industry and Climate Protection*, Amsterdam, August 2002

2002 Loo, S. van; Koppejan, J. *Handbook of Biomass Combustion and Co-Firing*; Twente University Press: Enschede, 2002

2003 Kemenade H.P. van, E. Mondt, A.J.A.M. Hendriks, P.H.J. Verbeek, *Liquid-Phase Separation with the Rotational Particle Separator*, Chem. Eng, Techn., 26, pp. 1176-1183,

2004 Golombok, M., L. Chewter, *Centrifugal separation for cleaning well gas streams*, Ind. Eng. Chem. Res., 43(7), 1734

2005 Frandsen, F.J.; Moiraghi, L.; Van Lith, S.; Jensen, A.J.; Glarborg, P. In *Aerosol in Biomass Combustion*; Obernberger, I., Ed.; Medienfabrik Graz: Graz, 2005, pp. 65–77

2005 Golombok, M., K. Bil , Ind. Eng. Chem. Res., 44(13), 4721

2005 Jöller, M.; Brunner, T.; Obernberger, I. *Energy & Fuels*, 19, pp. 311–323

2005 Kemenade, H.P. van, In *Aerosols in Biomass Combustion*; Obernberger, I., Ed.; Medienfabrik Graz: Graz, 2005, pp. 107–118

2005 Mondt, E., *Compact Centrifugal Separator of Dispersed Phases*, PhD thesis, Eindhoven University of Technology

2005 Wilhelm, J., Seibt, D., Bich, E., Vogel, E., Hassel, E., *Viscosity Measurements on Gaseous Sulfur Hexafluoride*, J. Chem. Eng. Data, 50, pp. 896-906

2005 Wissen, R.J.E. van, M. Golombok and J.J.H. Brouwers, Chem. Eng. Sci.60(16),4397

2006 BP, *Statistical Review of World Energy 2006*

2006 Royal Dutch Shell,*The Shell Global Scenario's to 2025*

2006 Wissen, R.J.E. van, M. Golombok and J.J.H. Brouwers, *Gas Centrifugation with Wall Condensation*, A.I. Chem. E. J. 52(3), 1271